Supporting Information for:

Synthesis of Heteroleptic bis-Phosphine bis-NHC Iron (0) Complexes: A Strategy to Enhance Small Molecule Activation

*Christian M Andre,[a] and Nathaniel K. Szymczak[a]**

[a]Department of Chemistry, University of Michigan, Ann Arbor, Michigan 48109, United States

Table of Contents

Experimental Procedures

General Considerations

All air- and moisture-sensitive manipulations were performed using standard Schlenk techniques or in an inert atmosphere glovebox with an atmosphere of purified nitrogen. The glovebox was equipped with a cold well designed for low temperature experiments as well as a −30 °C freezer for cooling samples and crystallizations. Solvents were purified using a Glass Contour solvent purification system through percolation through a Cu catalyst, molecular sieves, and alumina. Solvents were then stored over sodium and/or molecular sieves. Deuterated solvents were purchased from Cambridge Isotope Laboratories and used as received. NMR spectra were recorded on Bruker Avance Neo 500, and Varian Vnmrs 500/600/700 spectrometers at ambient temperature. ^{1}H and ^{13}C shifts are reported in parts per million (ppm) relative to TMS, with the residual solvent peak used as an internal reference. ^{31}P NMR spectra are referenced on a unified scale, where the single primary reference is the frequency of the residual solvent peak in the ^{1}H NMR spectrum. The following abbreviations are reported for NMR interpretation: broad (br), singlet (s), doublet (d), doublet of doublets (dd), triplet (t), multiplet (m). ^{13}C NMR resonances were observed as singlets unless otherwise stated. Infrared spectra were recorded using a Nicolet iS10 FT-IR spectrometer equipped with Smart Diamond Attenuated Total Reflectance (ATR) sampling accessory. Samples were either diluted in solid dry KBr and recorded as pellets, or were injected into a KBr solution cell with pathlengths of 0.20 mm. Electrospray-ioniziation time-of-flight (ESI/TOF) mass spectra were collected in acetonitrile using the Agilent 6230 TOF and Agilent 6520 Q-TOF mass spectrometers. Electrochemical measurements were performed on a Bio-Logic SP200 potentiostat/galvanostat with a built-in electrochemical impedance spectroscopy (EIS) analyzer. CV were measured in THF with (0.4 M) [NBu4][BArF 4])as the electrolyte with a glassy carbon working electrode, a platinum counter electrode, and a Ag wire / $AgNO_3$ electrode in a glass tube filled with the electrolyte solution with a CoralPor™ tip. All measurements were performed under an N2 atmosphere in a glovebox. Following each measurement, ferrocene was added to the analyte solution and all potentials were subsequently referenced to the Fc/Fc^{+} redox couple.

Tert-butanol, trimethylsilyltriflate, and hexamethyldisiloxane was purchased from commercial vendors, vacuum distilled, and dried over molecular sieves before transferring to a nitrogen glovebox. Iron (II) hexamethyldisilazide ($Fe(HMDS)_2$),[1] bis(diethylphosphino)ethane (depe),[2] trimesitylphosphine oxide ($OPMes_3$),[3] and potassium graphite (KC_8) [4] were prepared by literature procedure. $FeN_2(depe)_2$ was prepared via a modified literature procedure[5] where reduction by $KC_8$was performed in THF for 2 hours. $FeCO(depe)_2$ was also prepared by a modified literature procedure,[6] in which $FeN_2(depe)_2$ solution was charged with 30 psig CO in a J Young tube overnight. 1,1'-dibutyl-3,3'-methylene-dimimidazolium di(hexafluorophosphate) was prepared according to a literature prcedure[7] and converted to the PF_6^- salt by salt metathesis in water.

Synthetic Procedures

Synthesis of $[Fe(MeCN)_2(depe)(^{butyl}CC)]\ [PF_6]_2$ (2). In an inert atmosphere glovebox, to a 20 mL scintillation vial was added $Fe(HMDS)_2$ (136 mg, 0.362 mmol) and a stir bar, followed by a solution of **1** (200 mg, 0.362 mol) in 10mL of MeCN. After capping the vial the solution was stirred for 3hrs, during which time the initial green suspension turned into a deep red solution. The solvent was evaporated under vacuum to give red solids, which were then briefly (~1 minutes) triturated in 10 mL of THF, and filtered to

separate a yellow solution from the red solids. These red solids were further rinsed with THF (10 mL) and the yellow extract was discarded. Extraction of the red solids with 7.5 mL MeCN into a 20mL scintillation vial yielded a deep red solution to which a stirbar was then added. To the stirring red solution, depe (74 mg, 0.362 mmol, dissolved in 3 mL MeCN) was added dropwise, yielding a rapid color change to dark orange. The reaction mixture was then concentrated under vacuum to 1 mL to form a thick dark solution. 15 mL of pentane was added followed by gentle agitation of the mixture. Once settled, the top clear layer of the mixture was decanted off by pipette, and the colored solution left was evaporated under vacuum to yield orange solids **2** as orange solids (310 mg , 95%). Crystals of **2-cis** suitable for XRD were obtained by dissolving tetrabutylammonium tetraphenyl borate ([TBA][BPh_4]) in a concentrated solution of **2** in CH_2Cl_2, and chilling in a -30°C freezer overnight.

2-*cis*: ^{1}H NMR (600 MHz, CH_2Cl_2) δ: 7.53 (1H, ^{Imz}C**H**), 7.38 (1H, ^{Imz}C**H**), 7.28 (1H, ^{Imz}C**H**), 7.04 (1H, ^{Imz}C**H**), 6.19 (d, 1H, $(N)_2C\mathbf{H}_2$, *J* = 14.4 Hz), 5.27 (d, 1H, $(N)_2C\mathbf{H}_2$, *J* = 14.4 Hz), 4.35 (dt, 1H, $(N)C\mathbf{H}_2$, *J* = 12.4, 7.2 Hz), 4.15 (dt, 1H, $(N)C\mathbf{H}_2$, *J* = 12.5, 7.1 Hz), 3.92 (m, 2H, $(N)C\mathbf{H}_2$), 2.46 (3H, $NCC\mathbf{H}_3$), 2.33 (3H, $NCC\mathbf{H}_{3z}$), 2.15 (2H, $C\mathbf{H}_2$), 2.08 (m, 2H, $C\mathbf{H}_2$), 1.93 (2H, $C\mathbf{H}_2$), 1.84 (2H, $C\mathbf{H}_2$), 1.77 (2H, $C\mathbf{H}_2$), 1.63 (m, 2H, $C\mathbf{H}_2$), 1.50 (m, 4H, $C\mathbf{H}_2$), 1.41 (m, 4H, $C\mathbf{H}_2$), 1.27-1.39 (br m, 4H, $C\mathbf{H}_2$), 1.20 (dt, 3H, C**H**3, *J* = 11, 7.5 Hz), 0.98 (m, 12H, $C\mathbf{H}_3$), 0.70 (dt, 3H, $C\mathbf{H}_3$, *J* = 14.7, 7.3 Hz). **^{13}C{ ^{1}H} NMR** (126 MHz, C6D6) δ: 189.1 (m, *NH**C***), 188.1 (m, *NH**C***), 134.2 (s, N**C**CH_3), 132.0 (s, N**C**CH_3), 124.7 (s, ^{Imz}C), 123.3 (s, ^{Imz}C), 123.2 (s, ^{Imz}C), 122.2 (s, ^{Imz}C), 62.5, 59.3, 50.9, 49.4, 33.8, 33.6, 20.5, 19.9, 19.0-20.1 (m) 13.7, 13.6, 9.0 (m), 7.8 (m), 4.7 (s, NC**C**H_3), 4.4 (s, NC**C**H_3). **^{31}P{1H} NMR** (202 MHz, CH_2Cl_2) δ: 75.87 (d, 1P, *J* = 15Hz), 62.93 (d, 1P, *J* = 15Hz), -144.46 (2P, **P**F_6).

2-*trans*: **^{1}H NMR** (600 MHz, CH_2Cl_2) δ: 7.58 (2H, ^{Imz}C**H**), 7.24 (2H, ^{Imz}C**H**), 6.12 (1H, $(N)_2C\mathbf{H}_2$), 6.01 (1H, $(N)_2C\mathbf{H}_2$), 4.06 (2H, $(N)C\mathbf{H}_2$), 3.87 (2H, $(N)C\mathbf{H}_2$), 2.29 (3H, $NCC\mathbf{H_3}$), 2.28 (3H, $NCC\mathbf{H_3}$) – remaining features obscured by **2-*trans*. ^{31}P{^{1}H} NMR** (202 MHz, CH_2Cl_2) δ: 62.56 (2P), -144.46 (2P, **P**F_6).

2: IR (KBr, cm^{-1}): 2169 (w,$\nu_{\mathbf{NC}Me}$). **HRMS** (ESI+/TOF, m/z) calculated for [Fe(MeCN)(HCOO)(depe)(^{butyl}CC)]$^+$ = 567.2674, found 567.2671 (eluent contains NaCOOH / HCOOH buffer)

2 (64.4 mg, .0720 mmol) was dissolved in ca. 0.5mL DCM in a J Young tube. To this was added a 10% v/v hexamethyldisiloxide/DCM solution (50µL, .0235 mmol) as an internal standard to find 91% purity by ^{1}H NMR (Figure S19).

Synthesis of [Fe(CO)(MeCN)(depe)(^{butyl}CC)] [PF_6]$_2$ (3). To a J-Young NMR tube was loaded an orange solution of **2** (75 mg, 0.084 mmol) dissolved in 2mL of CH_2Cl_2. The tube was charged with 30 psig of CO gas, sealed, and agitated for 6 h. The tube was brought into an inert atmosphere glovebox, then the contents were transferred to a 20 mL scintillation vial and the solvent was removed under vacuum to yield pale-yellow solids. These solids were washed with 5 mL of diethyl ether and were dried under vacuum to yield pale yellow solids (70 mg, 96%).

^{1}H NMR (600 MHz, CH_2Cl_2) δ: 7.57 (2H, ^{Imz}C**H**), 7.17 (2H, ^{Imz}C**H**), 6.37 (d, 1H, $(N)C\mathbf{H}_2$, *J* = 15 Hz), 6.14 (d, 1H, $(N)C\mathbf{H}_2$, *J* = 15 Hz), 4.04 (dt, $(N)C\mathbf{H}_2$, 2H, *J* = 12 Hz), 3.94 (dt, $(N)C\mathbf{H}_2$, 2H, *J* = 12 Hz), 2.48 (3H, $NCC\mathbf{H}_3$), 2.27 (m, 2H, $C\mathbf{H}_2$), 2.12 (m, 6H, $C\mathbf{H}_2$), 1.82 (m, 4H, $C\mathbf{H}_2$), 1.69 (m, 2H, $C\mathbf{H}_2$), 1.58 (m, 2H, $C\mathbf{H}_2$), 1.37 (m, 6H, $C\mathbf{H}_3$), 1.32 (m, 2H, $C\mathbf{H}_2$), 0.92 (t, 6H, $C\mathbf{H}_3$, *J* = 7 Hz), 0.83 (m, 6H, $C\mathbf{H}_3$). **^{13}C{^{1}H} NMR** (176 MHz, CH_2Cl_2) δ: 218.3 (t, **C**O, *J* = 23Hz), 179.5 (dd, NH**C**, *J* = 36, 21 Hz), 134.5 (s, N**C**CH_3), 126.0 (s, ^{Imz}**C**), 122.2 (s, ^{Imz}**C**), 63.7 (s, $(N)_2\mathbf{C}H_2$), 51.2 (s, **C**H_2), 21.5 (t, **C**H_2, *J* = 8Hz), 21.4 (t, **C**H_2, *J* = 8Hz), 19.8 (s, $C\mathbf{H}_2$), 18.6(m), 13.4 (s, **C**H_3), 8.0 (s, **C**H_3), 7.9 (s, **C**H_3), 4.3 (s, NC**C**H_3). **^{31}P{^{1}H} NMR** (283 MHz, CH_2Cl_2) δ: 64.64 (s, 2P, depe), 144.5 (m, 2P,

PF_6). **IR** (KBr, cm^{-1}): 2169 (w,$\nu_{\mathbf{NC}Me}$), 1947 (s, ν_{CO}); **HRMS** (ESI+/TOF, m/z) calculated for [Fe(CO)(MeCN)(depe)(^{butyl}CC)]$^{2+}$ = 295.6451, found 295.6467.

3 (67.4 mg, .076 mmol) was dissolved in ca. 0.5mL DCM in a J Young tube. To this was added a 10% v/v hexamethyldisiloxide/DCM solution (50µL, .0235 mmol) as an internal standard to find 84% purity by ^{1}H NMR (Figure S20).

Synthesis of [Fe(N_2)(depe)(^{butyl}CC)] (4). To a 20 mL scintillation vial was added **2** (100 mg, 0.112 mmol), 5mL of THF, and a stirbar. After briefly stirring to dissolve most of **2,** the mixture was frozen using liquid nitrogen. KC_8 (34 mg, 0.246 mmol) was added, and the mixture was allowed to thaw while stirring. The resulting black suspension stirred for 30 min and was then filtered to yield a red solution. Solvent was removed from the solution via evaporation to yield red solids. These solids were extracted with 15 mL of pentane and filtered to give a deep red solution. Evaporation of solvent under vacuum yielded **4** as a greasy red solid (43 mg, 69%). The IR spectrum of a pentane solution of **4** exhibited a strong band at 1954 cm^{-1}, however this band was not present in the solid-state spectrum. Crystals suitable for X-ray diffraction were obtained from chilling a concentrated pentane solution of **4** to -25°C overnight.

^{1}H NMR (500 MHz, C_6D_6) δ: 6.44 (2H, ^{Imz}C**H**), 6.35 (2H, ^{Imz}C**H**), 4.97 (m, 2H), 4.72 (m, 1H), 4.56 (d, 2H, $(N)_2$C**H**$_2$, *J* = 10 Hz), 3.62 (m, 2H), 1.99 (br, 4H), 1.57-1.79 (m, 4H), 1.38–1.56 (m, 14H), 1.26 (m, 4H), 1.17-1.33 (m, 4H), 0.95-1.15 (br, 4H), 0.90 (m, 8H), 0.60-0.84 (4H). **^{13}C{^{1}H} NMR** (126 MHz, C_6D_6) δ: 212.5 (m, NH**C**), 118.3 (s, ^{Imz}**C**H), 116.8 (s, ^{Imz}**C**H), 60.0 (s, $(N)_2$**C**H_2), 50.2 (s, (N)**C**H_2), 34.4 (s, **C**H_2), 28.0 (t, *J* = 22 Hz), 26.7 (s), 20.40 (s, **C**H_2), 14.3 (s, **C**H_3), 8.9 (br, **C**H_3). **^{31}P{^{1}H} NMR** (202 MHz, C_6D_6) δ: 90.05 (s). **IR** (pentane, cm^{-1}): 1954 (s, ν_{N2}); **IR** (KBr, cm^{-1}): 1913 (s, ν_{N2}); **IR** (ATR, cm^{-1}): 1911 (s, ν_{N2}). **HRMS** (ESI+/TOF, m/z) calculated for [FeH(N_2)(depe)(^{butyl}CC)]$^+$ = 551.2833, found 551.2831

4 (25.6 mg, .047 mmol) was dissolved in ca. 0.5mL C_6D_6 in a J Young tube. A crystal of naphthalene (17.9 mg, .140 mmol) was added to the sample and dissolved as an internal standard to find 90% purity by ^{1}H NMR (Figure S21).

Synthesis of [Fe(CO)(depe)(^{butyl}CC)] (5). To a 20 mL scintillation vial was added **3** (73 mg, 0.0829 mmol), 5mL of THF and a stirbar. After briefly stirring to dissolve most of **2,** the mixture was frozen using liquid nitrogen. KC_8 was added (40 mg, 0.299 mmol), and the mixture was allowed to thaw under stirring. The resulting black suspension stirred for 30 min, during which it turned dark green then dark red, and was then filtered to yield a red solution. Solvent was removed from the solution via evaporation to yield red solids. These solids were then extracted with 15 mL of pentane and filtered to yield a deep red solution. Removal of solvent under vacuum yielded **5** as an orange powder (37 mg, 81% yield). Crystals were obtained from slowly evaporating a THF solution of **5** to at room temperature over several days.

^{1}H NMR (700 MHz, C_6D_6) δ: 6.45 (s, 2H, ^{Imz}C**H**), 6.32 (s, 2H, ^{Imz}C**H**), 5.14 (m, 2H), 4.94 (1H), 4.84 (1H), 3.49 (m, 2H, C**H**$_2$), 1.54-1.91 (br m, 8H), 1.36-1.50 (br m, 12H), 1.02-1.34 (br m, 9H), 0.87-1.03 (br m, 9H). **^{13}C{^{1}H} NMR** (176 MHz, C_6D_6) δ: 222.9 (br, **C**O), 214.4 (br, NH**C**), 118.3 (^{Imz}**C**H), 116.7 (^{Imz}**C**H), 50.9 (s, $(N)_2$**C**H_2), 33.4 (**C**H_2), 28.2 (t, *J* = 23 Hz), 27.8 (br), 20.5 (**C**H_2), 14.4 (**C**H_2), 8.9 (**C**H_3). **^{31}P{^{1}H} NMR** (283 MHz, C_6D_6) δ: 95.85 (br, depe). **IR** (pentane, cm^{-1}): 1794 (s, ν_{CO}); **IR** (KBr, cm^{-1}): 1737 (s, ν_{CO}), 1901 (m), 1848 (m) **; HRMS** (ESI+/TOF, m/z) calculated for [FeH(N_2)(depe)(^{butyl}CC)]$^+$ = 551.2720, found 551.2723.

5 (36.2 mg, .066 mmol) was dissolved in ca. 0.5mL C_6D_6 in a J Young tube. A crystal of naphthalene (16.1 mg, .126 mmol) was added to the sample and dissolved as an internal standard to find 90% purity by ^{1}H NMR (Figure S22).

[FeH(N$_2$)(depe)(^{butyl}CC)] OTf (6). To a 20 mL scintillation vial was added **2** (6 mg, .011 mmol), 5mL of THF, and a stirbar. While this solution is stirring, [NH_2Ph_2] [OTf] (3.5 mg, .011 mmol) was added dropwise as a solution in 2mL of THF to form a yellow solution. The solution was concentrated under vacuum to 1mL in volume, and 5mL of pentane were added to precipitate light colored solids. The suspension was filtered to collect the solids, which were then extracted with 2 mL of THF and used without further purification.

^{1}H NMR (700 MHz, THF) δ: 7.74 (s, 2H, ^{Imz}C**H**), 7.15 (s, 2H, ^{Imz}C**H**), 6.75 (d, 1H, (N)$_2$C**H**$_2$), 5.54 (d, 1H, (N)$_2$C**H**$_2$), 4.24 (m, 2H, (N)C**H**$_2$), 4.08 (m, 2H, (N)C**H**$_2$, -16.72 (t, 1H, *J* = 60 Hz) ; **^{13}C{^{1}H} NMR** (176 MHz, THF) δ 196.31, 122.63, 120.13, 49.50, 33.98, 22.02, 19.81, 13.17, 7.69, 6.70 ; **^{31}P NMR** (202 MHz, THF) δ: 81.9 (d, depe, *J* = 59 Hz); **IR** (KBr, cm^{-1}): 2072 (s, ν_{N2}). **HRMS** (ESI+/TOF, m/z) calculated for [FeH(N$_2$)(depe)(^{butyl}CC)]$^+$ = 551.2833, found 551.2831

Synthesis of [Fe(N$_2$SiMe$_3$)(depe)(^{butyl}CC)]OTf (7). To a 20 mL scintillation vial was added **4** (60 mg, 0.11 mmol), 5mL of Et_2O, and a stirbar. This was chilled to -78°C over 20 minutes using a dry ice / acetone cooling bath while stirring. One equivalent of TMSOTf (24.5 mg, 0.11 mmol) was dissolved in ca. 1mL of Et_2O. This TMSOTf solution was added dropwise by syringe to the chilled, stirring solution of **4** over the course of 1 – 2 minutes. This immediately yields an opaque brown color that gradually becomes an opaque green suspension. Once the TMSOTf addition is complete, the reaction mixture is filtered and washed with chilled Et_2O to collect dark green solids. These green solids are quickly extracted with 10 mL of THF, which is then concentrated under vacuum to ca. 2 mL to yield a dark green solution. This is placed in a -30°C freezer for a couple hours to yield green, hair-like, polycrystalline **7** (63 mg, 75% yield). Addition of any solvent other than THF yields a color change to yellow and degradation to **6** as evidenced by ^{1}H and ^{31}P NMR.

^{1}H NMR (700 MHz, THF) δ: 7.68 (s, 2H, ^{Imz}C**H**), 7.16 (s, 2H, ^{Imz}C**H**), 6.56 (d, 1H, (N)$_2$C**H**$_2$), 4.43 (d, 1H, (N)$_2$C**H**$_2$), 4.23 (br, 2H, (N)C**H**$_2$), 3.95 (br, 2H, (N)C**H**$_2$), 2.2-1.85 (br, 4H), 1.6-1.4 (br, 4H), 1.32-1.03 (br m, 16H), 0.84 (m, 6H, C**H**$_3$), 0.61 (m, 6H, C**H**$_3$), 0.19 (s, 9H, SiC**H**$_{3fi}$); **^{13}C{^{1}H} NMR** (176 MHz, C_6D_6) δ: 199.6 (m, NH**C**), 122.5 (br, (SO$_3$)**C**F$_3$), 122.1 (s, ^{Imz}**C**), 120.6 (s, ^{Imz}**C**), 49.7 (s, (N)$_2$**C**H$_2$), 33.4 (**C**H$_2$), 25.1 (t, *J* = 20 Hz), 22.8 (m), 22.5 (m), 19.8 (s, **C**H$_2$), 13.5 (s, **C**H$_2$), 8.3 (s, **C**H$_3$), 7.1 (s, **C**H$_3$), -0.8 (s, Si**C**H$_3$); **^{31}P{^{1}H} NMR** (202 MHz, THF) δ: 85.33 (s, depe); **^{29}Si{^{1}H} NMR** (139 MHz, THF) δ: -5.4 (s, **Si**Me$_3$); **IR** (ATR, cm^{-1}): 1693 (s br, ν_{N2}).

Protonation of FeN$_2$(depe)$_2$ to yield [FeH(N$_2$)(depe)$_2$]OTf. To a vial was added FeN$_2$(depe)$_2$ (7 mg, .0141 mmol) and ca. 0.2 mL THF. While gently swirling this solution, [NH_2Ph_2] [OTf] (4 mg, .0125 mmol) was added as a solution in ca. 0.2 mL THF. This immediately yielded a color change from orange to light green. The mixture was filtered to remove green solids and yield a pale-yellow solution that is analyzed without further purification.

Note regarding IR spectra of 4 and 5:

We note large differences between solution- and solid-phase ν_{N2} and ν_{CO} stretches for **4** and **5** (>30 cm^{-1}). Differences in coordination geometry between solid and solution phase may contribute to differences between the solution/solid IR data. To address this hypothesis, we performed DFT studies on both the intermediate (τ = 0.4) and square planar geometries. We found that the respective ν_{N2} and ν_{CO} of **4** and **5**

are insignificant (< 10 cm^{-1}). Therefore, we cannot attribute the experimentally determined difference in solid/solution phase to coordination geometry. Although intermolecular interactions in the solid state can also influence the IR resonances, such interactions are not evident in the SC-XRD data of **4** and **5**.

NMR Spectra

Figure S1. ^{1}H NMR spectrum (d3-MeCN, 25 °C) of **1**.

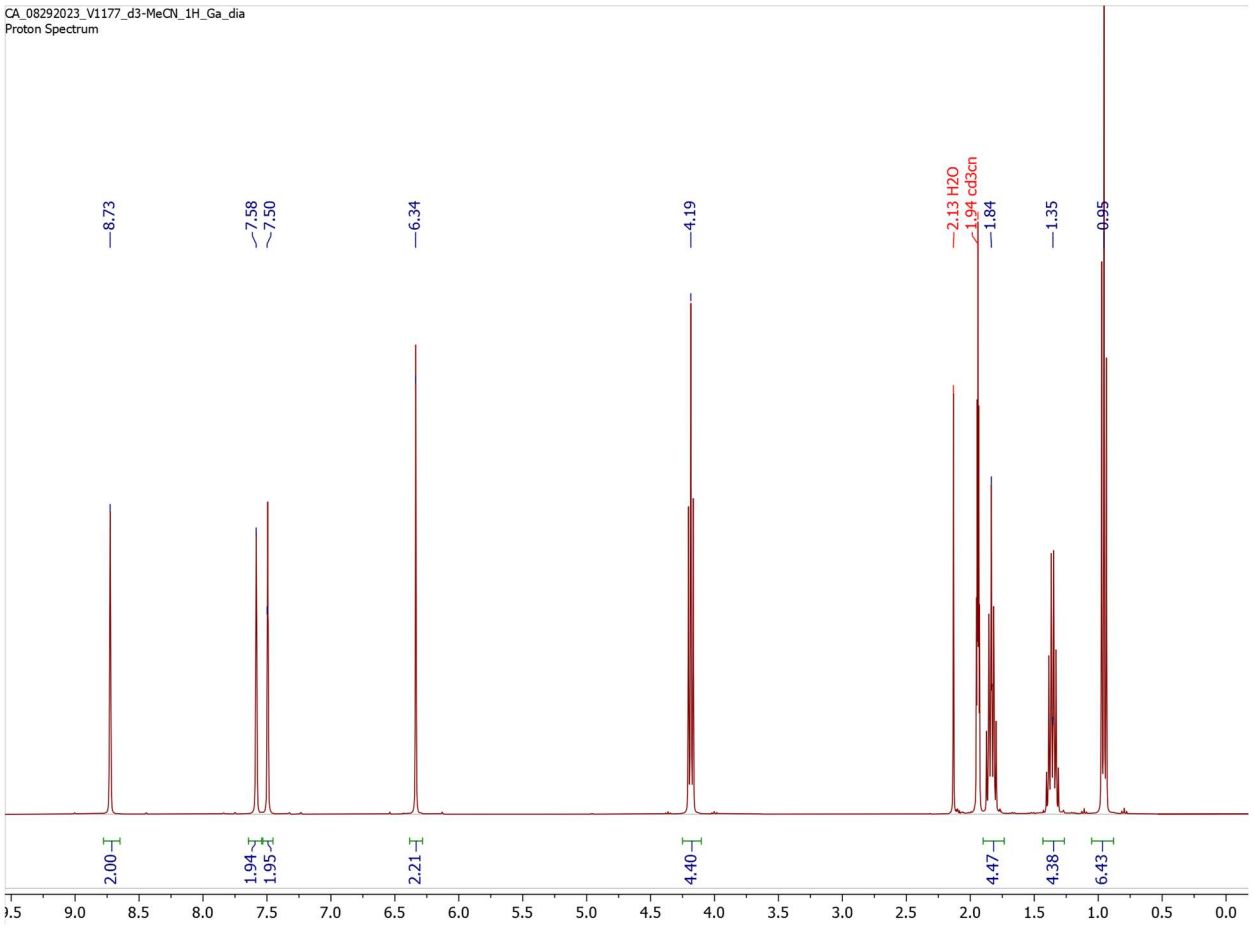

Figure S2. ^{1}H NMR spectrum (MeCN, 25 °C) of **1a**.

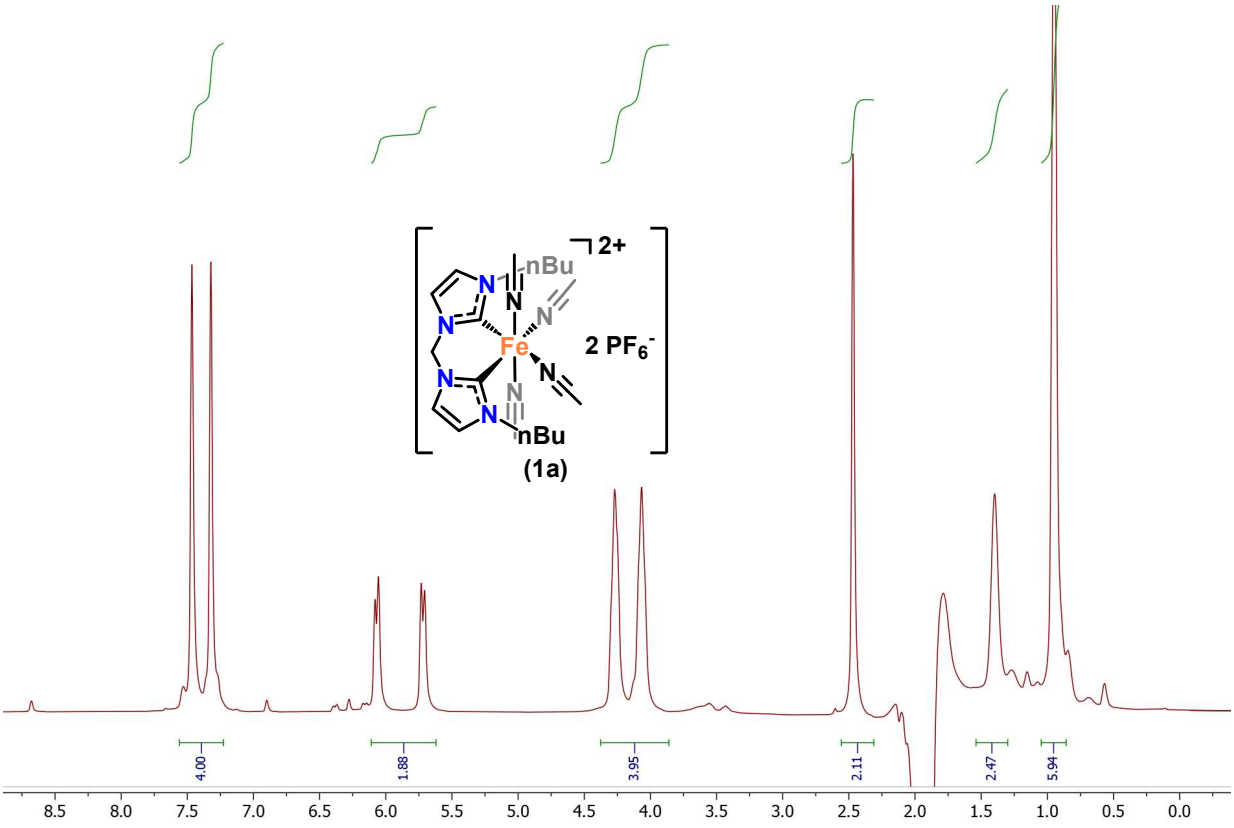

Figure S3. ^{1}H NMR spectrum (CH_2Cl_2, 25 °C) of **2**

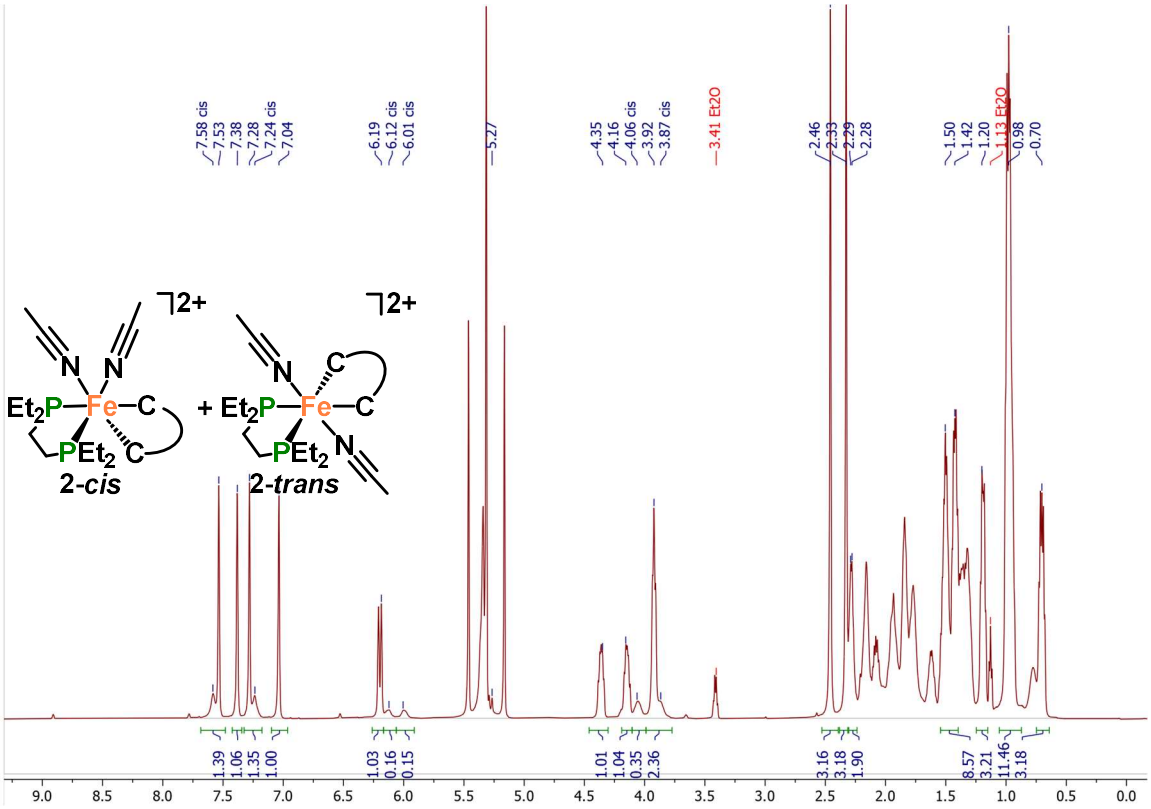

Figure S4. ^{1}H NMR spectrum (MeCN, 25 °C) of **2**

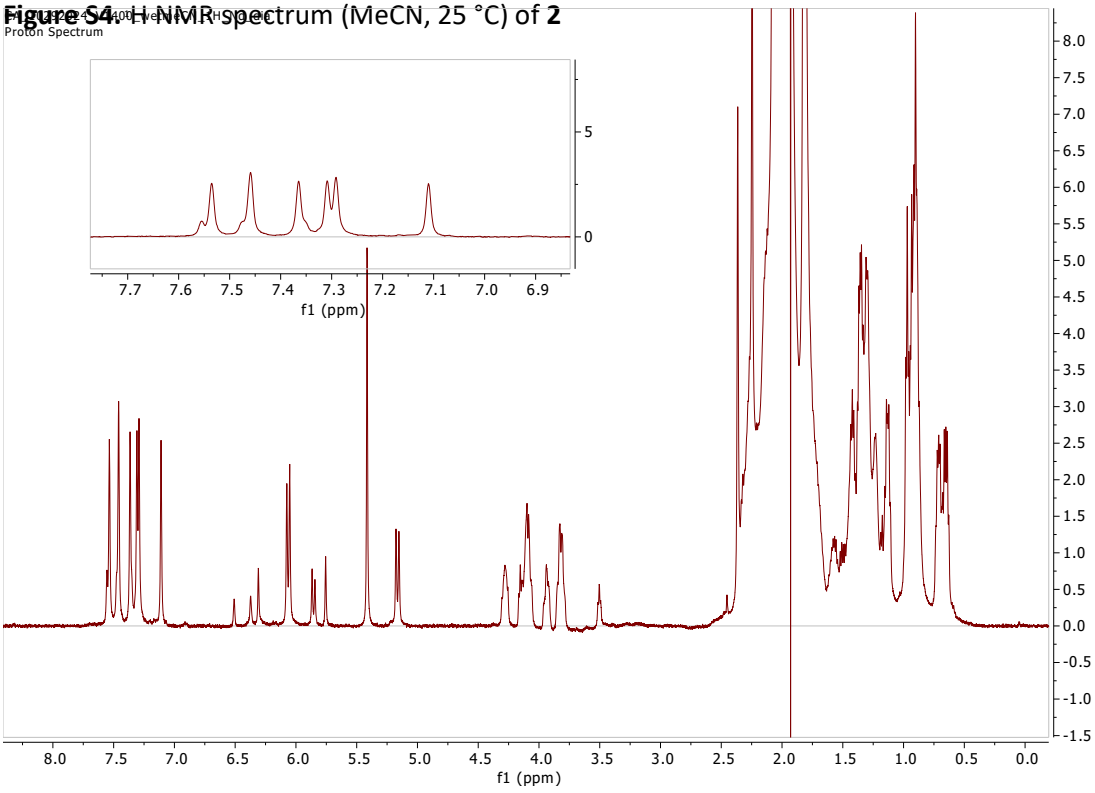

Figure S5. ^{31}P NMR spectrum (CH_2Cl_2, 25 °C) of **2**

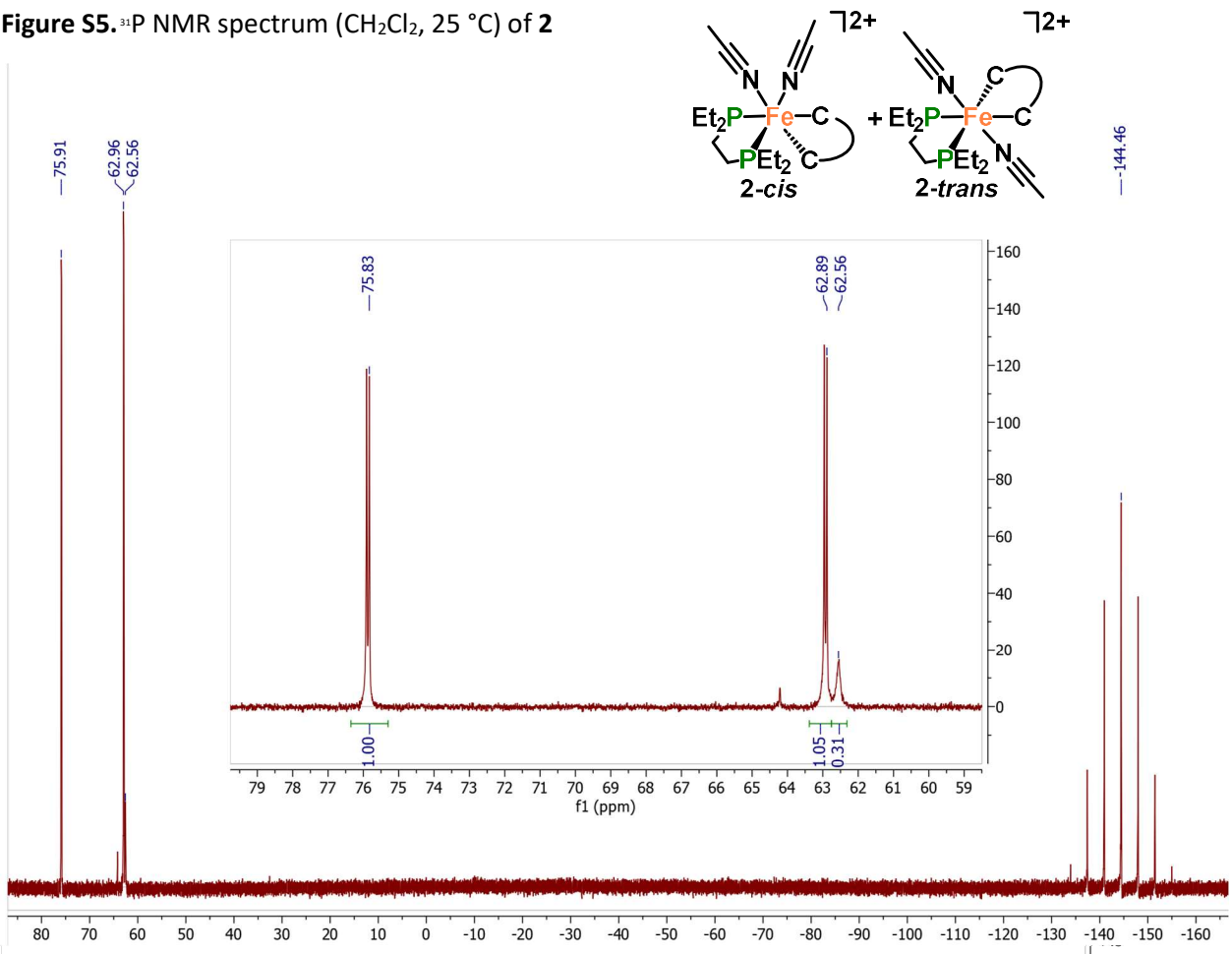

Figure S6. ^{31}P NMR spectrum (MeCN, 25 °C) of **2**

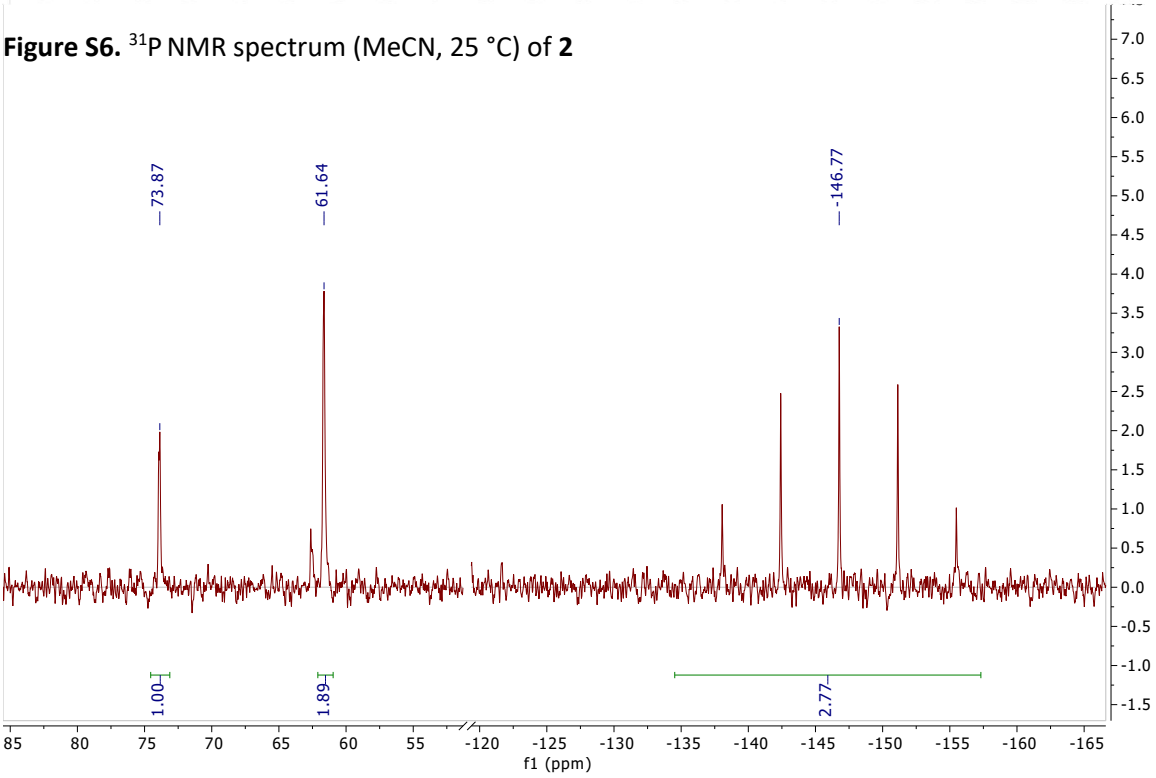

Figure S7. ^{13}C NMR spectrum (CH_2Cl_2, 25 °C) of **2**

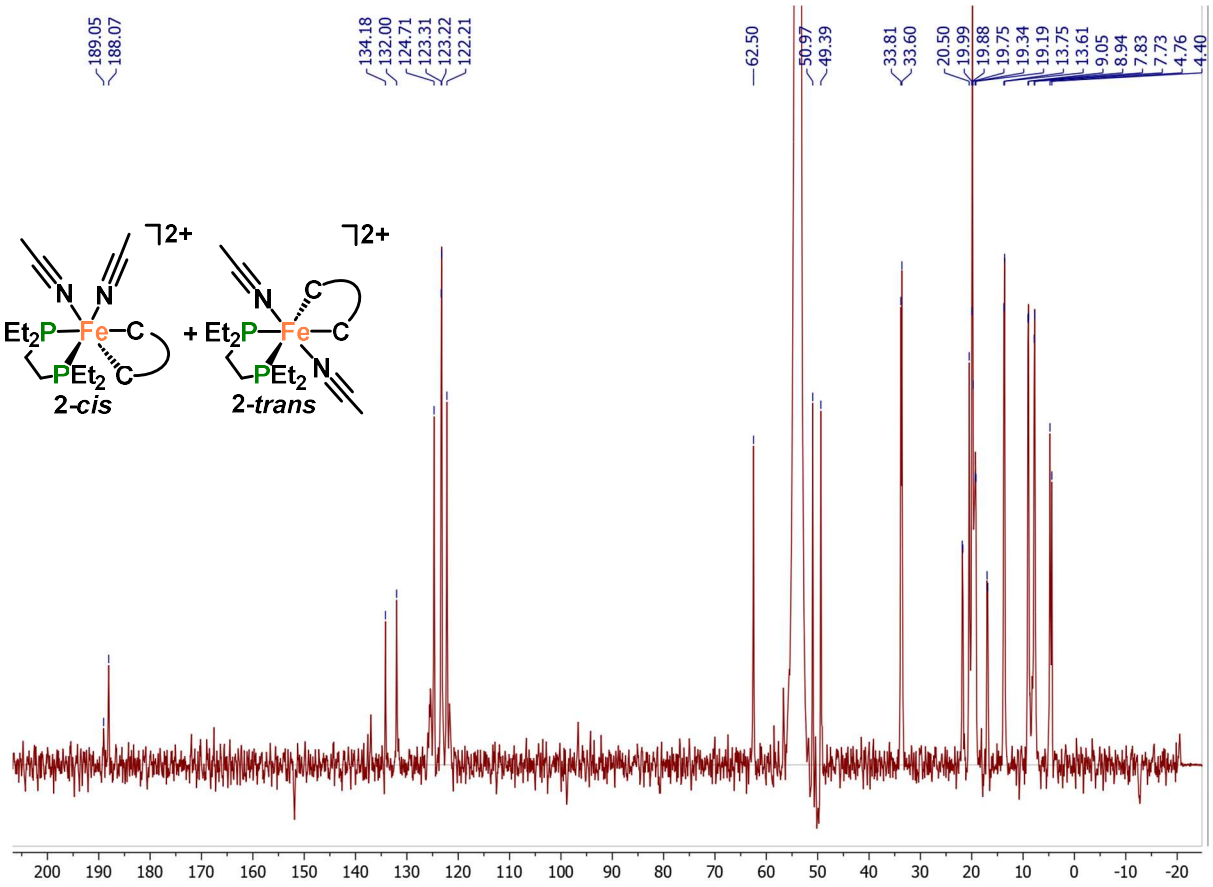

Figure S8. ^{1}H NMR spectrum (CH_2Cl_2, 25 °C) of **2** following addition of d_3-MeCN (blue)

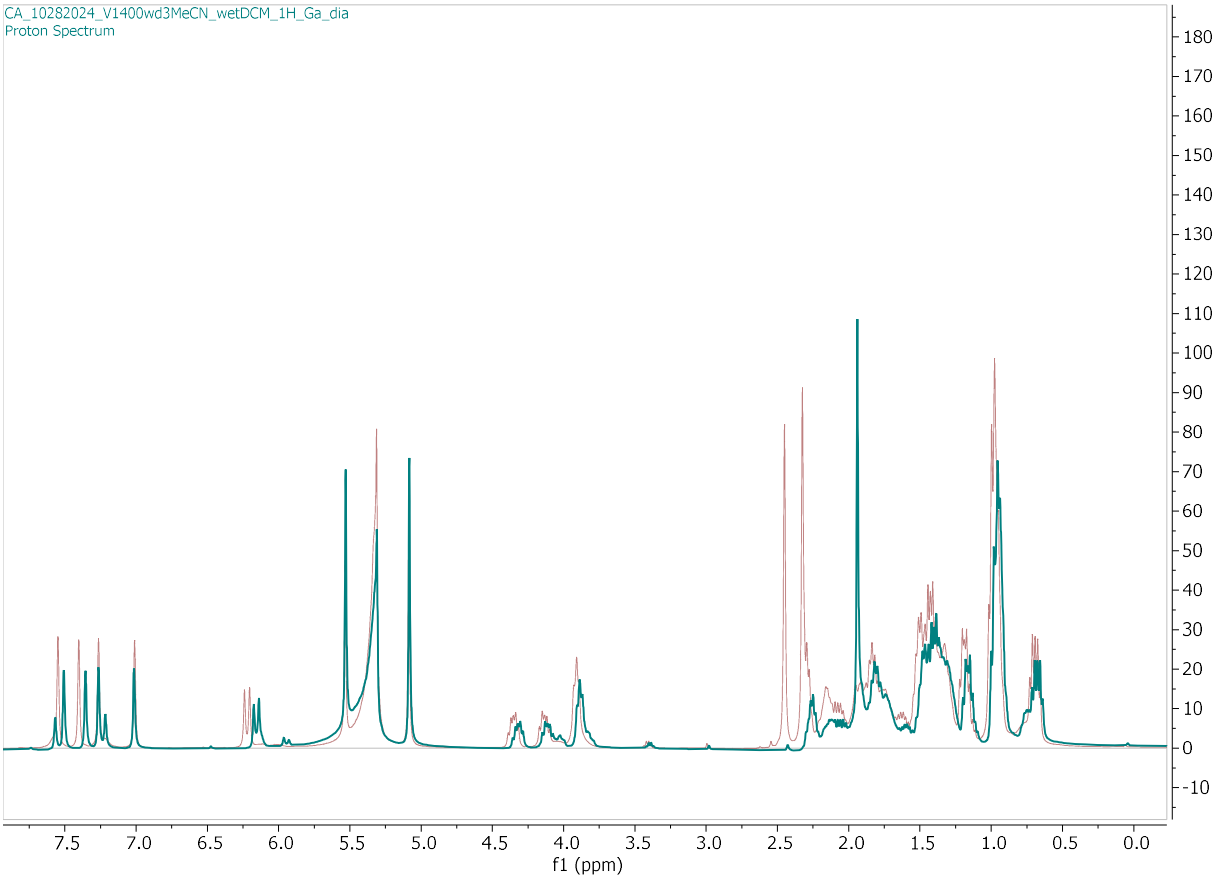

Note: To a 0.4mL CH_2Cl_2 solution of **2** in an NMR tube was added a drop of deuterated MeCN. NMR spectra taken immediately after. Overlay in light red is initial ^{1}H NMR spectrum of **2** in CH_2Cl_2.

Figure S9. ^{1}H NMR spectrum (CH_2Cl_2, 25 °C) of **3**

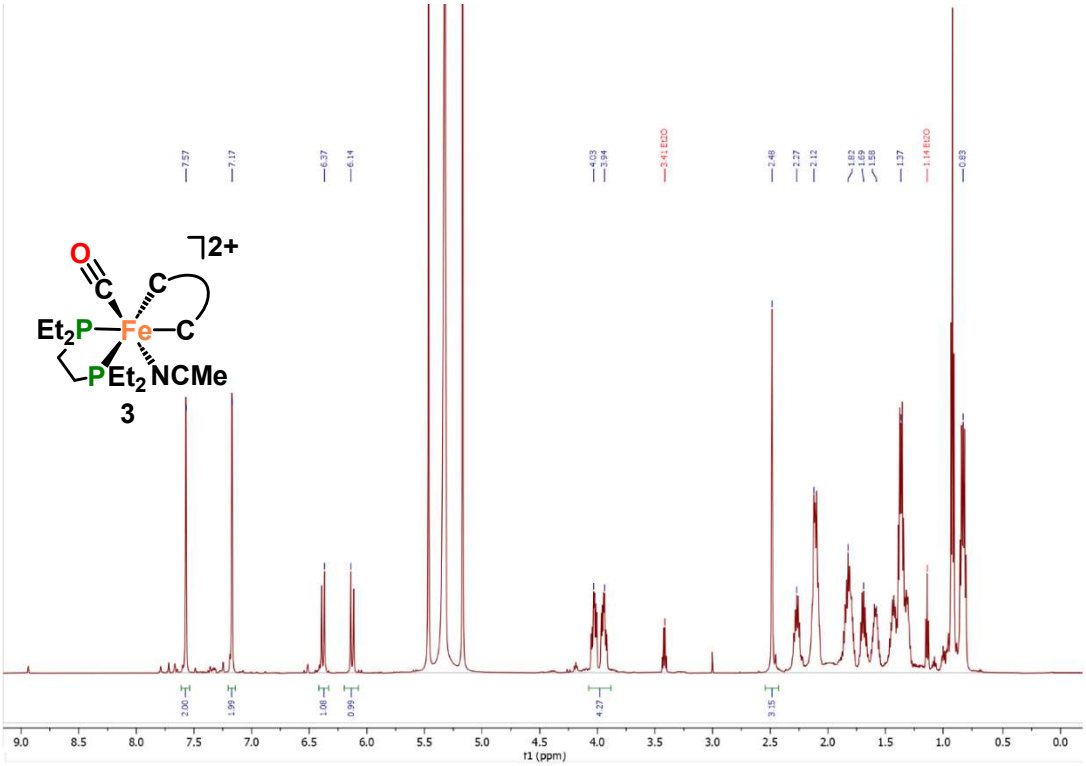

Figure S10. ^{31}P NMR spectrum (CH_2Cl_2, 25 °C) of **3**

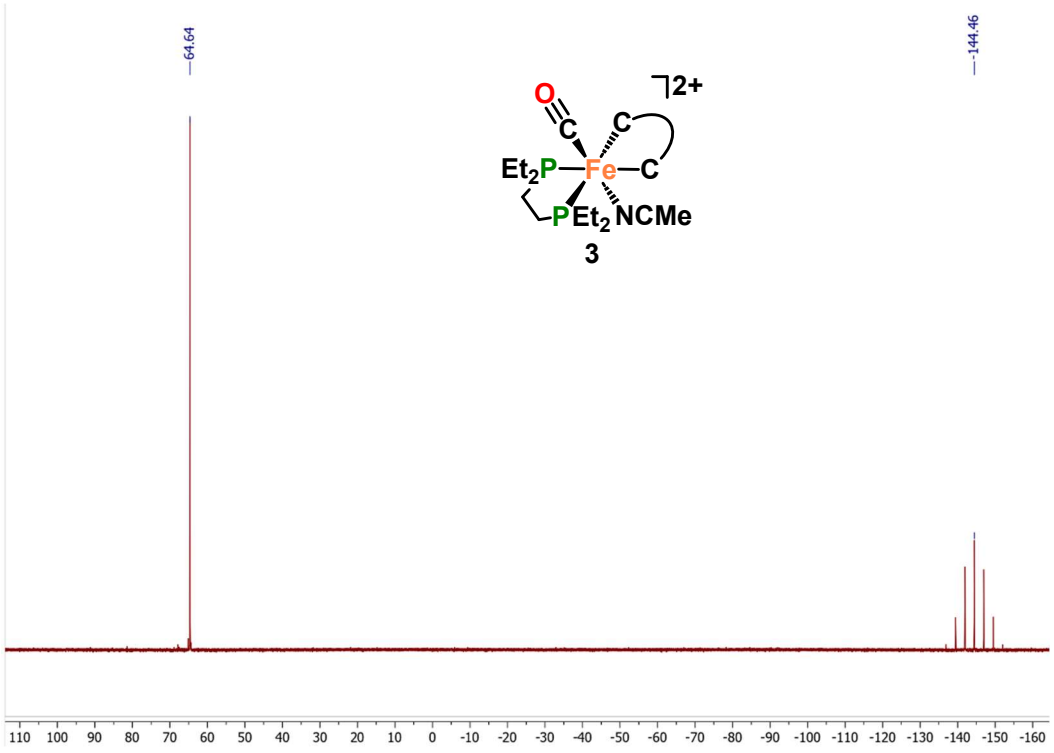

Figure S11. ^{13}C NMR spectrum (CH_2Cl_2, 25 °C) of **3**

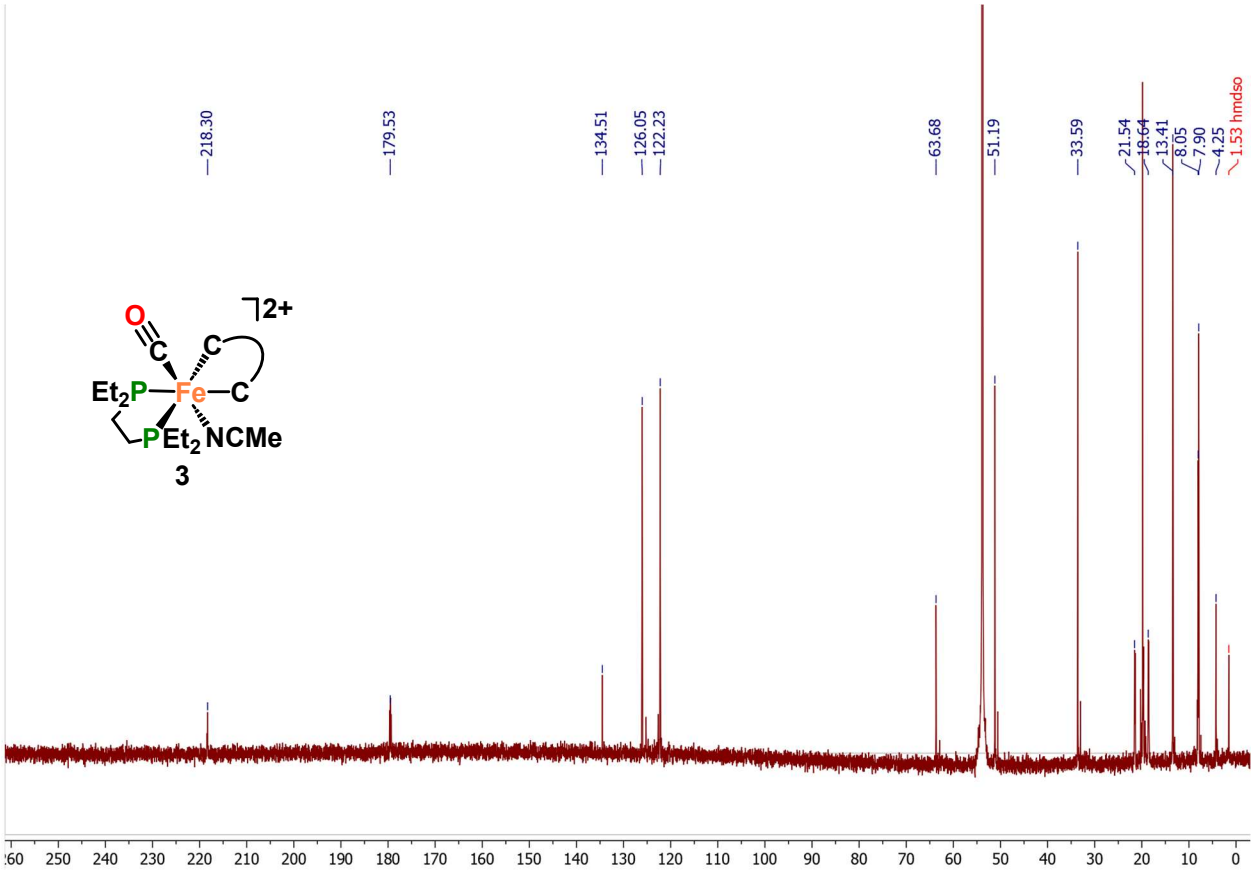

Figure S12. ^{1}H NMR spectrum (C_6D_6, 25 °C) of **4**

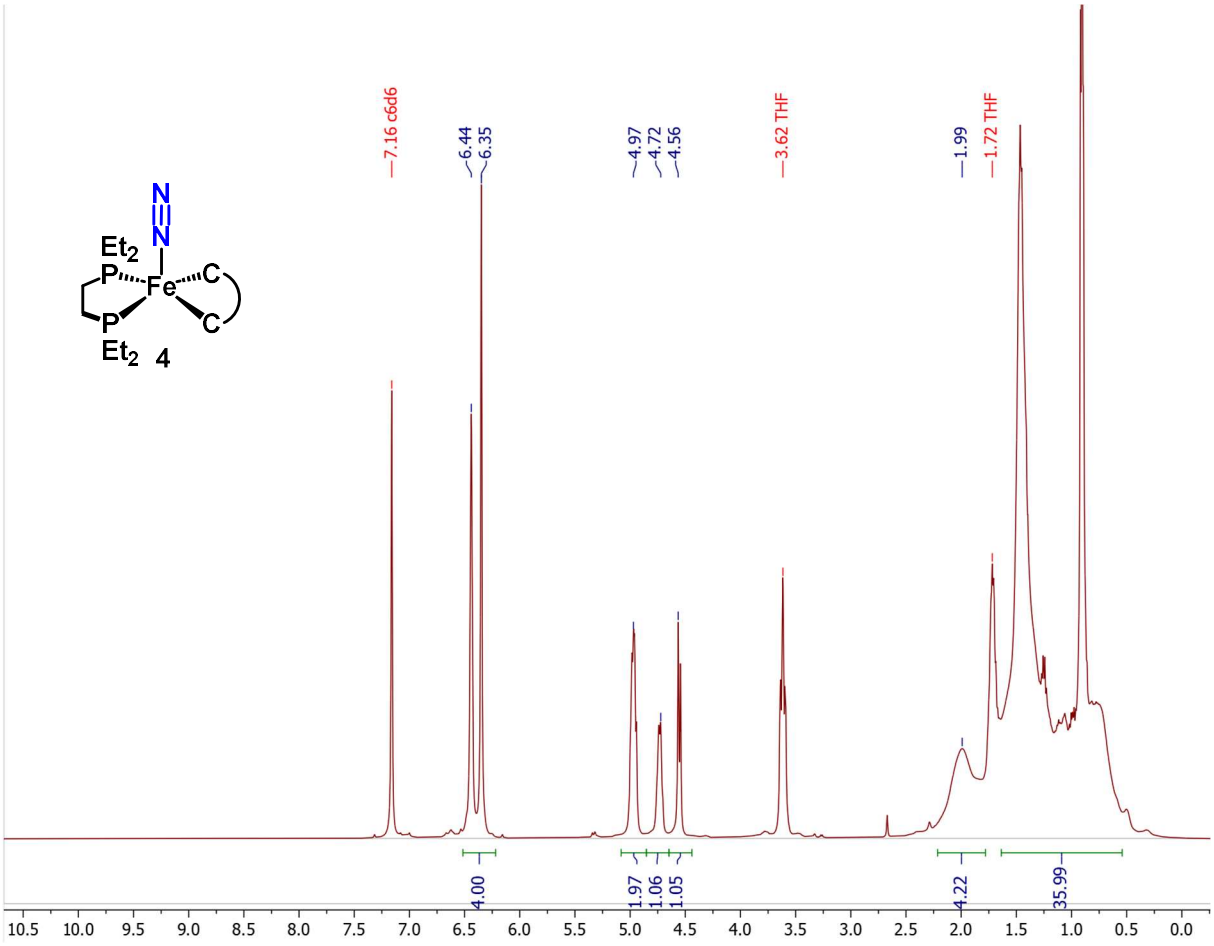

Figure S13. ^{31}P NMR spectrum (C_6D_6, 25 °C) of **4**

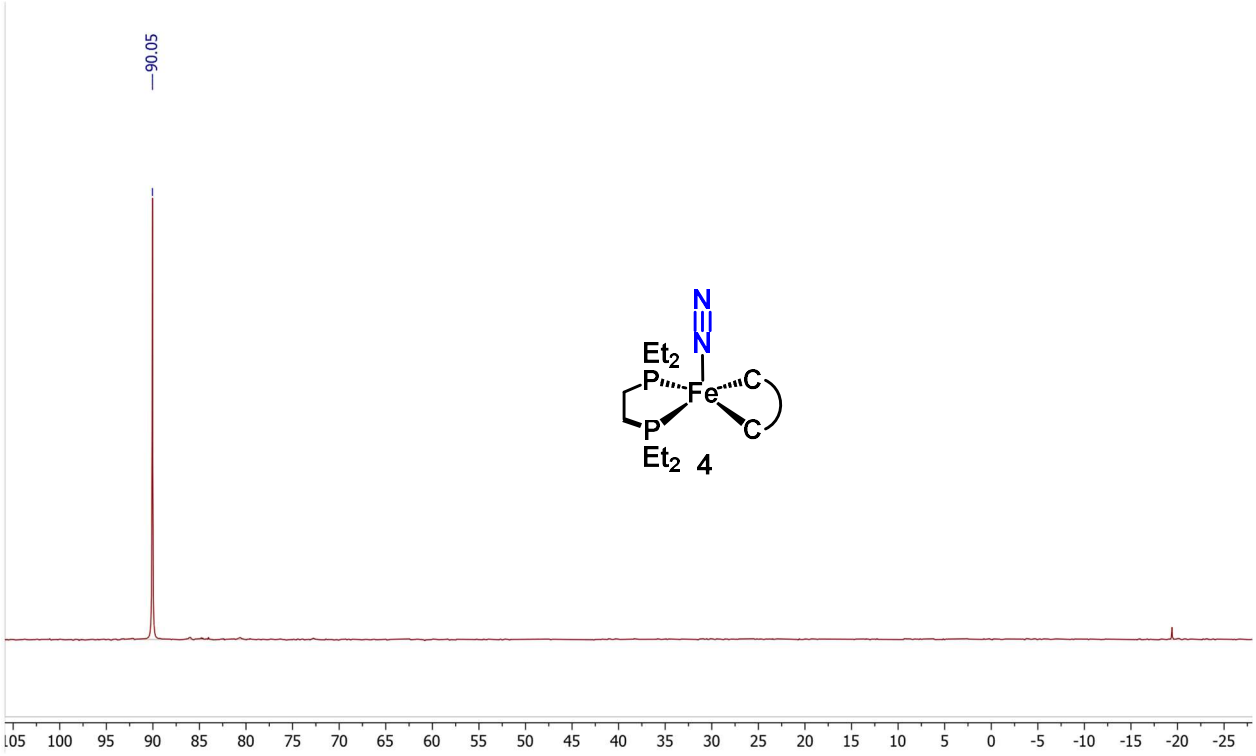

Figure S14. ^{13}C NMR spectrum (C_6D_6, 25 °C) of **4**

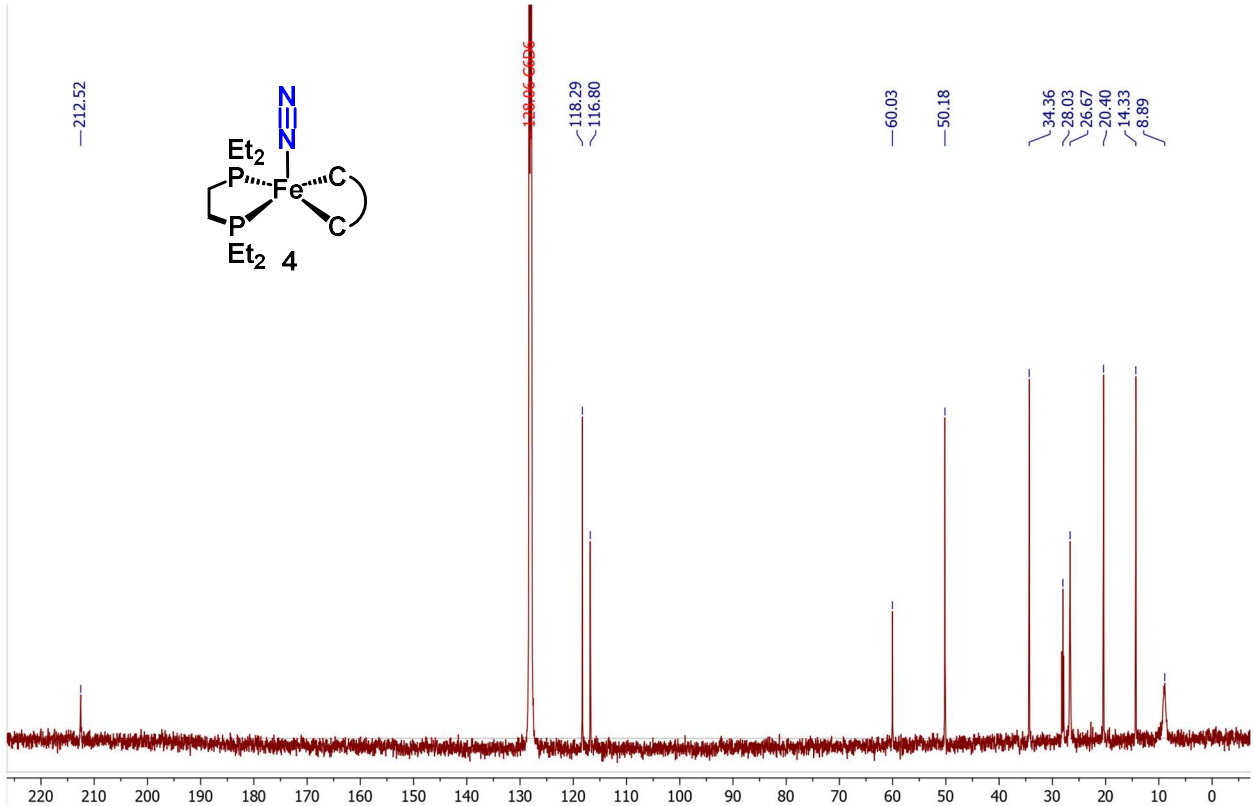

Figure S15. ^{1}H NMR spectrum (C_6D_6, 25 °C) of **5**

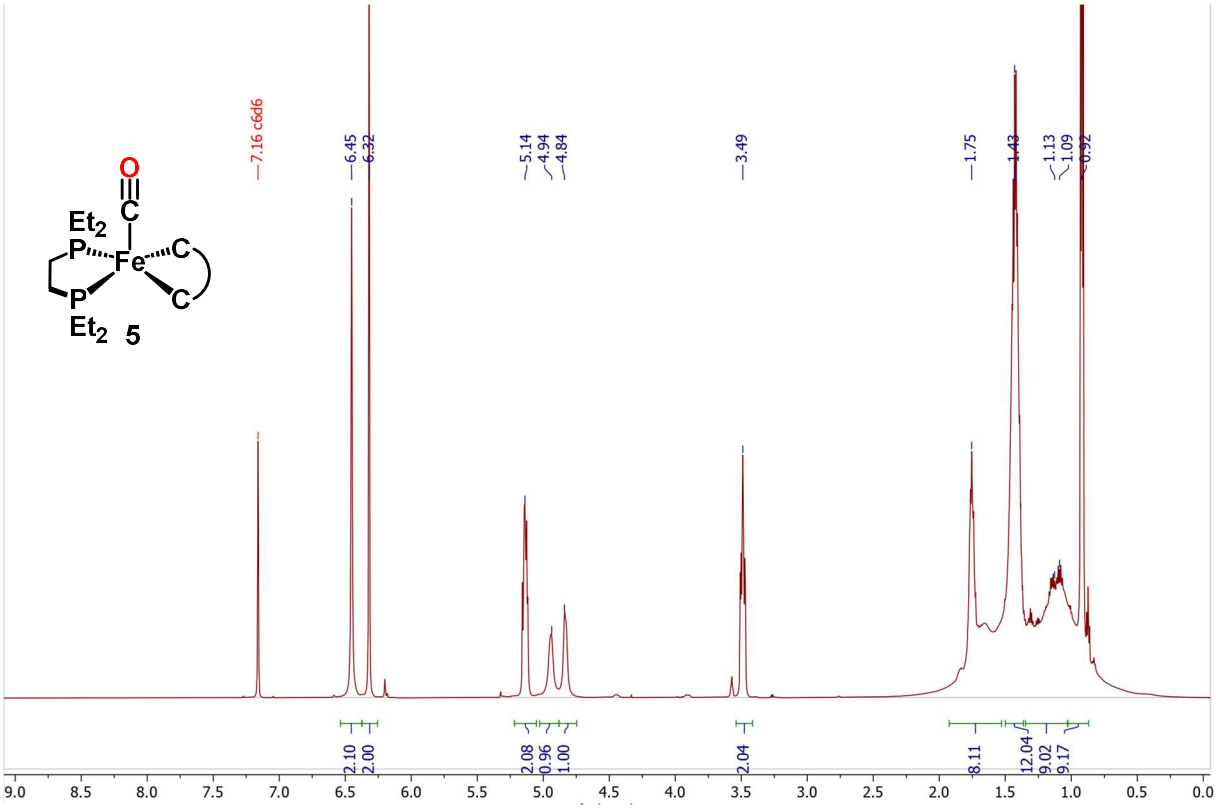

Figure S16. ^{31}P NMR spectrum (C_6D_6, 25 °C) of **5** Note: Features other than δ 95.85 are impurities

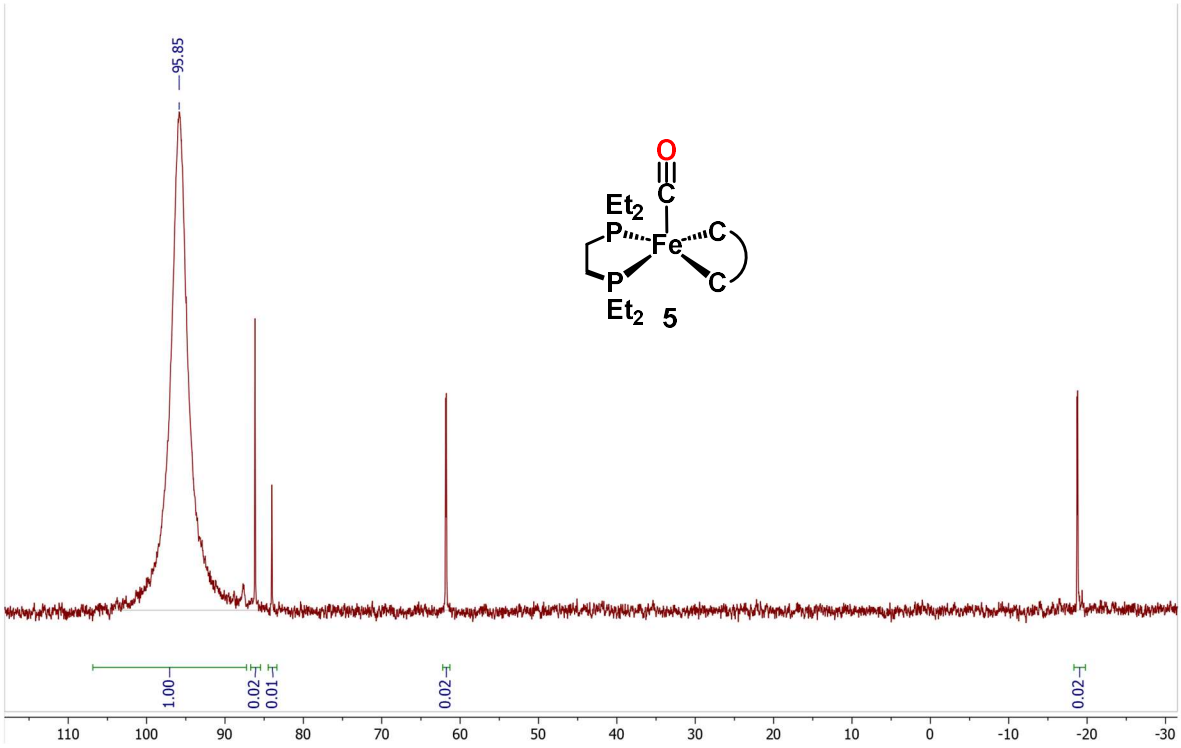

Figure S17. ^{13}C NMR spectrum (C_6D_6, 25 °C) of **5**

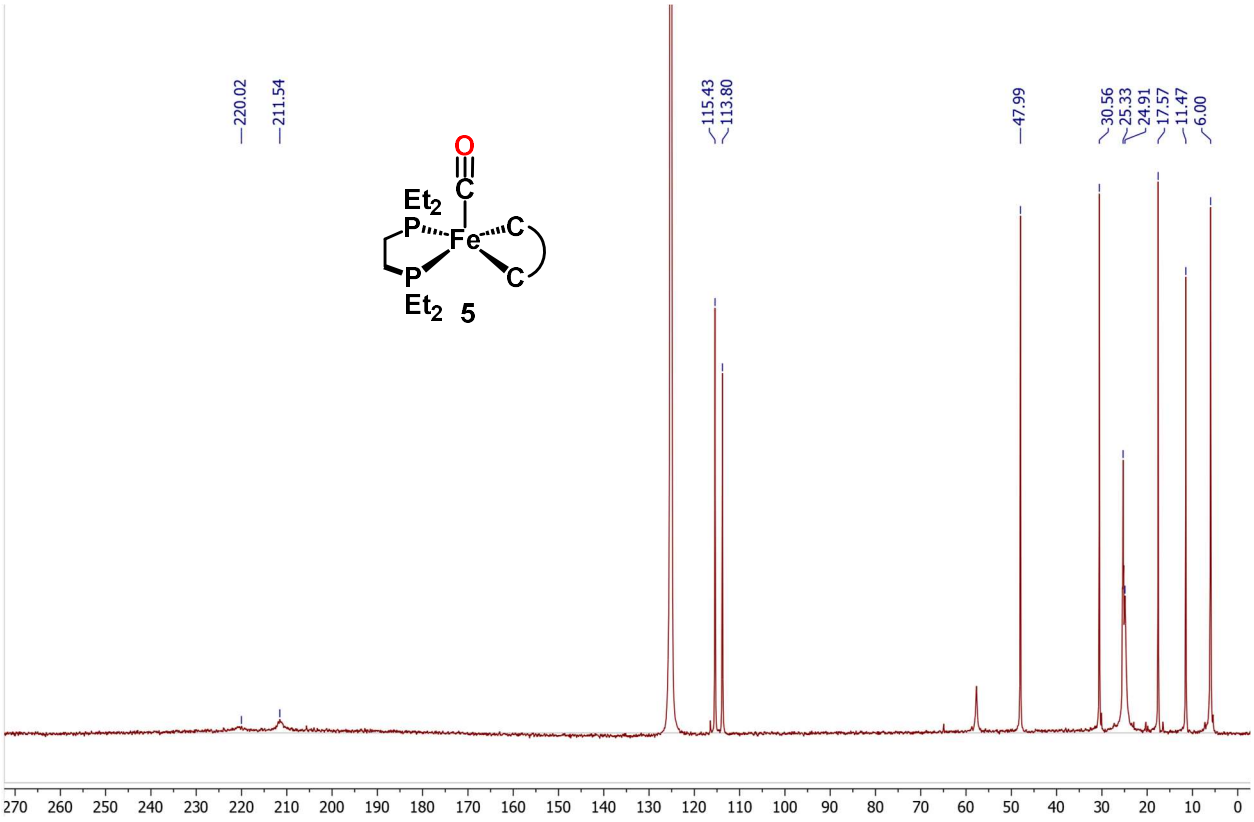

Figure S18. Variable temperature ^{1}H NMR spectrum (THF, 25 °C) of **4**

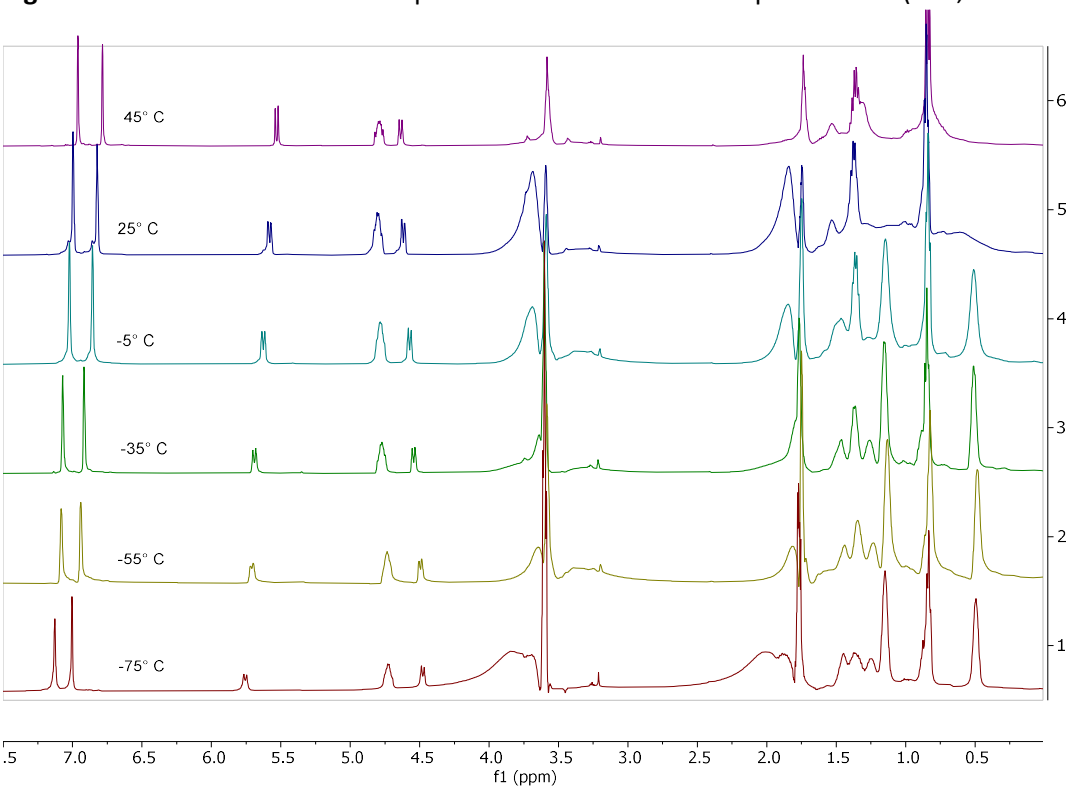

Figure S19. Variable temperature $^{31}P\{^{1}H\}$ NMR spectrum (THF, 25 °C) of **4**

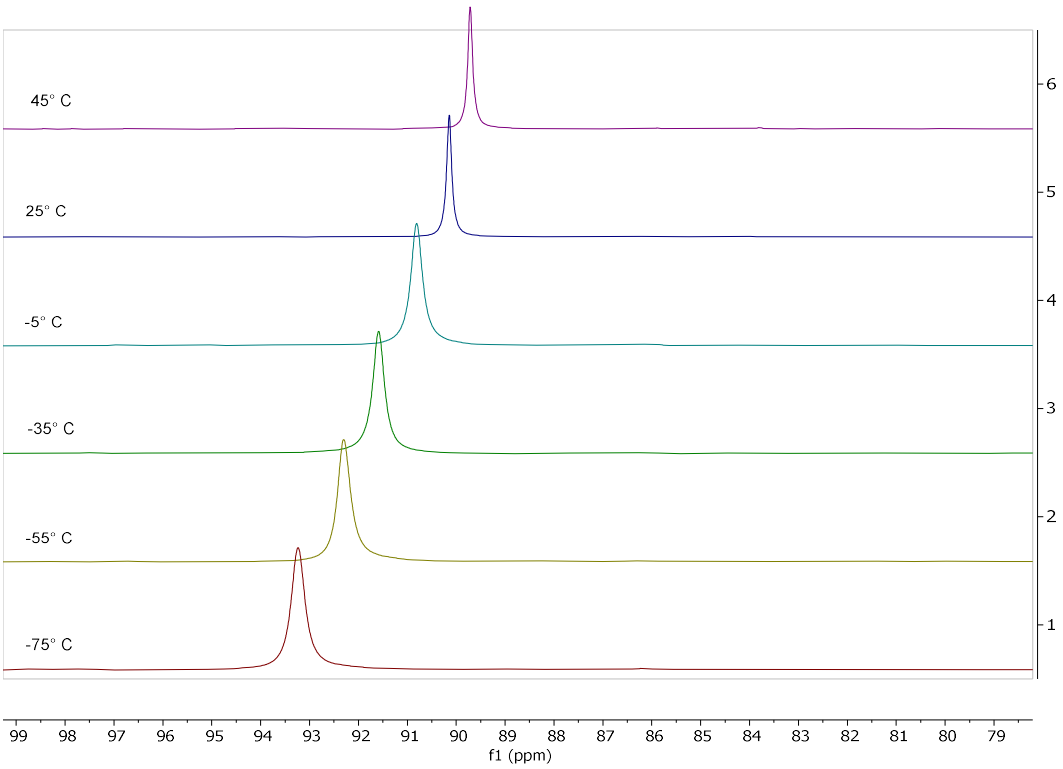

Figure S20. Variable temperature ^{1}H NMR spectrum (THF, 25 °C) of **5**

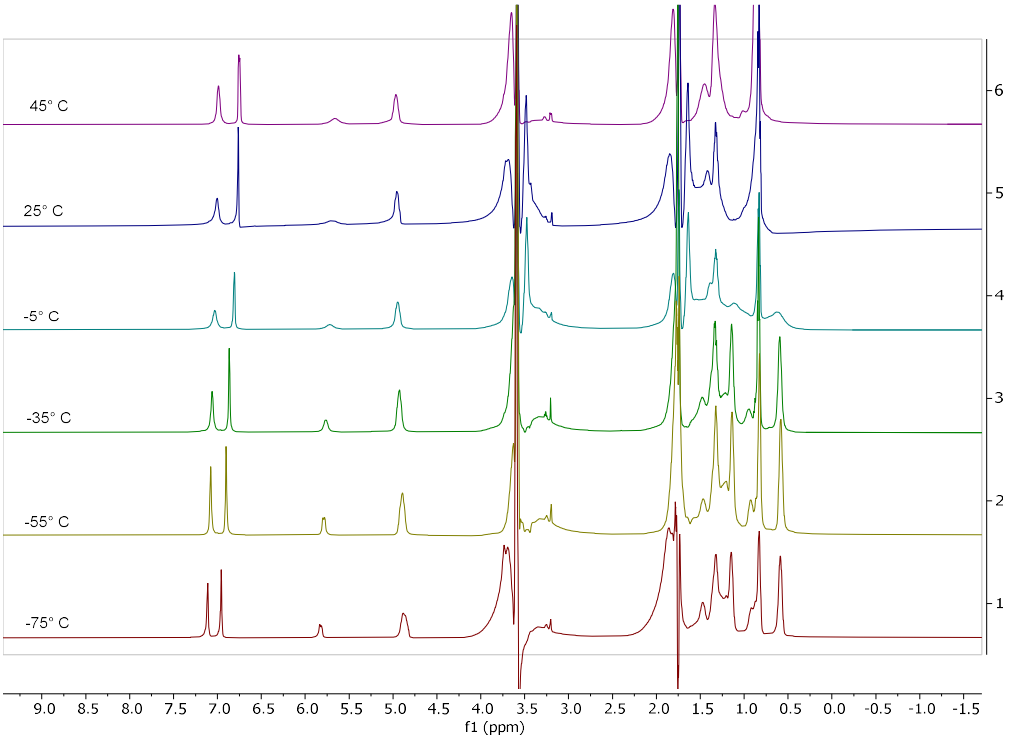

Figure S21. Variable temperature $^{31}P\{^{1}H\}$ NMR spectrum (THF, 25 °C) of **5**

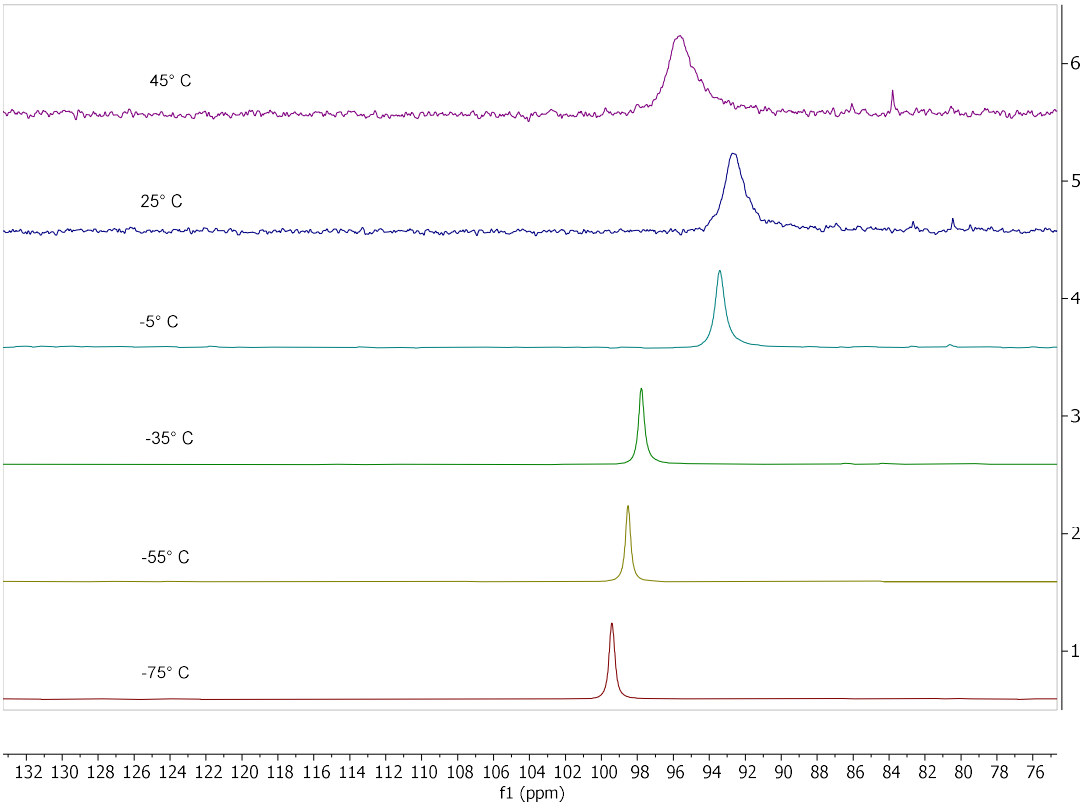

Figure S22. ^{1}H NMR spectrum (THF, 25 °C) of [**6**]OTf from reaction of **4** with $[NH_2Ph_2]OTf$

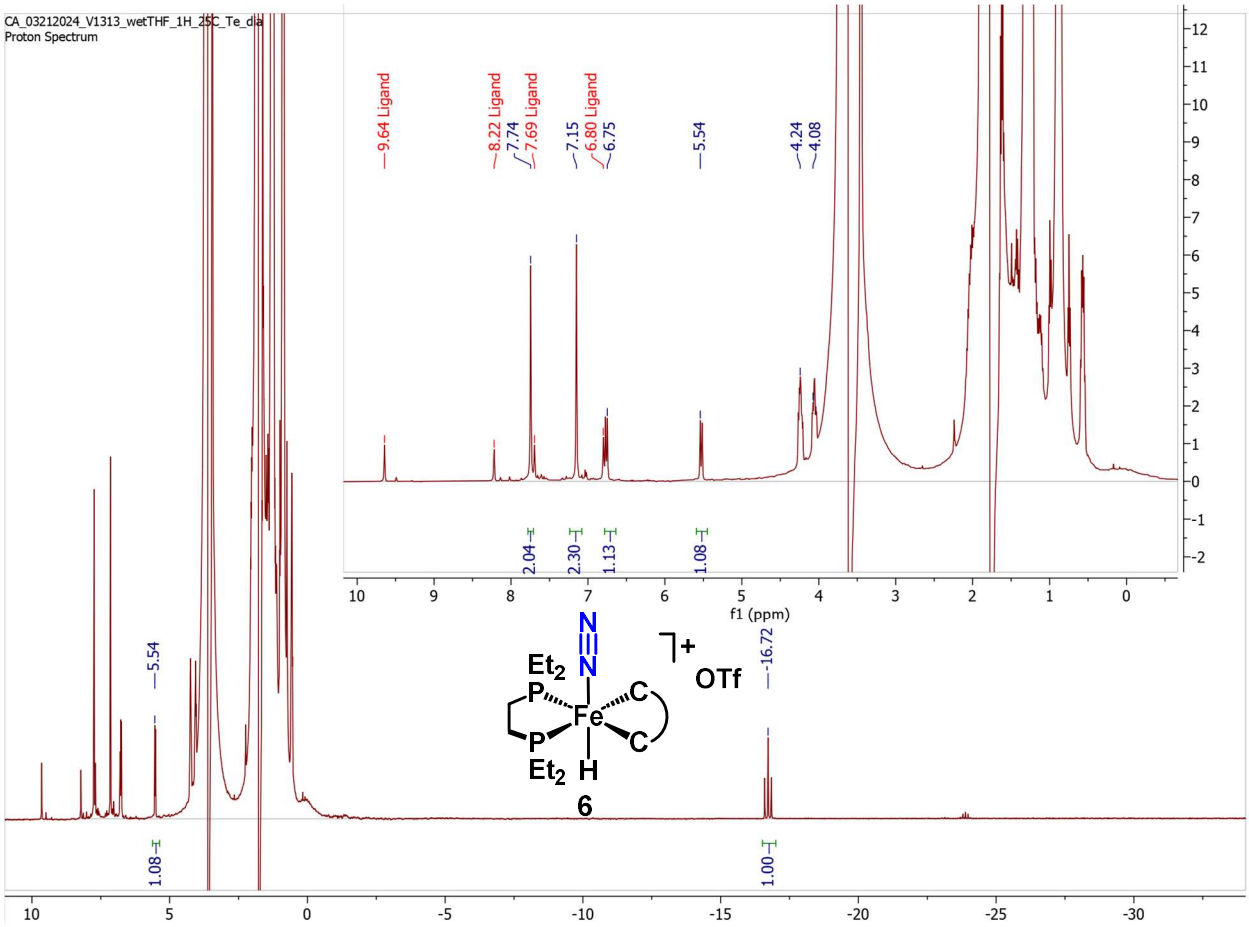

Note: Protonated bis-NHC ligand (**1**[OTf] marked Ligand) is a significant impurity that could not be separated by solubility

Figure S23. ^{13}C NMR spectrum (THF, 25° C) of [**6**]OTf from reaction of **4** with $[NH_2Ph_2]OTf$

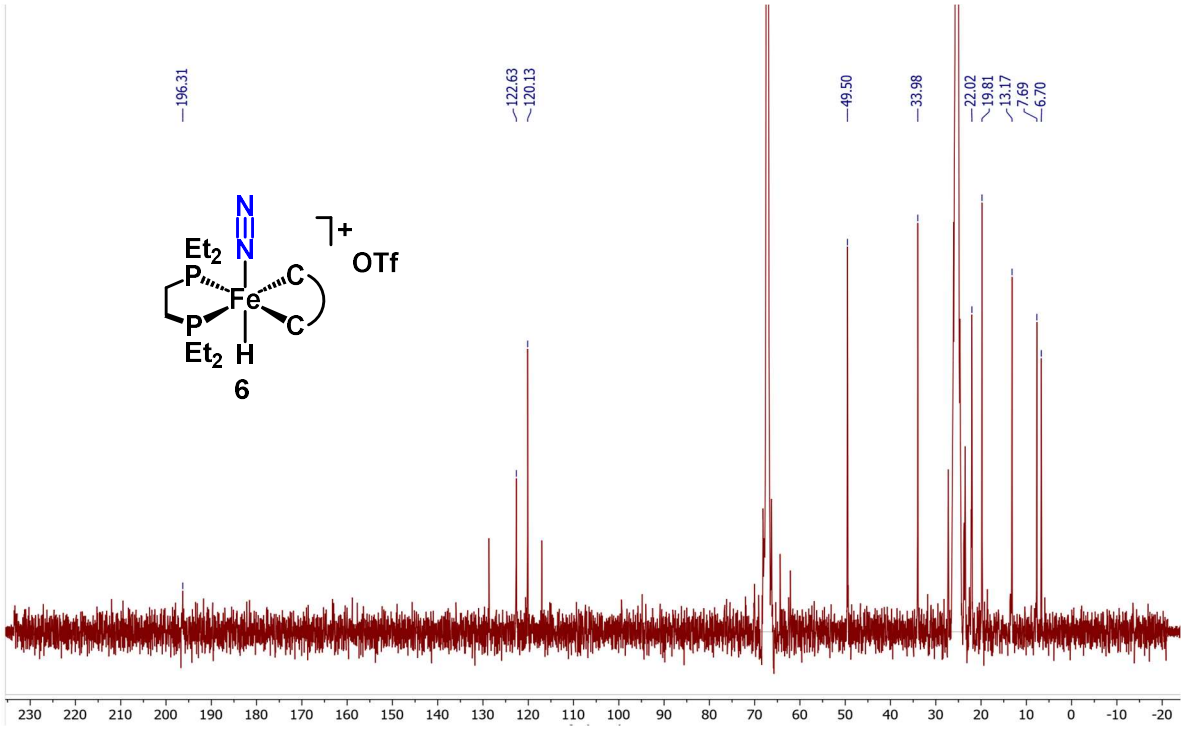

Figure S24. ^{31}P NMR spectrum (THF, 25° C) of [**6**]OTf from reaction of **4** with $[NH_2Ph_2]OTf$

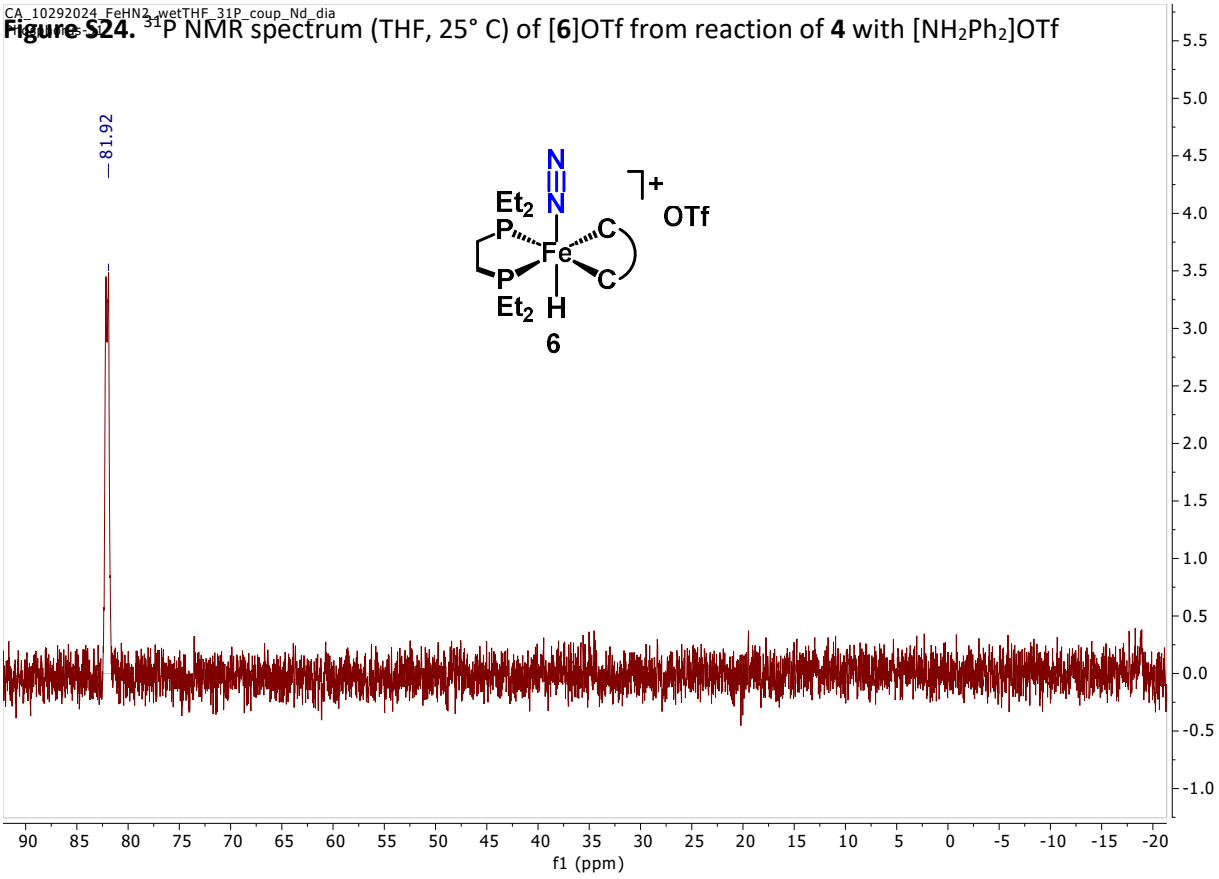

Figure S25. ^{1}H NMR spectrum (THF, 25°C) of [FeH(N_2)(depe)$_2$][OTf] from protonation of FeN_2(depe)$_2$

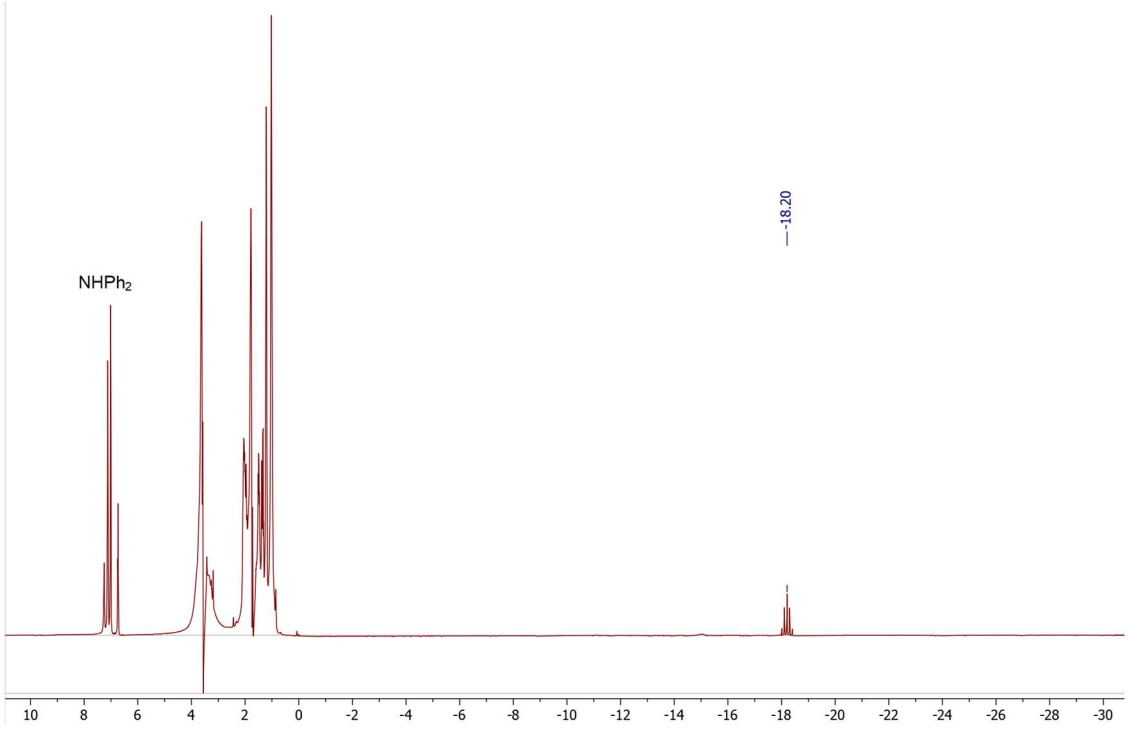

Figure S26. ^{31}P NMR spectrum (THF, 25°C) of crude [FeH(N_2)(depe)$_2$][OTf] from protonation of FeN_2(depe)$_2$

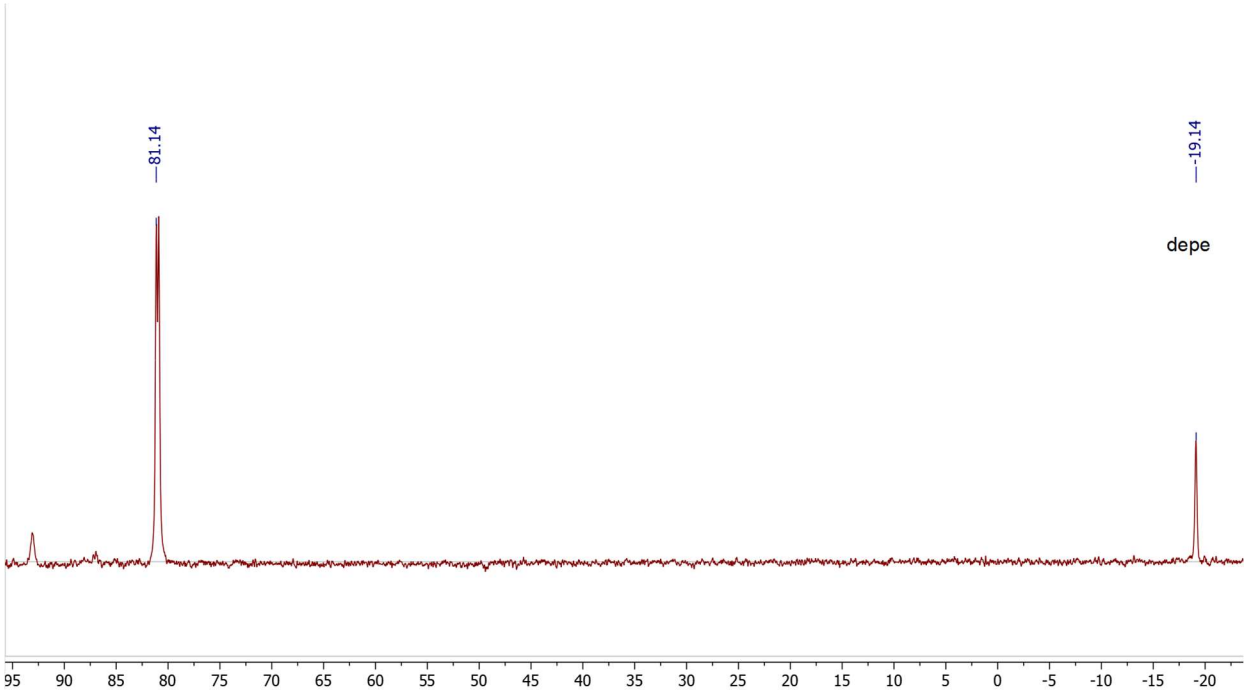

Figure 27. ^{1}H NMR spectrum (THF, 25°C) of **7**

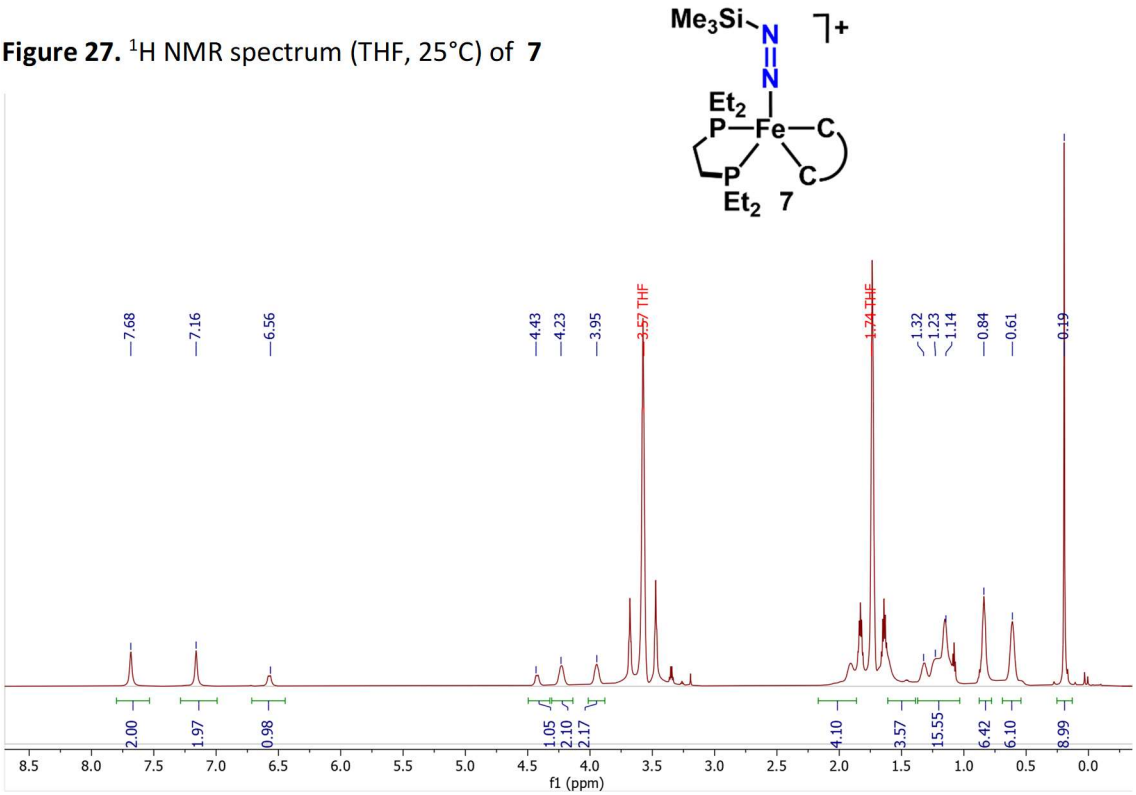

Figure 28. ^{31}P NMR spectrum (THF, 25°C) of **7**

Note: Miniscule impurity of the Fe hydride **6** is visible in this spectrum.

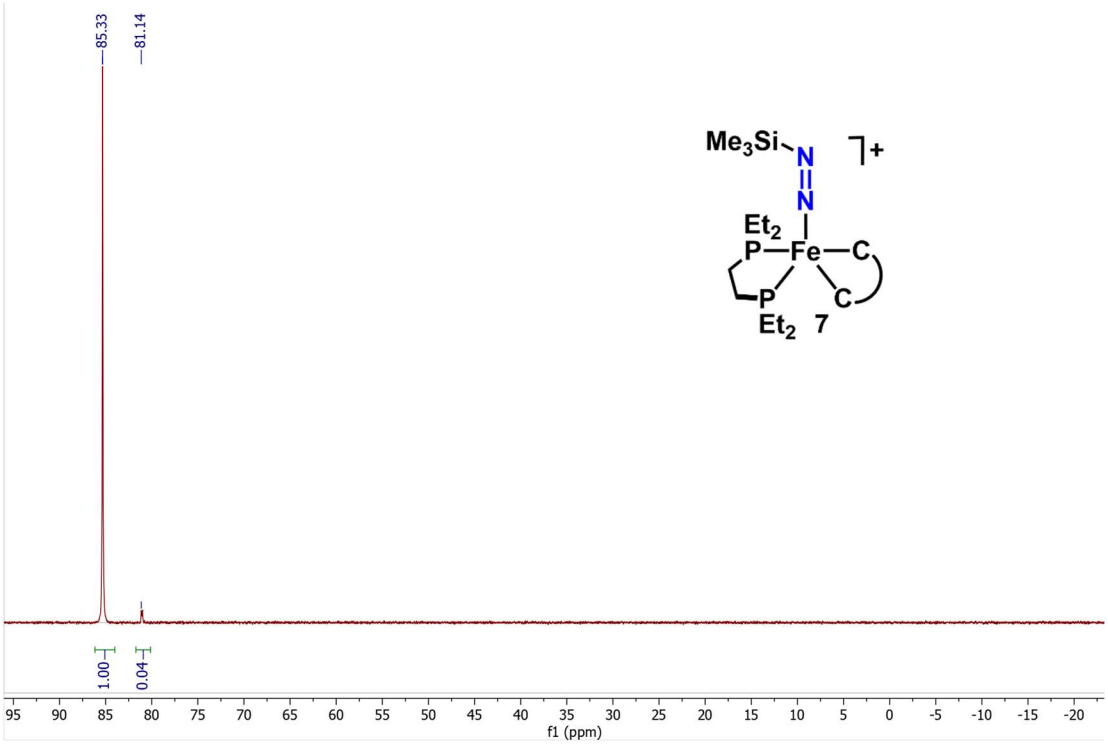

Figure 29. ^{13}C NMR spectrum (THF, 25°C) of **7**

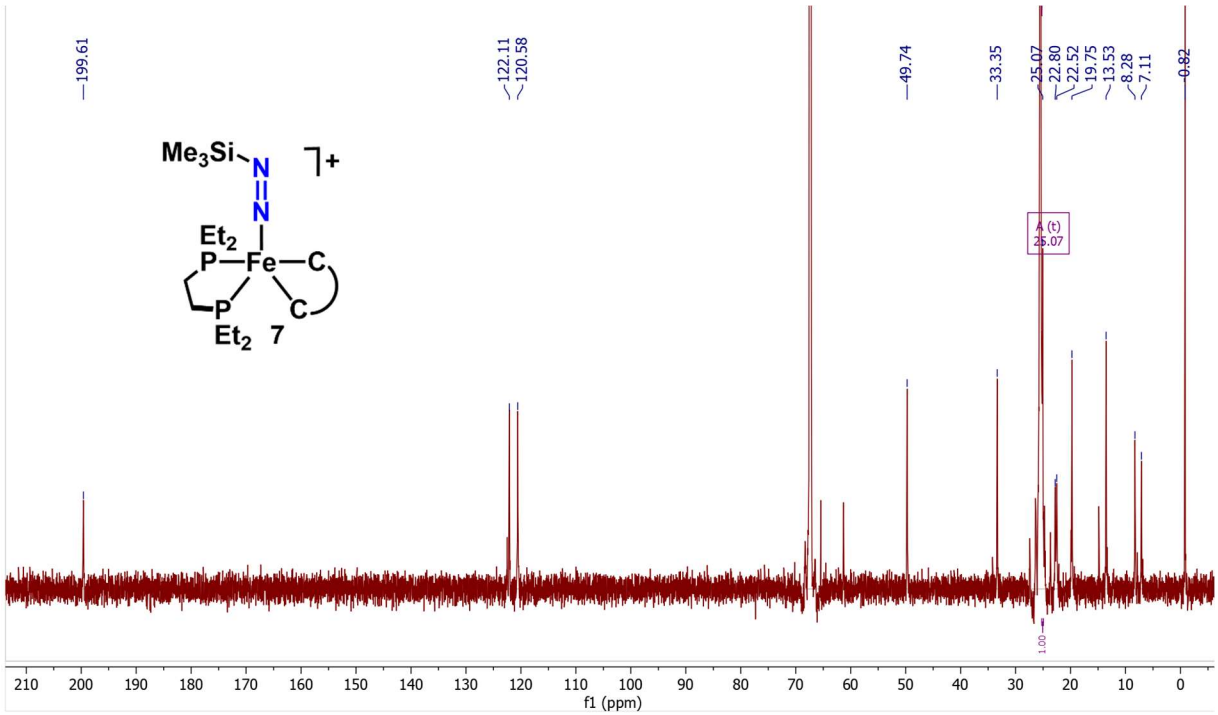

Figure 30. ^{19}F NMR spectrum (THF, 25°C) of **7**

Consistent with free triflate counterion

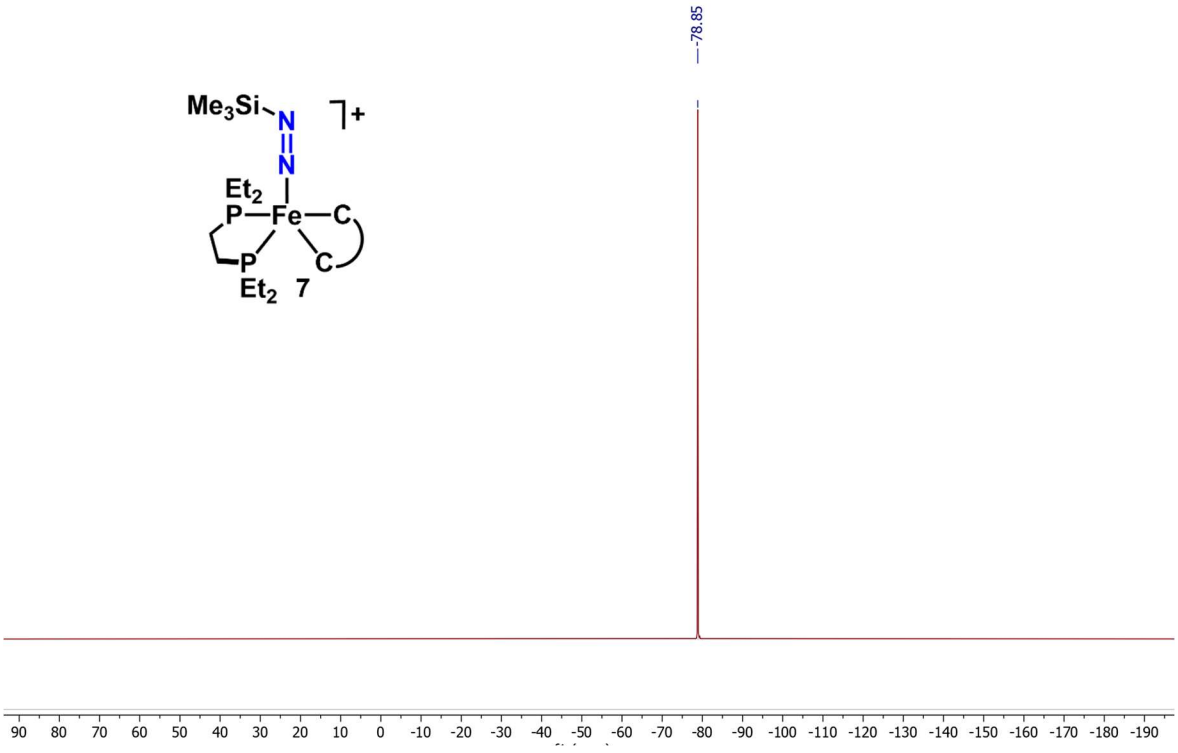

Figure S31. ^{29}Si NMR spectrum of **7**

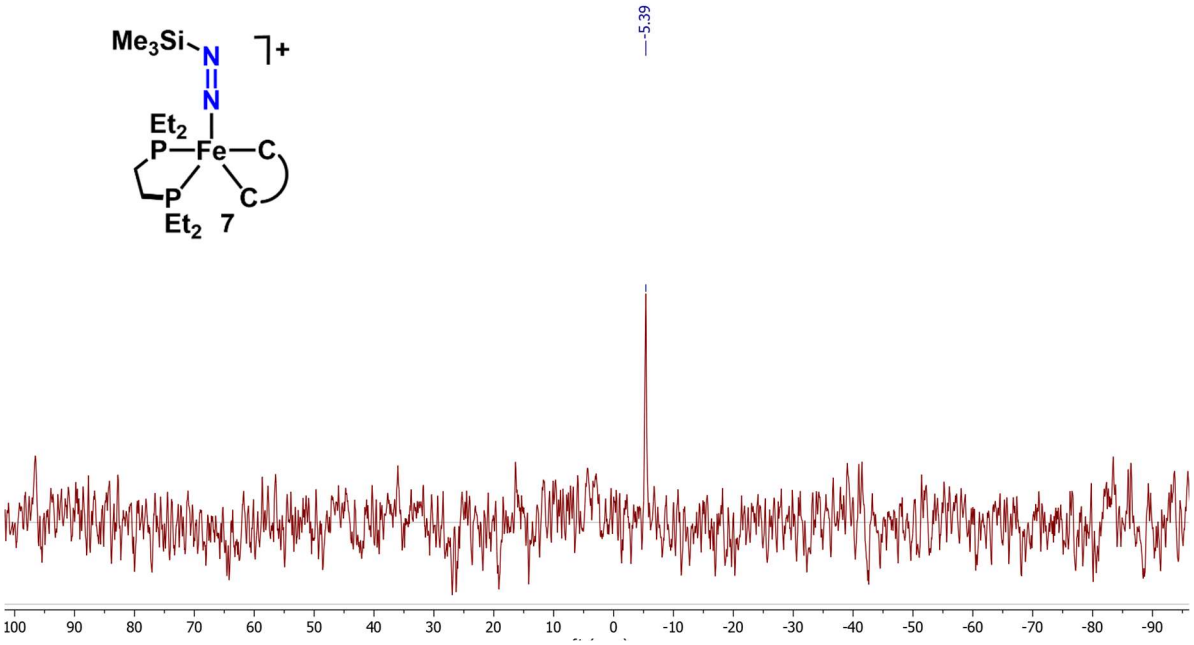

Figure S32. Quantitative NMR of **2** referenced to HMDSO (0.07 ppm)

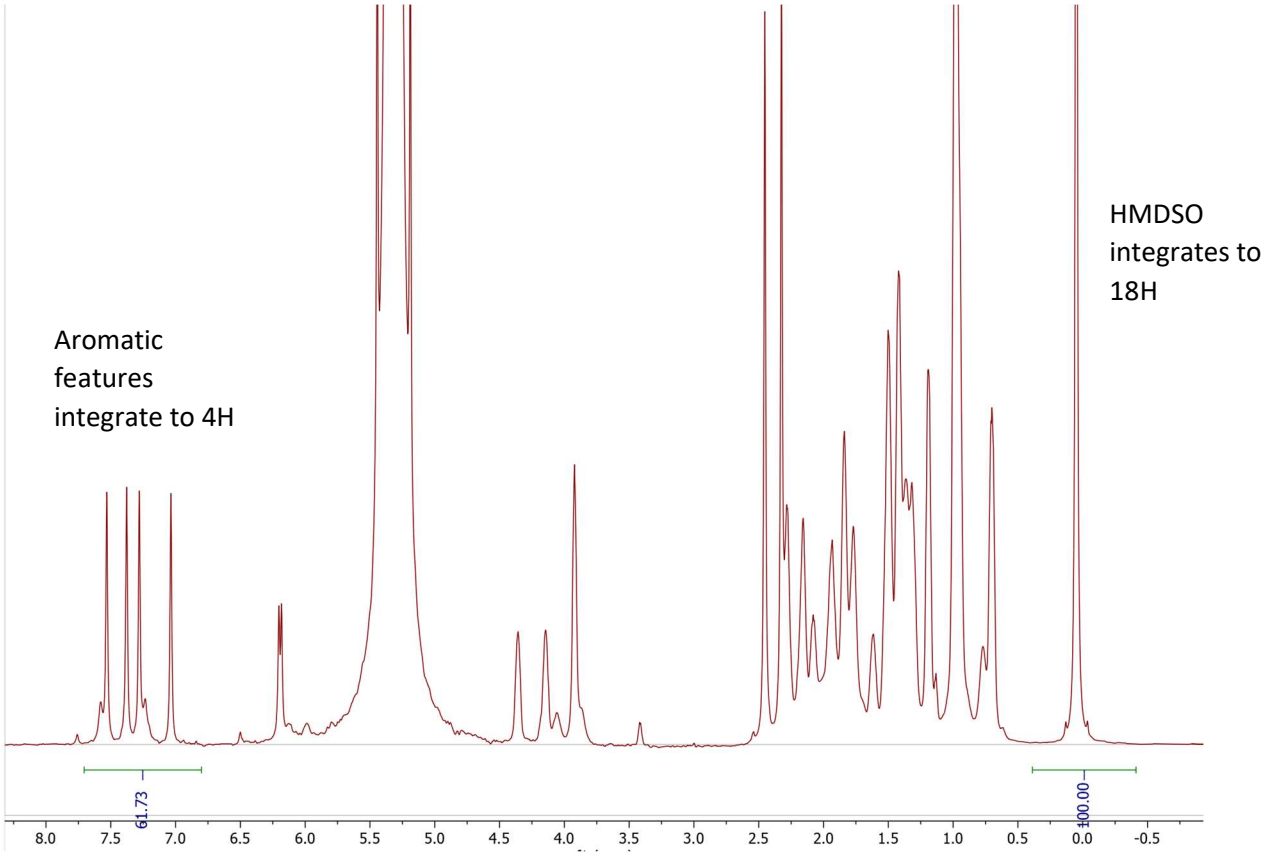

Figure S33. Quantitative NMR of **3** referenced to HMDSO (0.07 ppm)

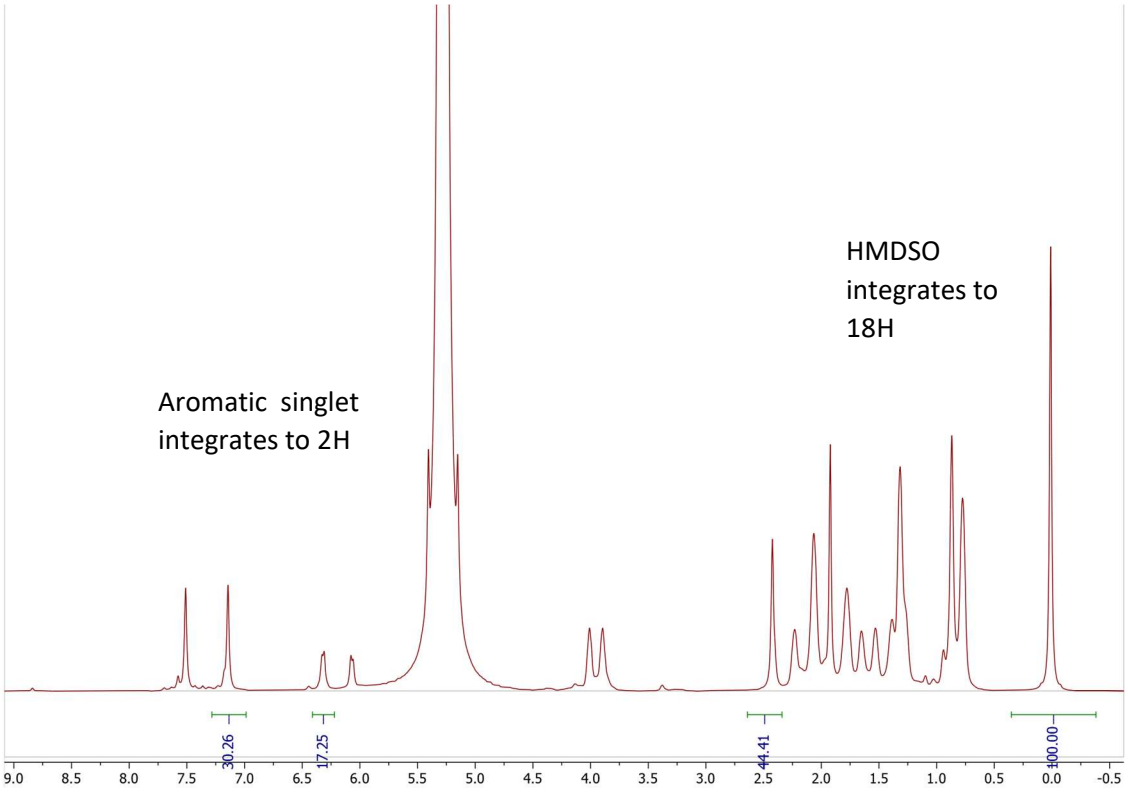

Figure S34. Quantitative NMR of **4** referenced to naphthalene (7.56 ppm)

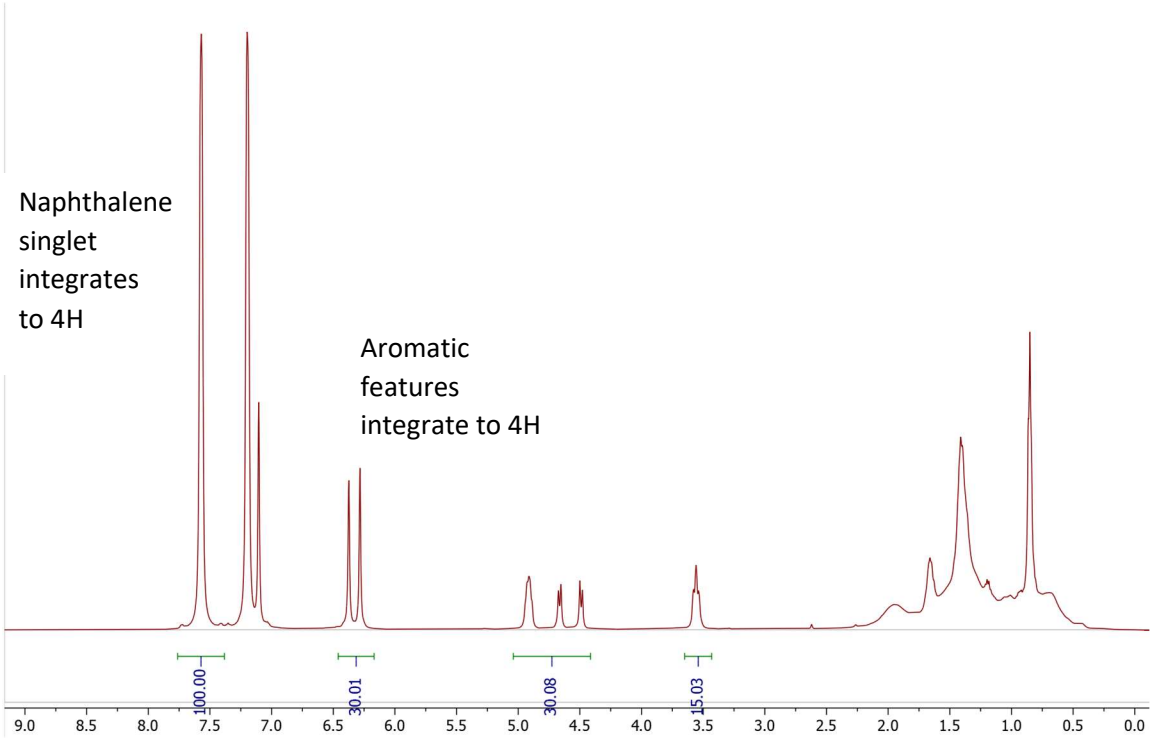

Figure S35. Quantitative NMR of **5** referenced to naphthalene (7.56 ppm)

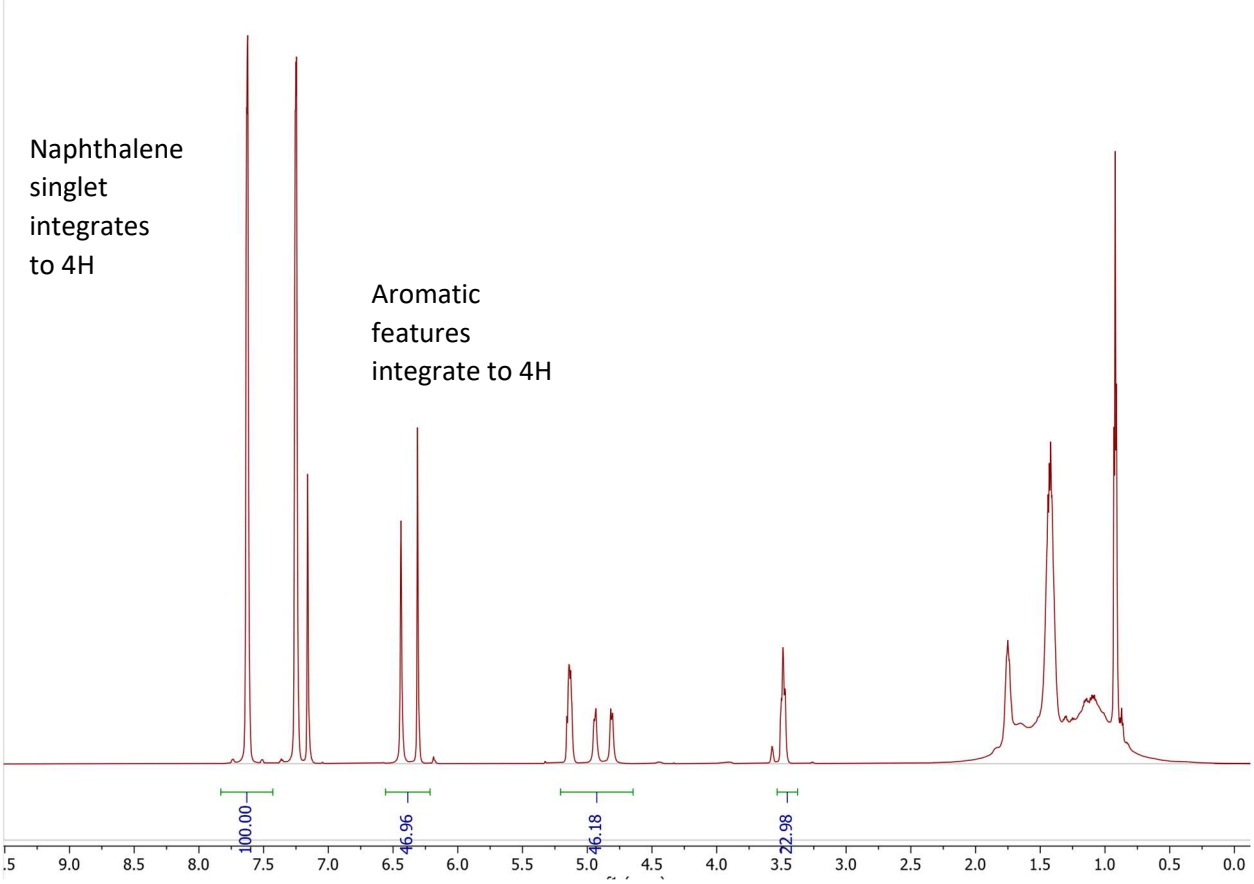

Figure S36. Infrared spectrum (KBr) of **2**.

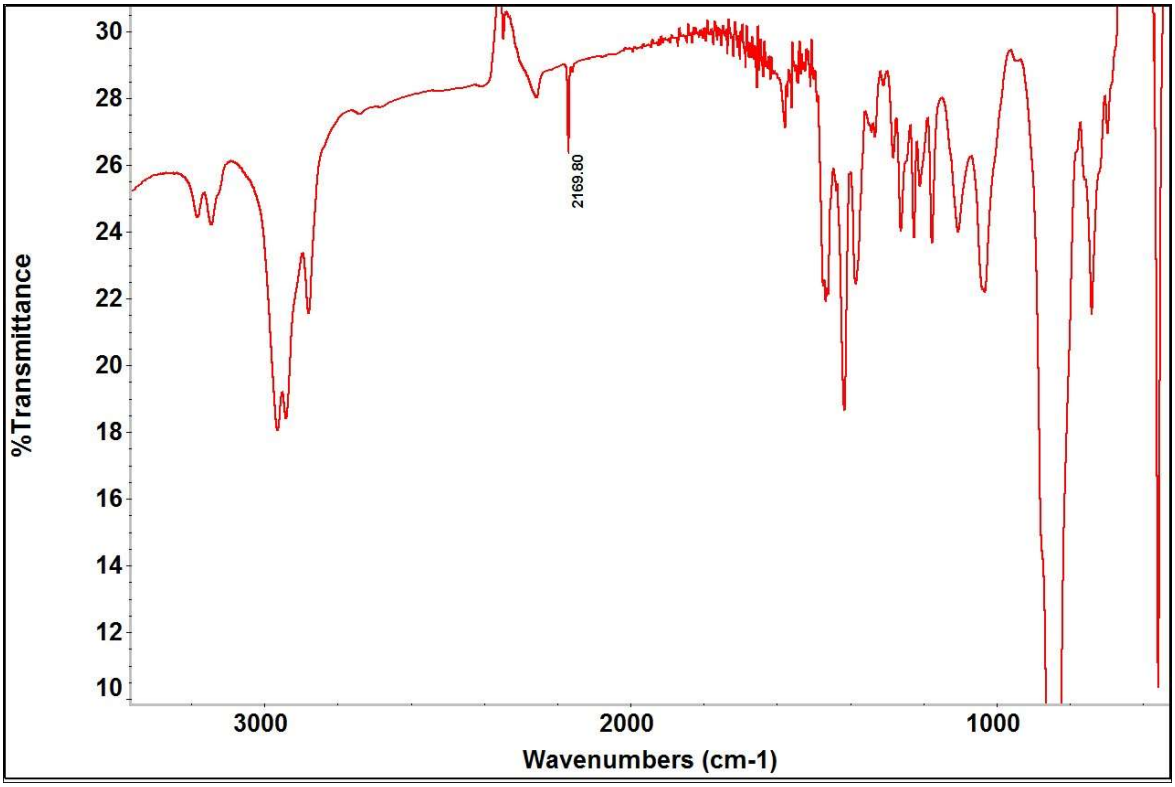

Figure S37. Infrared spectrum (KBr) of **3**.

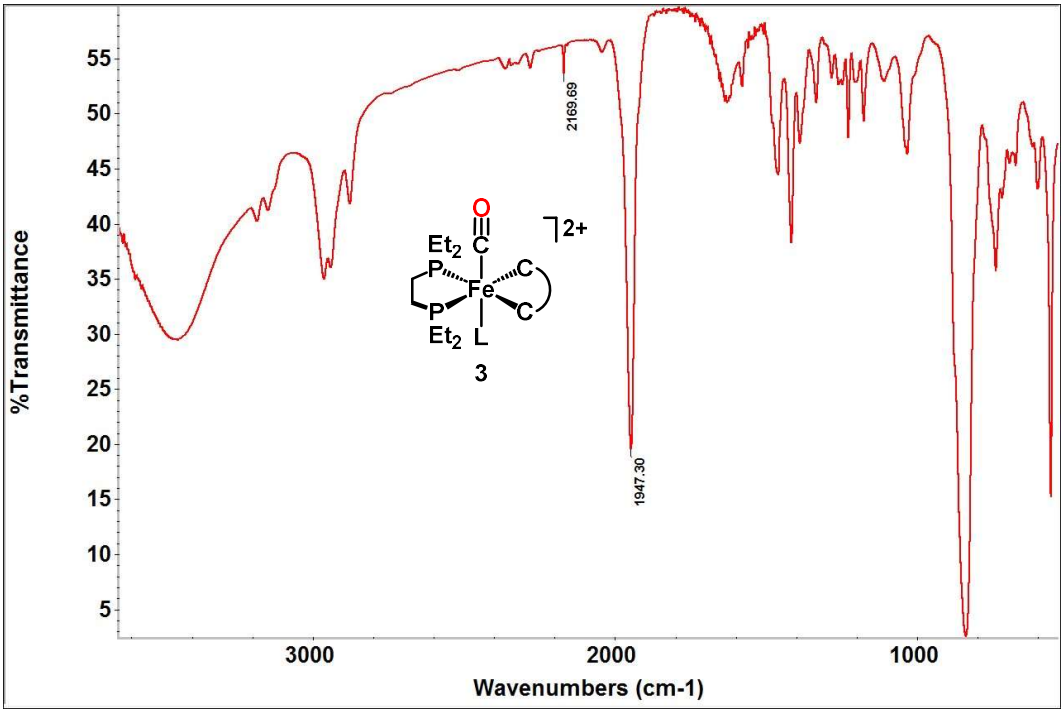

Figure S38. Infrared spectrum (Pentane solution) of **4**.

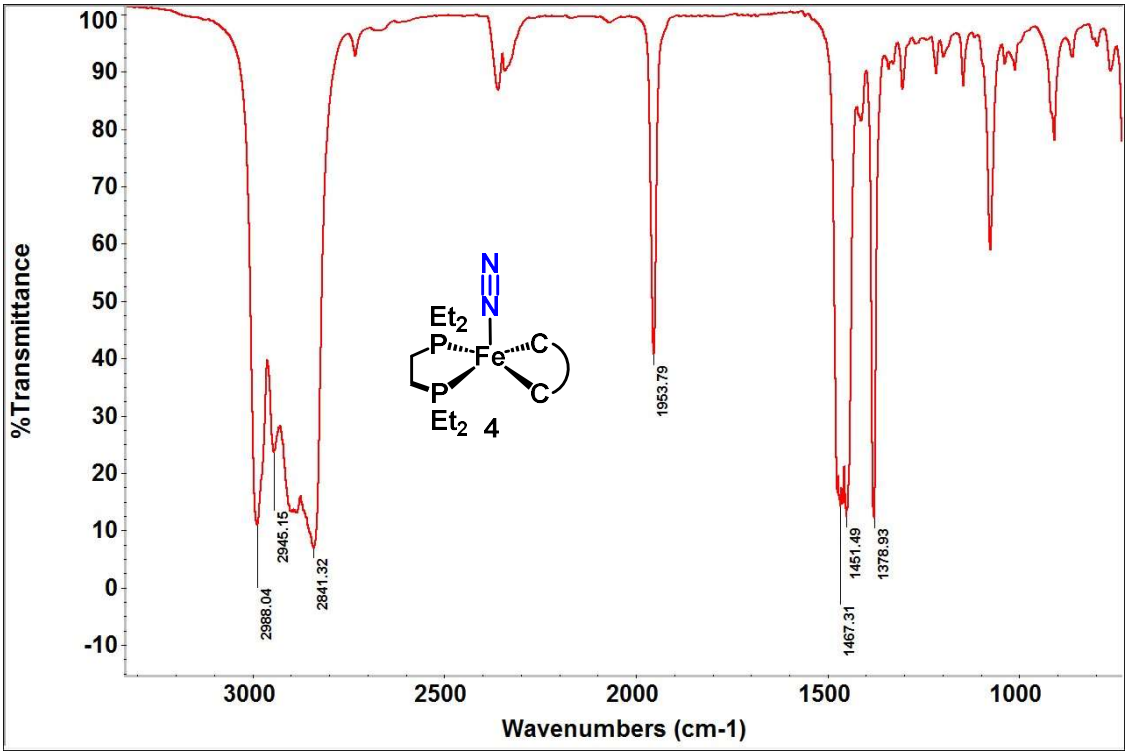

Figure S39. Infrared spectrum (ATR) of **4**. This spectrum was collected in an inert atmosphere glove box.

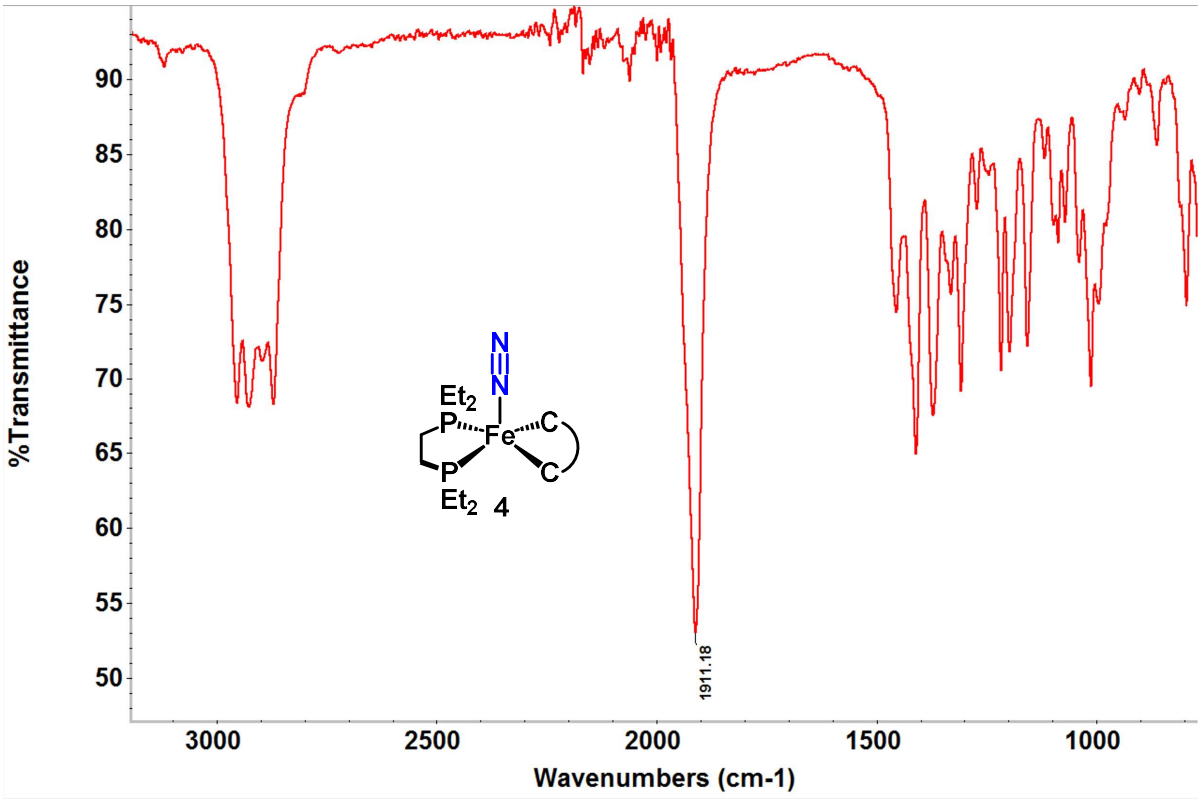

Figure S40. Infrared spectrum (KR) of **4.**

Note: Scans collected continuously over 5 minutes that reflects rapid decomposition of **4** into **6** in the presence of air.

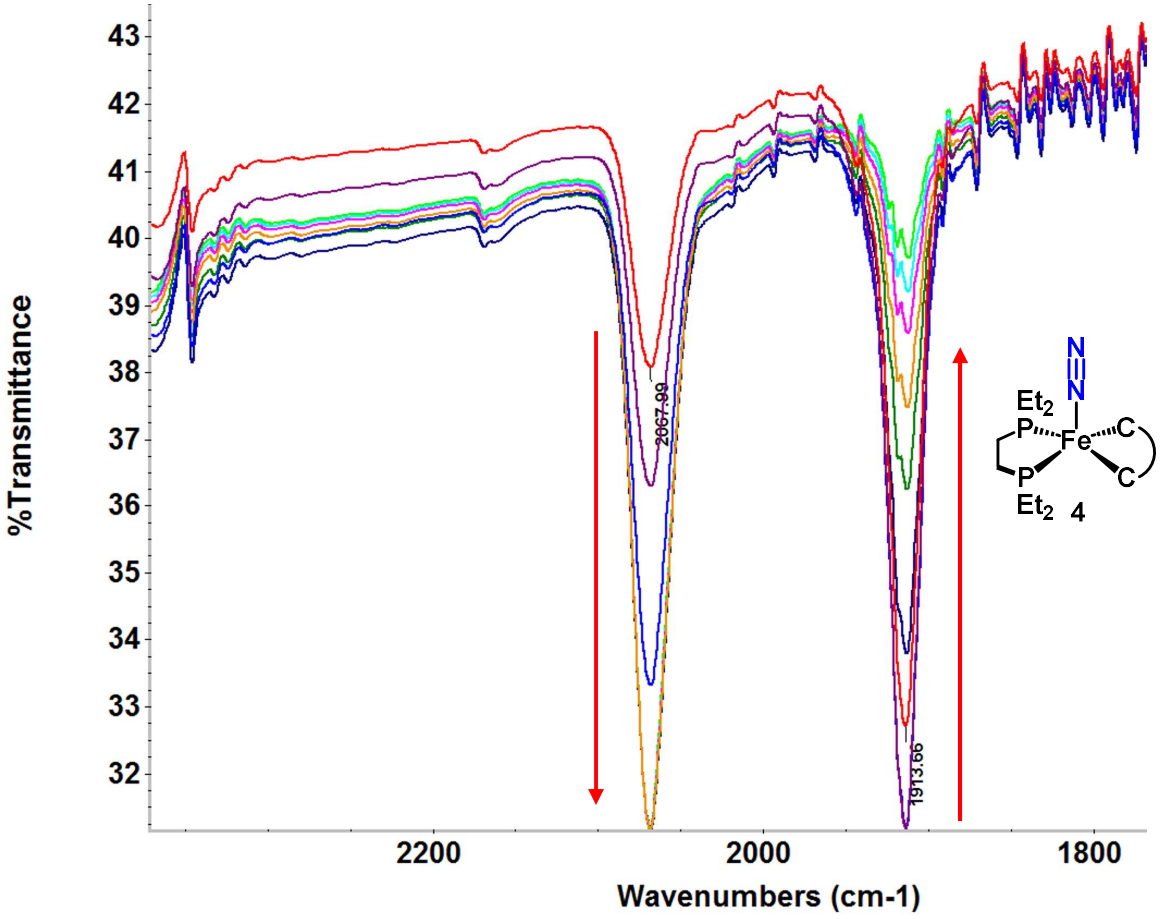

Figure S41. Infrared spectrum (KBr) of **5**.

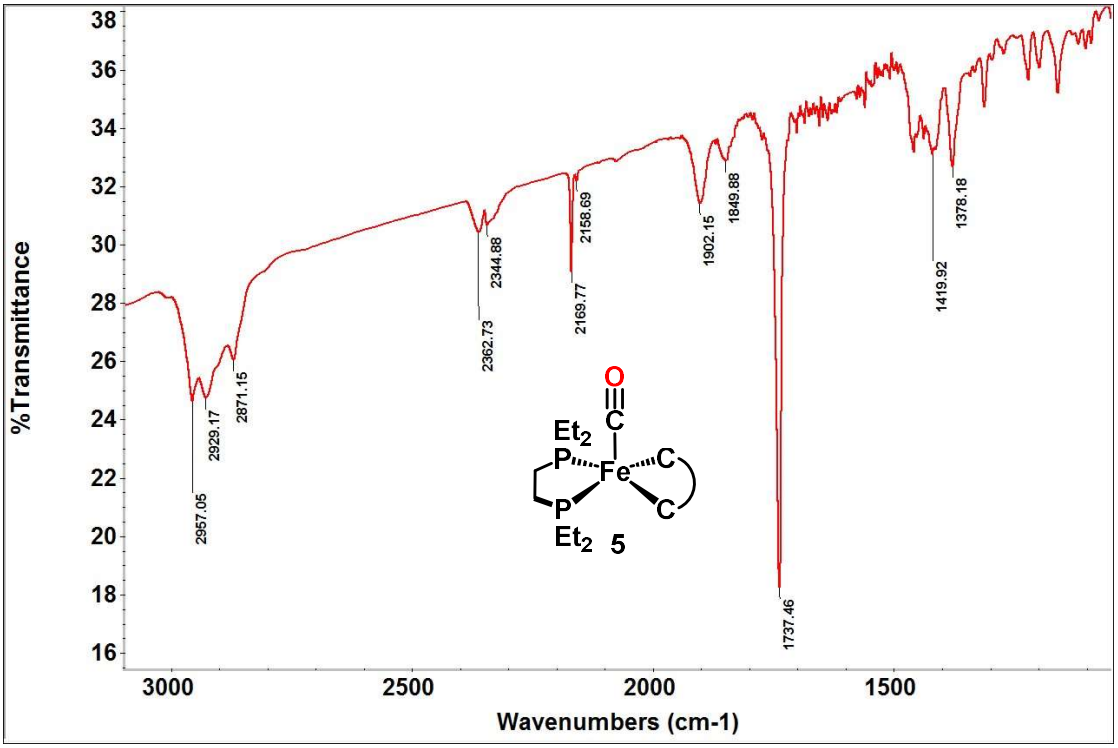

Figure S42. Infrared spectrum (Pentane solution) of **5**.

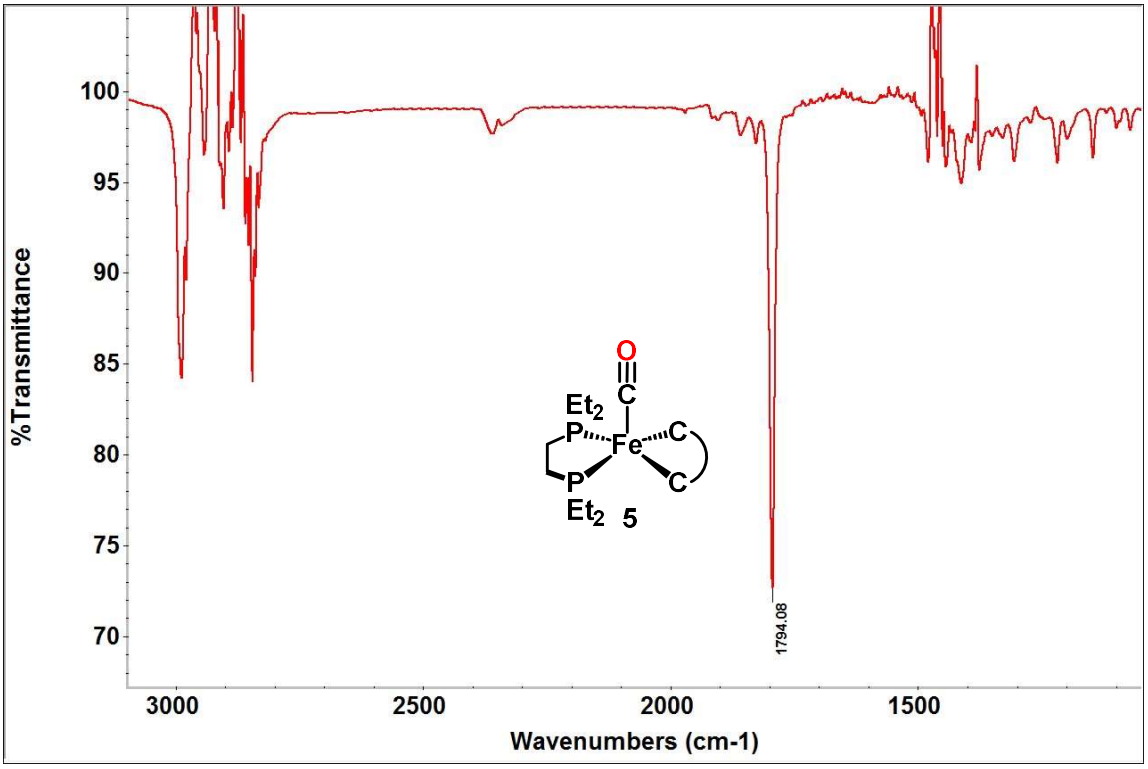

Figure S43. Infrared Spectrum (THF solution) of **6**[OTf].

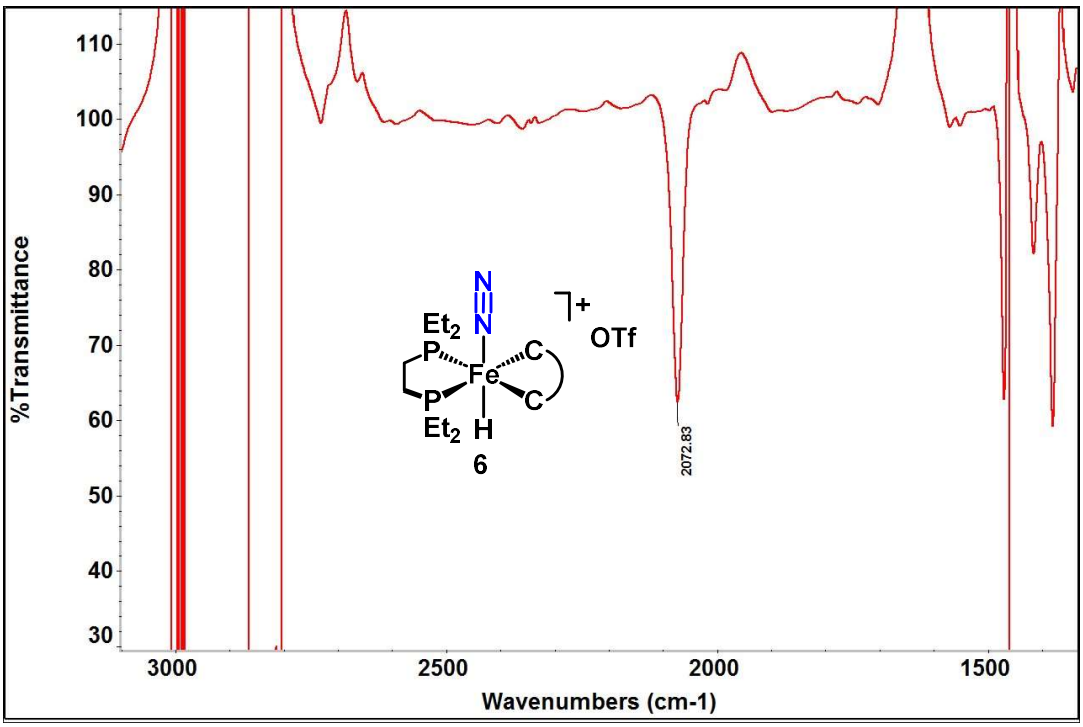

Figure S44. Infrared Spectrum (KBr) of **6**[^{t}BuO] from reaction of **4** with ^{t}ButOH Note: The 4 cm^{-1} shift from 2062 cm^{-1} characteristic of [**6**]OTf is attributed to the change in counterion ($^{t}BuO^{-}$ vs OTf^{-}) in this reaction mixture

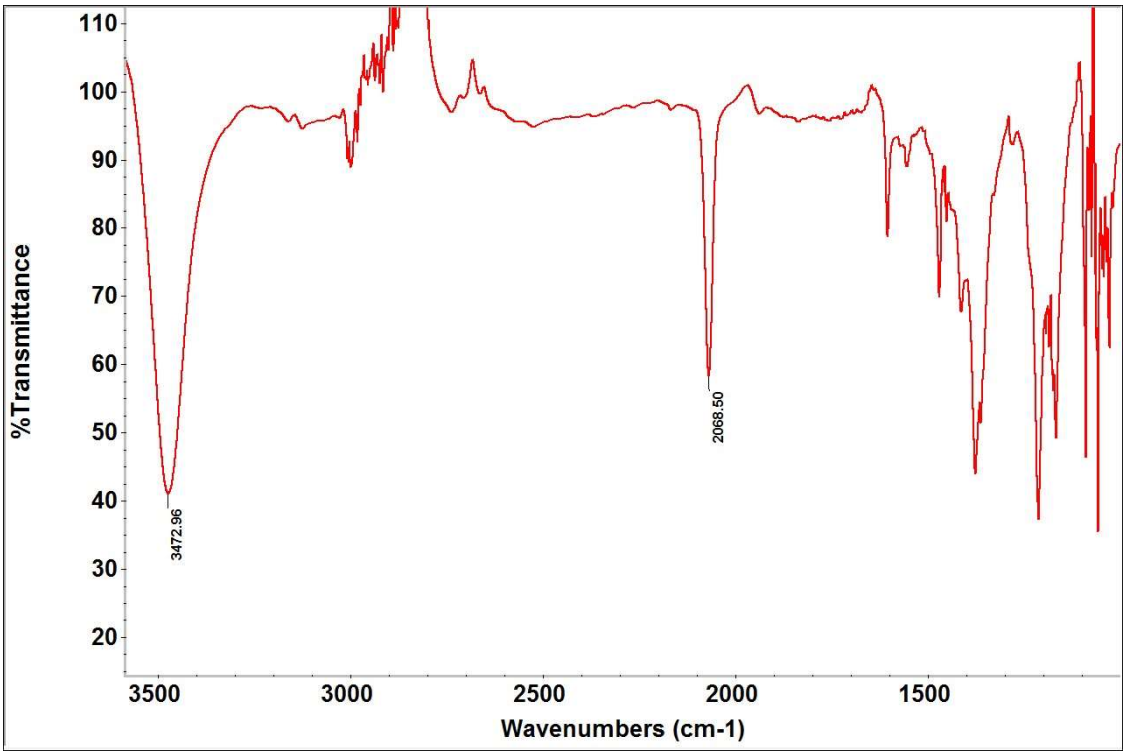

Figure S45. Infrared Spectrum (THF solution) of crude [$FeH(N_2)(depe)_2$][OTf] from protonation of $FeN_2(depe)_2$

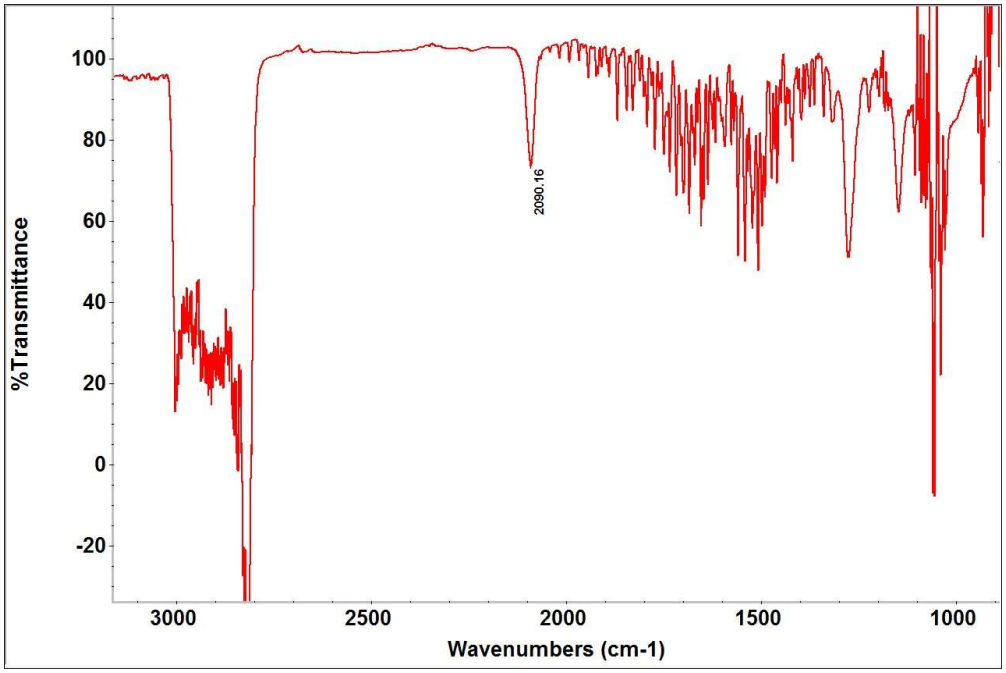

Figure 346. Infrared Spectrum (ATR) of **7**

Note: Slight impurities of **6** and another oxidized iron dinitrogen complex (potentially the $Fe^{I}N_2$) are visible at 2065 cm^{-1} and 2024 cm^{-1}

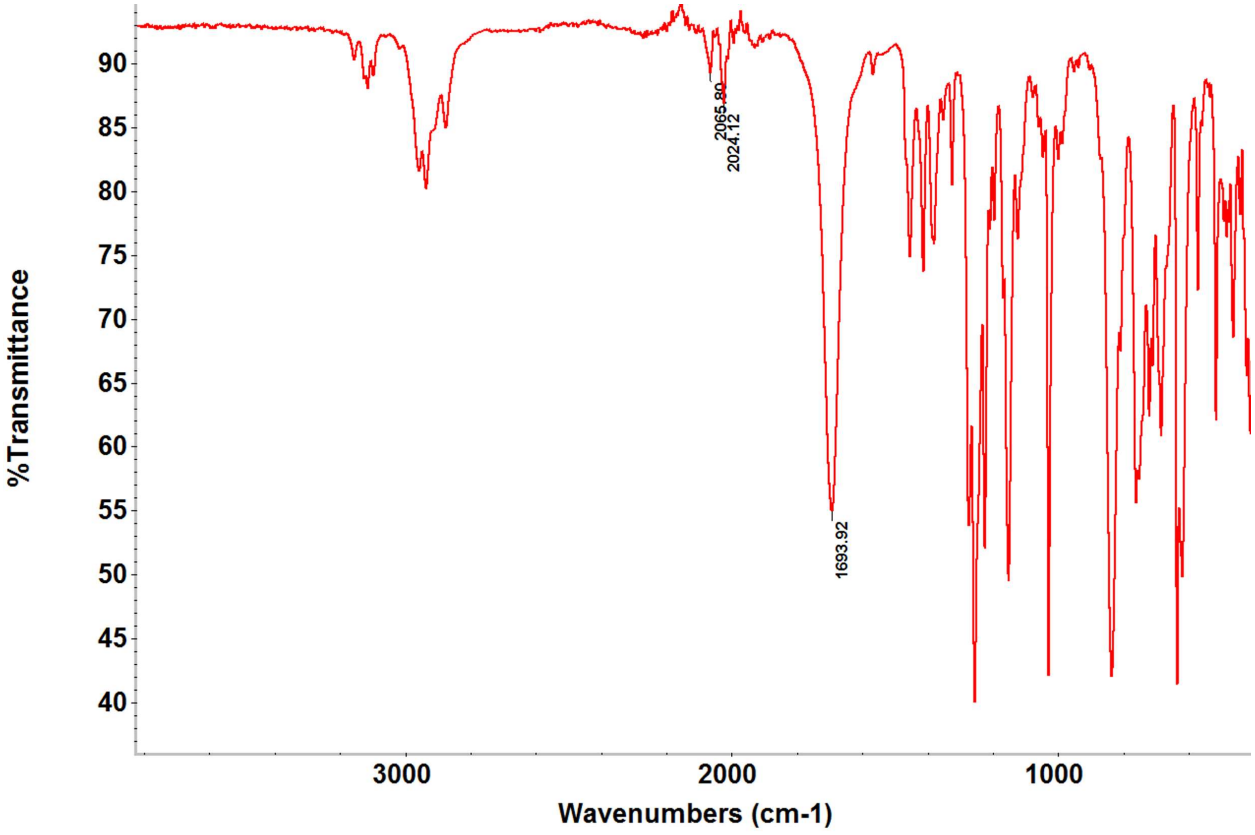

Figure S47. Electrochemical analysis of $FeCO(depe_2)$ (6.3 mM) recorded in THF solvent with 0.4M $[TBA][PF_6]$.

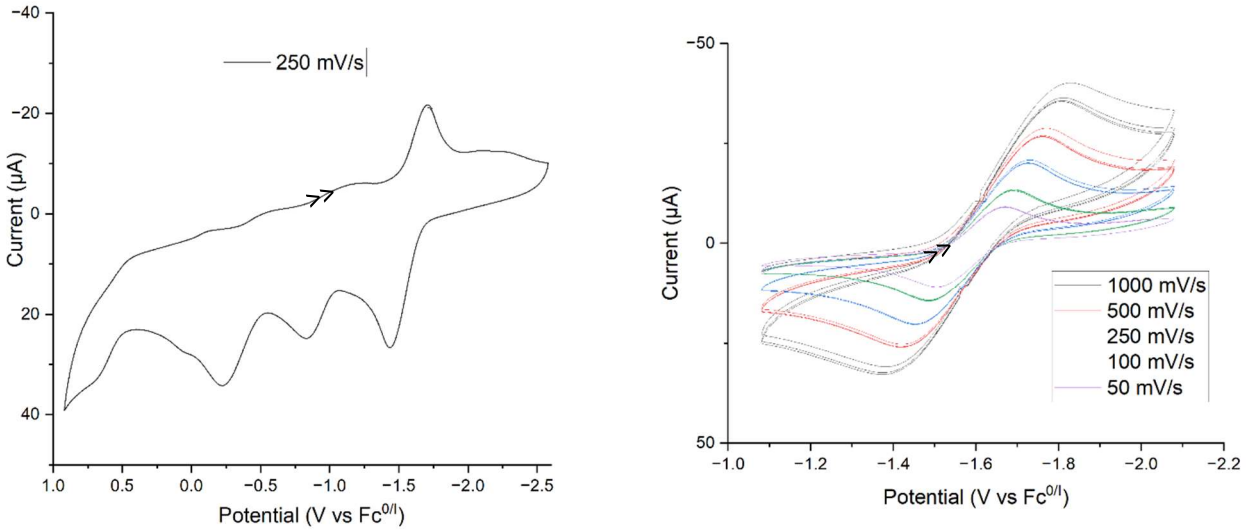

Figure S48. Electrochemical analysis of **4** (3.2mM) recorded in THF solvent with 0.4M $[TBA][PF_6]$.

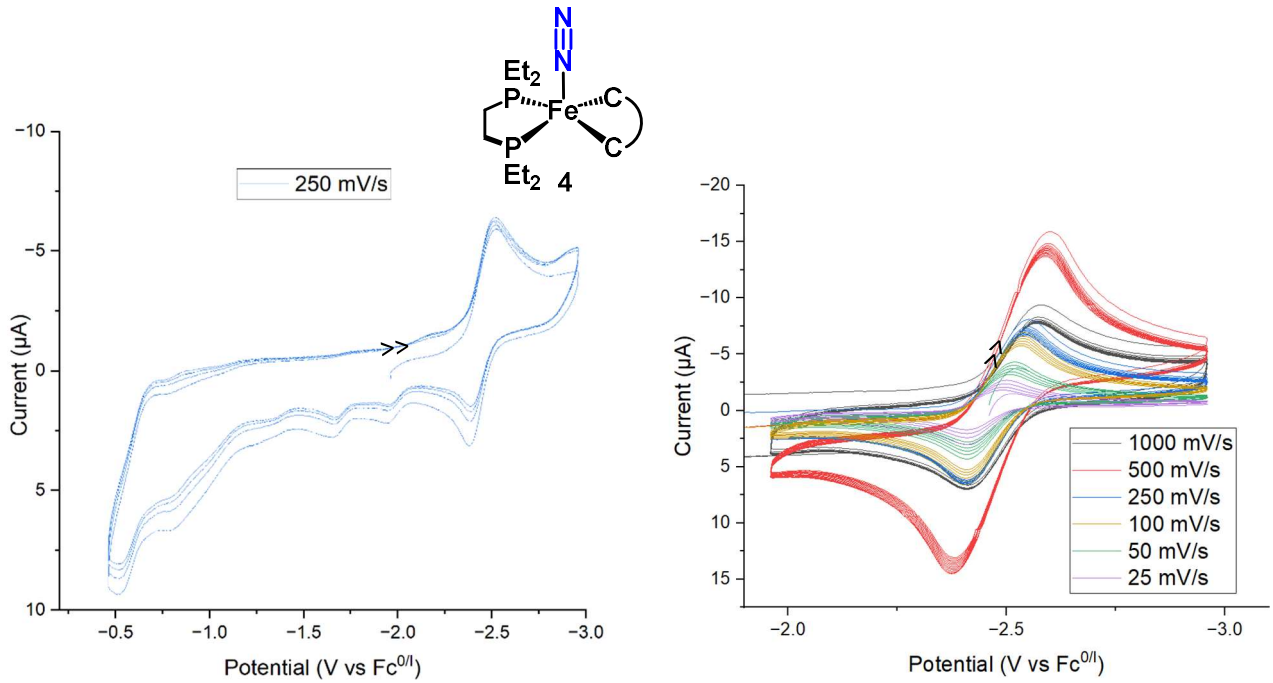

Figure S49. Electrochemical analysis of **5** (3.2mM) recorded in THF solvent with 0.4M [TBA][PF_6].

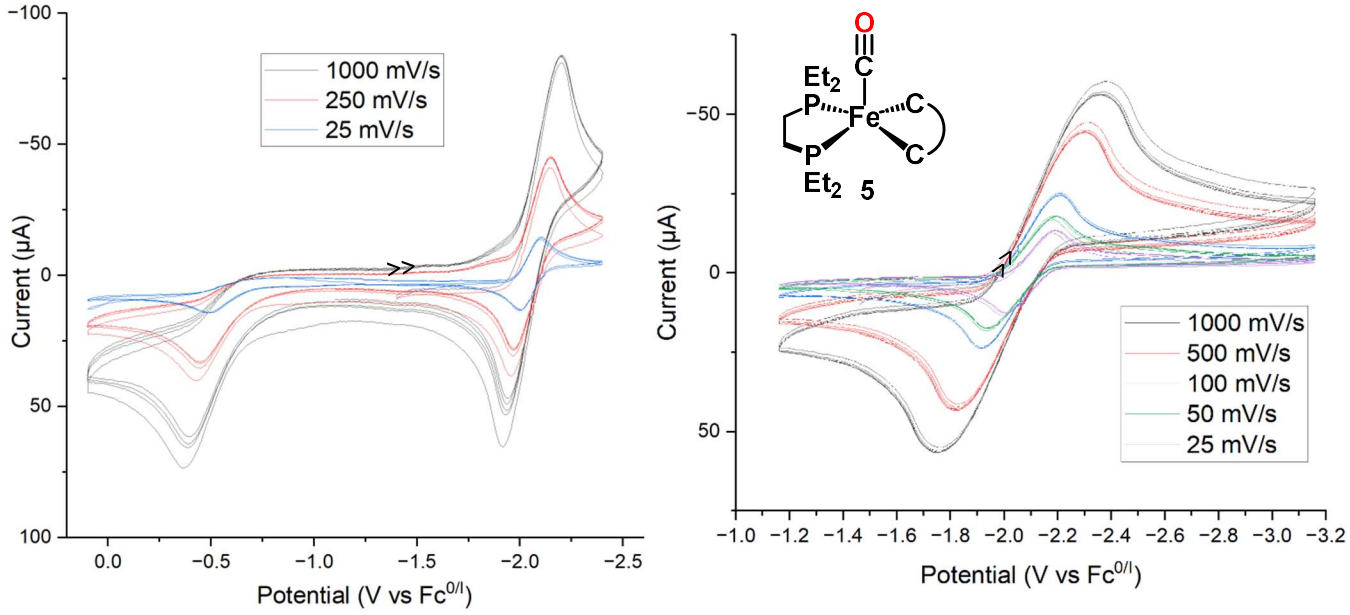

Time Resolved NMR Experiments for Fe^0 compounds protonation by tertbutanol

Procedure for reaction between tert-butanol and 4. To a vial was added 4.5 mg of $OP(Mes)_3$ (11 µmol, as internal standard) followed by 390 µL of a 21 mM solution of **4** (8.2 µmol) in THF. After agitating to form a homogeneous solution, the contents were transferred to a J-Young tube. An NMR spectrum was taken with the parameters described below. In an inert atmosphere glovebox, the contents of the tube were then frozen at -196°C. To the tube was added 90 µL of 1.08 M tert-butanol solution (97 µmol) in THF such that it froze in the tube before reaching the bottom, and the tube was sealed. The tube was kept frozen until it was brought to the NMR instrument, which was set to 25 °C. For 30 sec, the tube was let to thaw and was shaken before placing it in the NMR instrument. The total time elapsed between thawing the NMR tube and the first spectral scan was 150 seconds. An array of inverse-gated (decoupler only on during acquisition) $^{31}P\{^1H\}$ NMR experiments was set up with the following parameters: acquisition time = 2.7 s, D1 = 15 s to give the total recycle time of 17.7s, pulse angle = 90°. Each acquisition took 293 seconds and the elapsed time at the half point of the acquisitions were used as the time point in the kinetic profile. The data analysis was performed using MestreNova software, where an integral graph of **4**, protonated product, $OPMes_3$ with integration region of 20 times the line width at half-height was constructed.

Reaction between tert-butanol and $FeN_2(depe)_2$. For preparing the sample, 390 µL of a 19.5 mM solution of **$FeN_2(depe)_2$** (7.6 µmol) in THF with 2.6mg $OP(Mes)_3$ was loaded into a J-Young tube. The same procedure as for protonating **4** was used, except the sample was not frozen. Tert-butanol solution was added at room temperature and the NMR tube was shaken at time = 0 s.

Figure S50. $^{31}P\{^{1}H\}$ NMR spectra (THF, 25°C) time profile of reaction between **4** and t-butanol.
Y: $OPMes_3$; Y1: **6**; Y2: **4**; Y3: depe

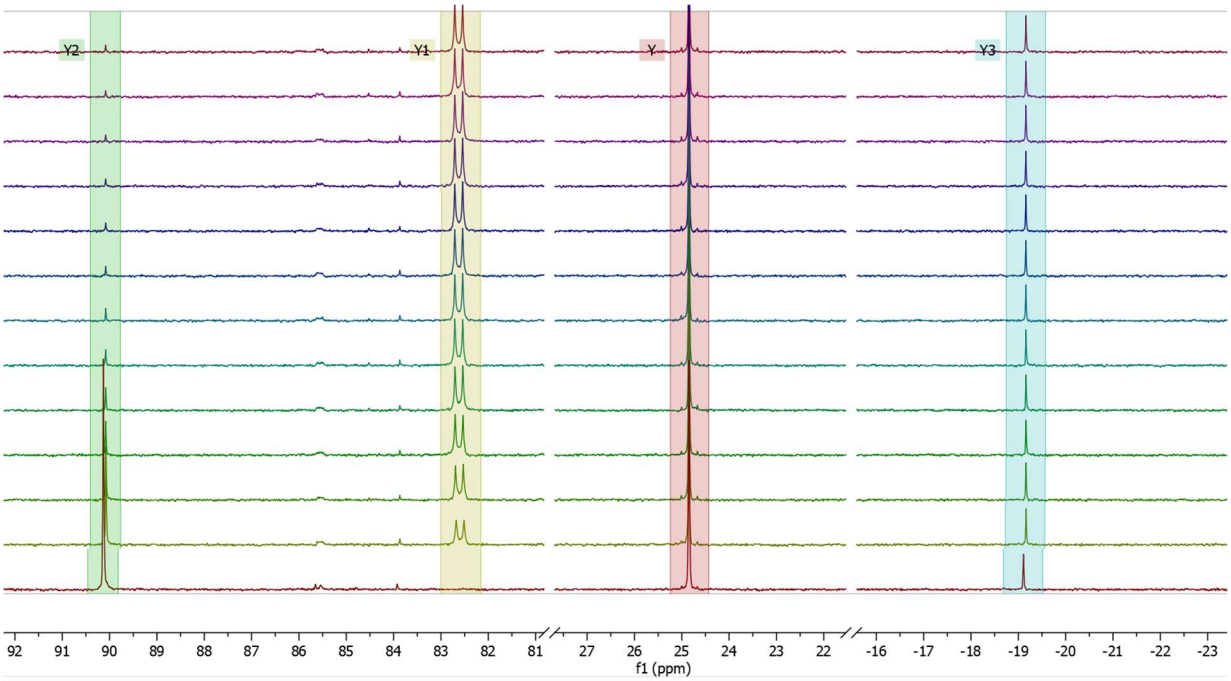

Table S1. ^{31}P NMR integrations over time for reaction of **4** with t-butanol

Time (s)	**$OP(Mes)_3$** (δ = 25.2 - 24.4 ppm)	**4** (δ= 90.5 - 89.7 ppm)	**6** (δ = 83.0 - 82.1 ppm)	**depe** (δ = -18.7 – -19.6 ppm)
0	1361.97	1362.34	16.9149	195.006
433	1123.78	485.378	653.297	190.582
1029	1116.03	155.442	905.848	170.322
1329	1115.6	280.769	829.946	158.259
1631	1111.72	98.7029	997.123	163.853
1929	1103.74	79.9039	1029.18	162.877
2223	1089.95	53.6626	1043.77	155.228
2526	1093.68	38.6132	1054.36	160.596
737	1103.24	48.2762	1061.17	173.199
2842	1114.9	42.5635	1058.47	156.125
3187	1104.88	25.3525	1063.21	164.269
3520	1111.2	18.0702	1066.06	150.464
3906	1105.36	28.3874	1060.49	168.748

Figure S51. Exponential fit to ^{31}P integrations of **4** and **6** over time.

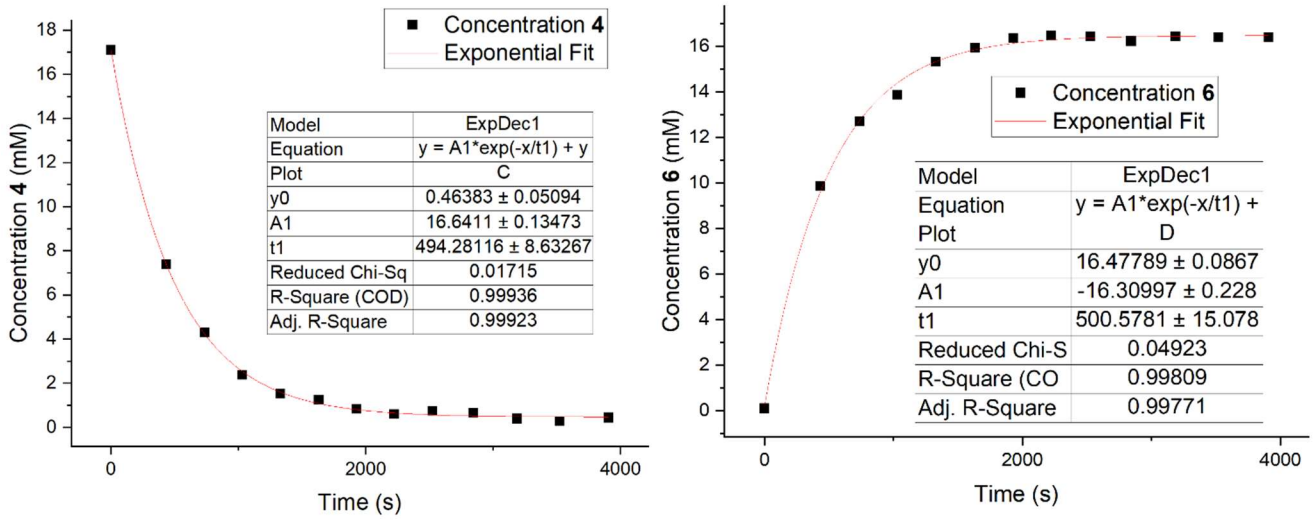

Figure S52. ^{1}H NMR spectrum (THF, 25°C) of final time-point in reaction of **4** with tert-butanol

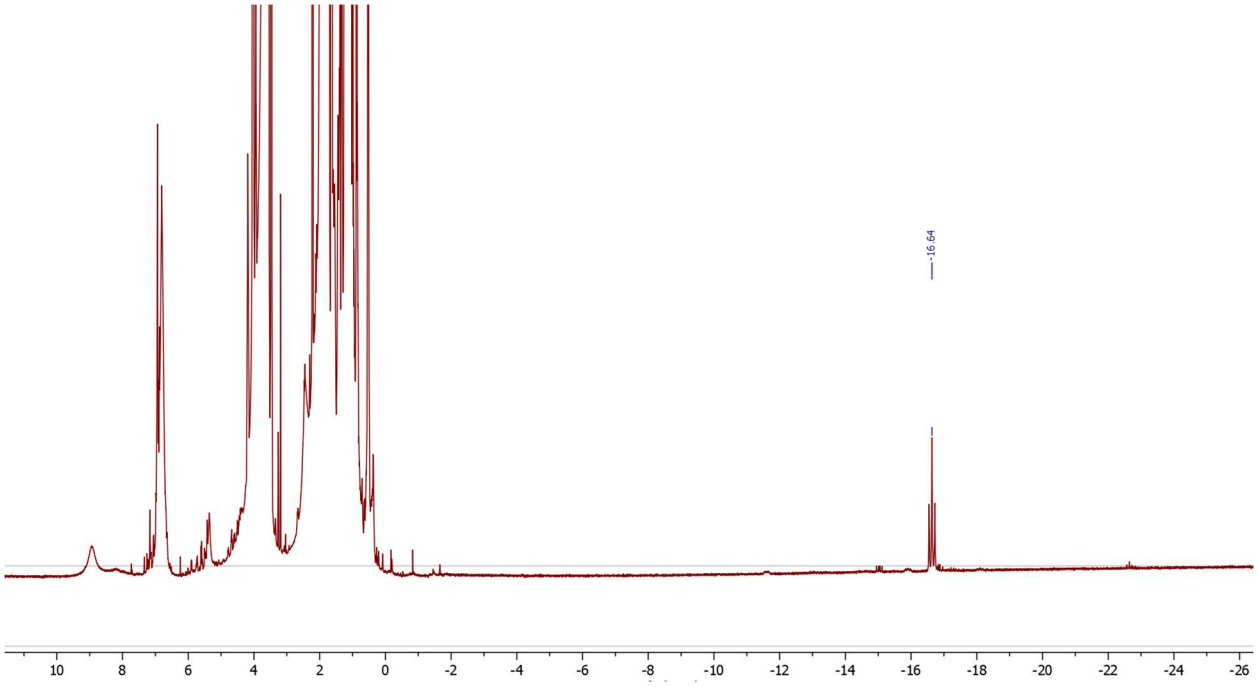

Figure S53. $^{31}P\{^{1}H\}$ NMR time profile of Reaction between $FeN_2(depe)_2$ and t-butanol in THF. Y: $OPMes_3$; Y1: $FeN_2(depe)_2$; Y2: $FeHX(depe)_2$; Y3: $FeHX(depe)_2$'

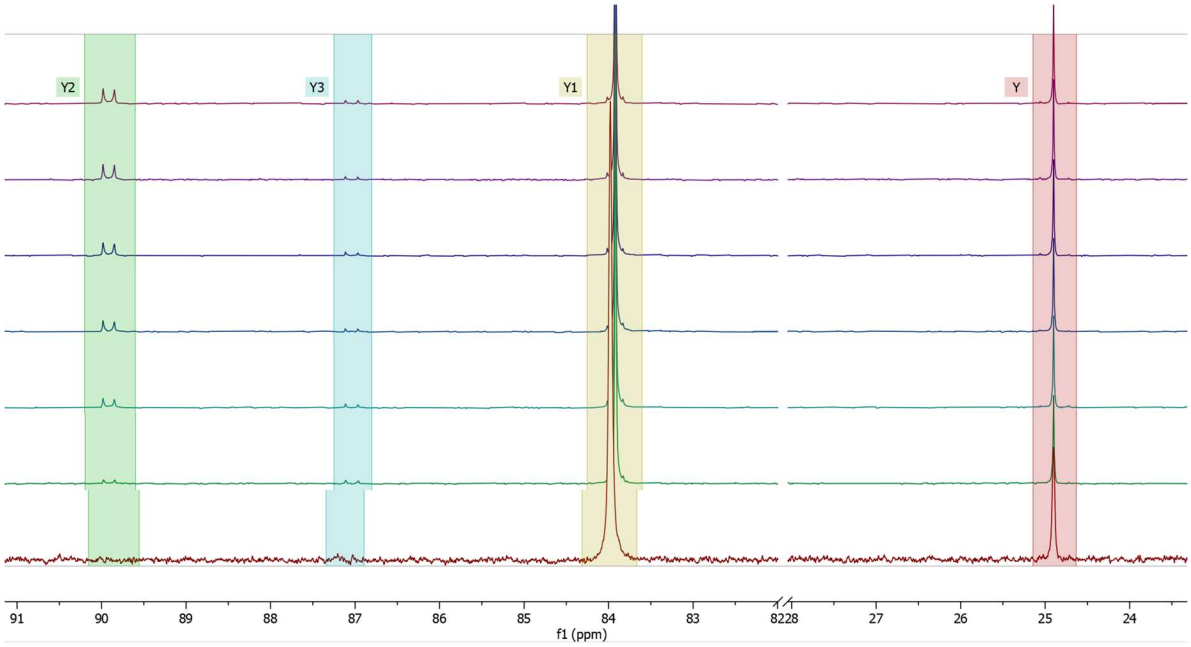

Table S2. ^{31}P NMR integrations over time for reaction of $FeN_2(depe)_2$ with t-butanol

Time (s)	**$OP(Mes)_3$** (δ 25.2-24.6 ppm)	**$FeN_2(depe)_2$** (δ 90.5-89.7 ppm)	**$FeHX(depe)_2$** (δ 90.2 – 89.6 ppm)	**$FeHX(depe)_2$'** (δ 87.3 - 86.8 ppm)
0	383.757	2071.1	-32.6891	-2.87768
351	447.942	2520.57	-15.2876	11.1656
3750	608.44	3263.97	13.4806	29.737
6905	417.056	2207.61	32.2845	25.7896
10199	721.918	3961.44	64.7284	37.9237
68057	1015.47	5102.52	279.396	49.5171
89749	979.26	4931.96	304.267	22.2889
163169	944.092	4855.39	403.398	47.2323
324835	603.03	2917.85	263.921	18.032
410670	1018.9	4761.45	487.337	62.9615

Figure S54. ^{1}H NMR spectrum (THF, 25°C) of final time-point in reaction of $FeN_2(depe)_2$ with tert-butanol

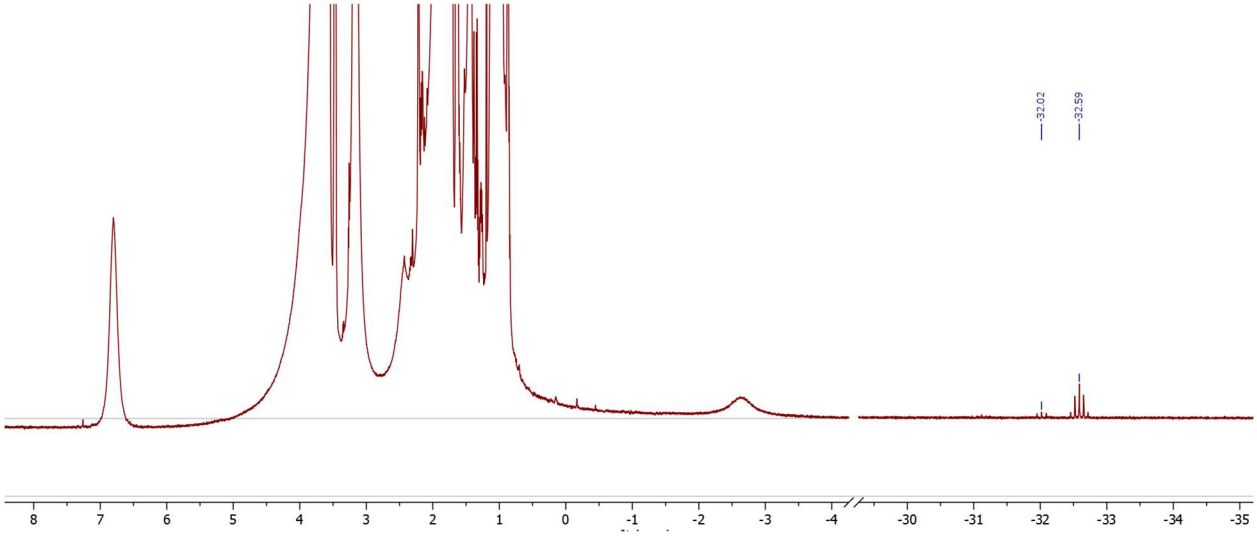

Computational Details

DFT calculations were performed using the Gaussian 09 revD01 software package[9]. Stationary point gas-phase geometries were calculated using a TPSS functional[10] and a def2-TZVP basis set[11] with empirical dispersion GD3.[12] The SMD solvation model with THF[13] was applied to each stationary point geometry to determine a solvation energy correction via $\Delta G_{solv} = E_{solv} - E_{gas}$. Solution phase free energies were then approximated with this value via $G_{solv} = G_{gas} + \Delta G_{solv}$. Redox potentials were standardized against the $Fe(Cp)_2$ / $[Fe(Cp)_2]^+$ redox couple via the Nersnt equation $\Delta E = \Delta G/(nF)$.

Table S3. Calculated Molecular Orbital Energies of **4** and $FeN_2(depe)_2$ at optimized geometries

	4	$FeN_2(depe)_2$
HOMO	-2.53 eV	-3.19 eV
HOMO-1	-3.00 eV	-3.20 eV
HOMO-2	-3.50 eV	-4.07 eV
HOMO-3	-3.66 eV	-4.12 eV

Figure S55. Calculated HOMO (top left), HOMO-1 (top right), HOMO-2 (bottom left) and HOMO-3 (bottom right) of **4**

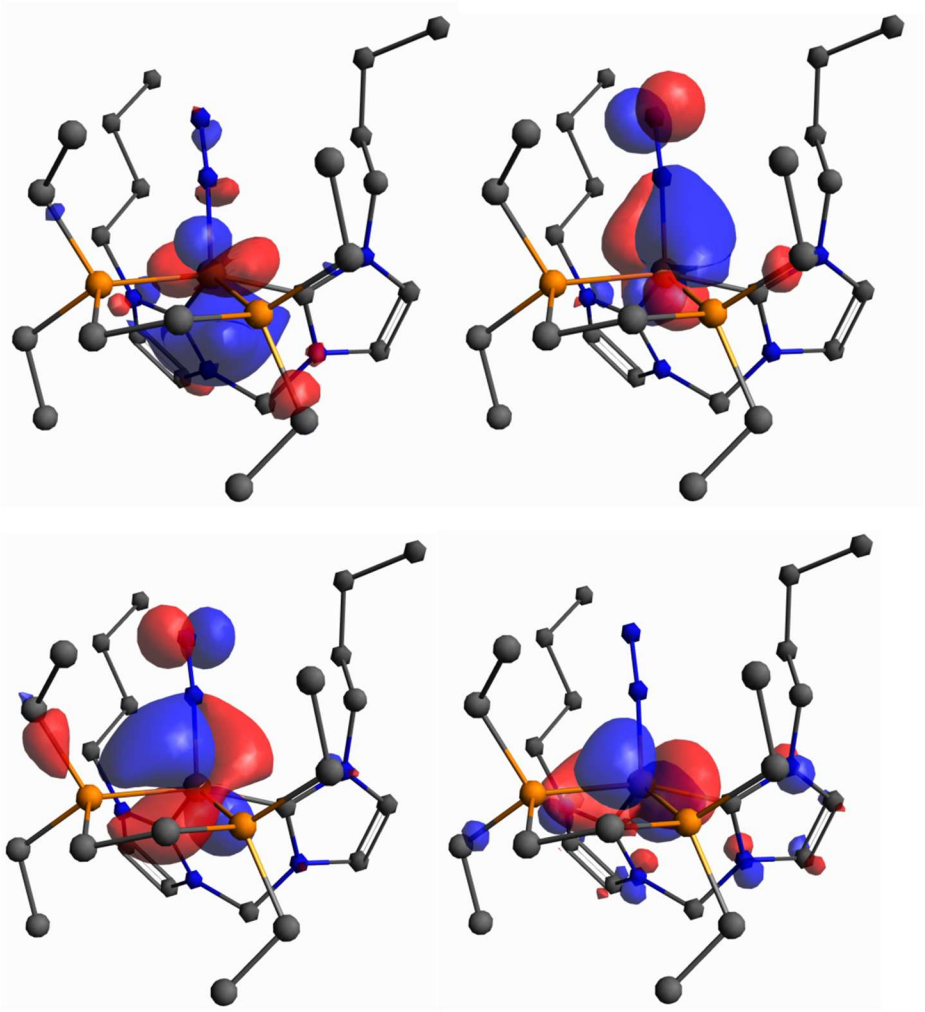

Figure S56. Calculated HOMO (top left), HOMO-1 (top right), HOMO-2 (bottom left) and HOMO-3 (bottom right) of $FeN_2(depe)_2$.

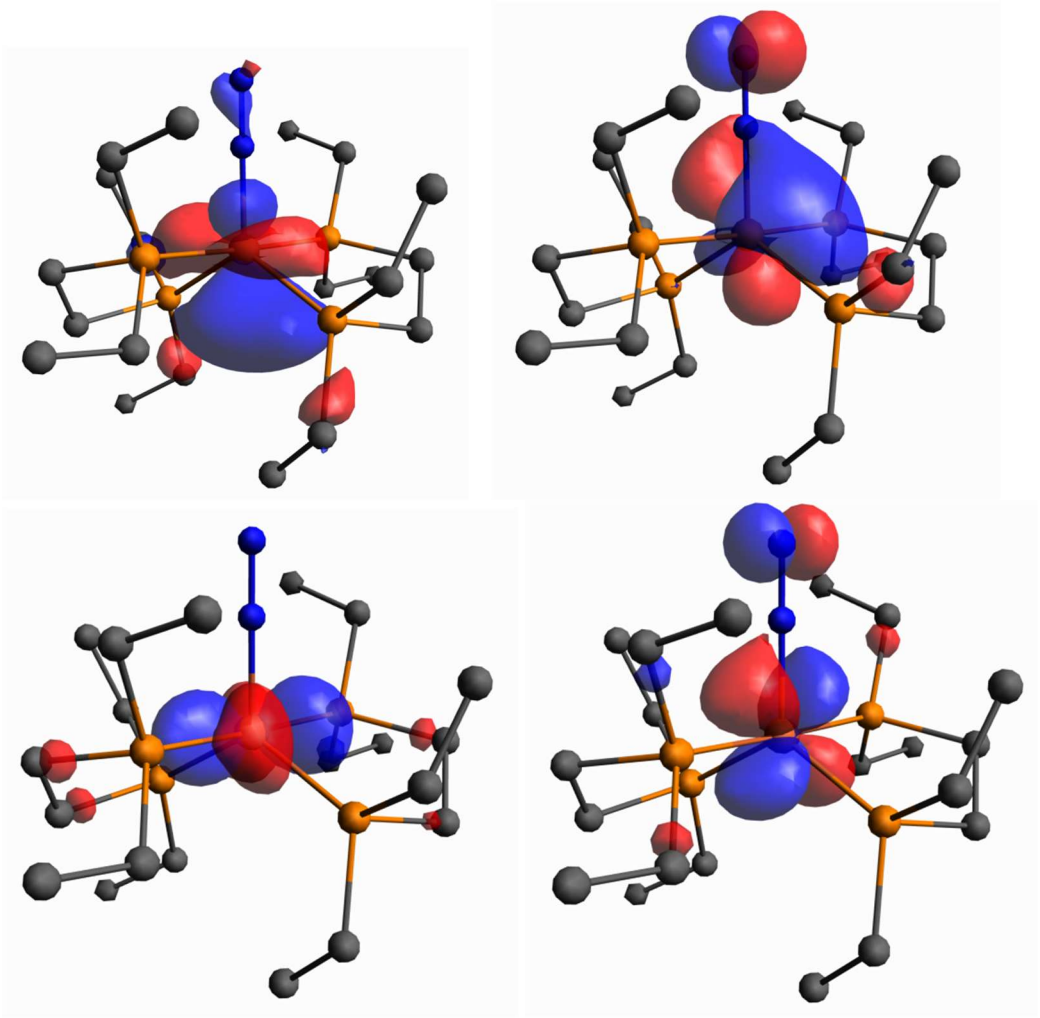

Table S4. Calculated and experimental values for **4** and $FeN_2(depe)_2$

4: $FeN_2(depe)(CC)$	**Calculated (DFT)**	**Experimental (crystal)**
N-N bond length (Å)	1.142	1.144(2)
Complex (0/I) redox couple vs $Fc^{0/I}$	-2.31	-2.48
τ geometric parameter	.4	.02
ν_{N2} (cm^{-1})	1937	1954 (C_5H_{12} soln)
$FeN_2(depe)_2$		
N-N (Å)	1.139	1.139(13)
Complex (0/I) redox couple vs $Fc^{0/I}$	-1.83	-2.00
τ geometric parameter	.9	.9
ν_{N2} (cm^{-1})	1961	1976

Table S5. Optimized coordinates of **4** for DFT calculations

Fe	3.31930000	3.91220000	14.74740000
P	3.50800000	1.77940000	15.23160000
P	3.79800000	3.27960000	12.71450000
N	0.70420000	4.41800000	16.05250000
N	0.96890000	5.55890000	14.02360000
N	2.12990000	3.97580000	17.57680000
N	4.78930000	4.69560000	15.43400000
N	2.71950000	6.52950000	13.27030000
N	5.73020000	5.17690000	15.87100000
C	0.91820000	4.23490000	18.20760000
C	0.01800000	4.50960000	17.25160000
C	2.33420000	5.39590000	13.96480000
C	2.02910000	4.07880000	16.20580000
C	5.24290000	3.94300000	11.73120000
C	3.79150000	5.03080000	19.07440000
C	3.38600000	3.78810000	18.30090000
C	4.11110000	6.92260000	13.02500000
C	0.15750000	4.59690000	14.73280000
C	2.24380000	0.83580000	16.19810000
C	0.53920000	6.71970000	13.40950000
C	4.97340000	1.13840000	16.18090000
C	0.80300000	1.02150000	15.74300000
C	4.22570000	1.47260000	12.57110000
C	3.57560000	0.70640000	13.71100000
C	5.23630000	4.97500000	19.57650000
C	1.62980000	7.32270000	12.93160000
C	5.97060000	8.51360000	13.68350000
C	2.54620000	3.48640000	11.34910000

C	6.55790000	8.59540000	12.28430000
C	4.46800000	8.24010000	13.69120000
C	6.55070000	3.99410000	12.52290000
C	6.32450000	1.48050000	15.57700000
C	5.58110000	6.17220000	20.45290000
C	1.33090000	2.58440000	11.45840000
H	0.15510000	3.74920000	14.31560000
H	5.37620000	4.14610000	20.07800000
H	4.92480000	1.48270000	17.06700000
H	7.52480000	8.87030000	12.32300000
H	6.12770000	9.39230000	14.14630000
H	1.73970000	8.12530000	12.44180000
H	3.99700000	3.60970000	17.69160000
H	6.42940000	7.80170000	14.17930000
H	6.48340000	7.69100000	11.85450000
H	3.96650000	1.16200000	11.68300000
H	2.26660000	4.43230000	11.34430000
H	4.66060000	6.19110000	13.37870000
H	6.84630000	3.07760000	12.78050000
H	0.69760000	0.99520000	14.80610000
H	7.29360000	4.35030000	11.98650000
H	4.00560000	-0.11220000	13.92410000
H	0.81740000	4.21080000	19.18720000
H	0.20350000	0.30340000	16.11470000
H	3.15590000	5.13690000	19.84920000
H	-0.90800000	4.70980000	17.26720000
H	4.25010000	6.97910000	12.03050000
H	7.07800000	1.17060000	16.13010000
H	4.99600000	4.82920000	11.41690000

H	5.82890000	4.93420000	18.80670000
H	6.40870000	1.06280000	14.70050000
H	3.26220000	2.99410000	18.91890000
H	6.54680000	6.22700000	20.71360000
H	5.32420000	3.40400000	10.95060000
H	2.31780000	1.09580000	17.14620000
H	5.20260000	1.41510000	12.61550000
H	-0.32560000	6.93310000	13.39410000
H	-0.75590000	4.92550000	14.82370000
H	3.00060000	3.35650000	10.49970000
H	5.40430000	6.98920000	20.00760000
H	2.49090000	-0.06040000	16.12790000
H	0.40880000	1.89260000	16.06630000
H	0.67700000	2.83310000	10.73950000
H	4.86960000	0.18700000	16.25770000
H	3.97480000	8.96090000	13.19620000
H	6.40250000	2.47350000	15.43510000
H	3.69170000	5.77980000	18.50100000
H	6.07590000	9.21540000	11.74240000
H	4.99200000	6.15510000	21.31180000
H	1.53880000	1.59630000	11.32890000
H	6.44140000	4.55740000	13.34130000
H	0.94780000	2.63170000	12.30760000
H	2.65590000	0.48610000	13.46890000
H	4.14970000	8.20010000	14.55320000

Table S6. Optimized coordinates of (**4** +) for DFT calculations

1 2

Fe	-0.06418000	-0.06314900	-0.16045400
P	0.46432500	2.09722500	0.13062500
P	2.13243000	-0.39742300	0.06773500
P	-2.25876400	0.28364400	0.07239200
P	-0.60470900	-2.21030000	0.23292600
C	0.57732700	4.19815200	2.11098200
C	-0.13270700	2.90530800	1.69133000
C	0.72039200	3.25172000	-2.47777500
C	-0.00285500	3.37053600	-1.13207300
C	2.31474200	2.30832400	0.22736400
C	2.97547700	1.14360000	-0.51034700
C	4.26380600	-0.58334100	2.04196400
C	2.74910500	-0.57921400	1.80579900
C	4.37589500	-1.52691800	-1.38495900
C	2.93534100	-1.75366400	-0.90387600
C	-0.97130100	-3.51254000	-2.29653000
C	-0.19213900	-3.55368800	-0.97694200
C	-0.25769000	-2.12208100	3.03978700
C	-0.00212600	-2.98561100	1.80119100
C	-2.45213500	-2.40584600	0.39608900
C	-3.13247200	-1.28140900	-0.38419100
C	-4.29751000	0.27927400	2.12844700
C	-2.82503400	0.57487500	1.81962800
C	-3.03581000	1.51505300	-2.36663000
C	-3.21146400	1.57243800	-0.84538000
H	0.11036200	4.60290900	3.01432600
H	0.51697300	4.96669500	1.33540800

H	1.63352900	4.02442800	2.33396200
H	-0.06468400	2.15210000	2.48496200
H	-1.20116500	3.09731400	1.53698600
H	0.39388600	4.05479800	-3.14530500
H	0.51357800	2.30015500	-2.96981200
H	1.80401200	3.34716800	-2.35867200
H	0.19615600	4.35273100	-0.68701000
H	-1.08459500	3.29770900	-1.27460100
H	2.60233800	2.29287200	1.28435100
H	2.61500700	3.28076700	-0.17524400
H	2.80341000	1.21612700	-1.59008700
H	4.05653000	1.11191100	-0.34509300
H	4.47048700	-0.60166700	3.11676400
H	4.74539200	0.30698500	1.62745000
H	4.73483700	-1.46458900	1.59985000
H	2.30540500	-1.50134100	2.19231000
H	2.27439500	0.23526600	2.36681700
H	4.72597800	-2.41330400	-1.92318800
H	5.06662300	-1.34005600	-0.56015000
H	4.43108500	-0.67978500	-2.07392800
H	2.28677300	-1.91533200	-1.77154500
H	2.86896900	-2.65920600	-0.28772000
H	-0.67677500	-4.35862500	-2.92477700
H	-0.77882600	-2.59620800	-2.85634300
H	-2.04929400	-3.59293200	-2.12669000
H	-0.38102700	-4.50212800	-0.45755000
H	0.88324200	-3.50350800	-1.16663800
H	0.23416900	-2.54644300	3.92019700
H	-1.32739600	-2.05623300	3.26171300

H	0.11846900	-1.10417200	2.88954000
H	1.07044900	-3.17564700	1.67274400
H	-0.48292700	-3.96620700	1.90198500
H	-2.70134200	-2.33176700	1.46043900
H	-2.76062600	-3.39944400	0.05564100
H	-3.00312900	-1.42443000	-1.46174900
H	-4.20584100	-1.21890200	-0.17829100
H	-4.52926700	0.58253500	3.15425900
H	-4.52314300	-0.78770300	2.04293800
H	-4.97296700	0.82368600	1.46225100
H	-2.59975400	1.62520600	2.03202000
H	-2.17001100	-0.00960300	2.47325800
H	-3.62262800	2.30462500	-2.84526100
H	-3.37583600	0.55750300	-2.77185200
H	-1.99001600	1.64486700	-2.65347300
H	-2.89544000	2.54651500	-0.45282300
H	-4.26814000	1.45663900	-0.57690100
N	0.17051400	-0.25087600	-3.10543400
N	0.04080000	-0.16018000	-1.99058400

Table S7. Optimized coordinates of $FeN_2(depe)_2$ for DFT calculations

0 1

Fe	0.01540600	-0.14142100	-0.30273300
P	-0.44812600	1.89633600	0.31711300
P	2.08434700	0.57180400	-0.48332700
P	0.47860400	-1.71327400	1.12113500
P	-2.04869000	-0.89355000	-0.19249000
C	1.09153200	2.95937200	0.42323000

C	2.12009200	2.42685700	-0.56834200
C	-1.05637000	-2.63475200	1.67221700
C	-2.07384400	-2.60378500	0.53774000
C	-1.28692300	2.41780400	1.91343100
C	-1.16162300	3.88846800	2.33290500
C	-1.49812200	2.91030500	-0.85473700
C	-0.90868700	3.00994200	-2.26391100
C	3.01262800	0.16463800	-2.03467300
C	3.36165000	-1.31843700	-2.17593200
C	3.37676200	0.23181500	0.81609000
C	4.78523300	0.78984900	0.58365800
C	1.54985300	-3.15067100	0.58328400
C	0.97710200	-3.90235300	-0.62067400
C	1.25322800	-1.48400900	2.81308600
C	0.78192600	-0.21219200	3.51266400
C	-2.95846800	-1.21725500	-1.77578900
C	-3.38063700	0.04453500	-2.53306400
C	-3.36877800	-0.05305900	0.81860000
C	-4.77237200	-0.66867700	0.81860700
H	1.47572300	2.87049400	1.44760700
H	0.85734700	4.01617100	0.25149700
H	1.83863000	2.68451500	-1.59443200
H	3.12413100	2.82717700	-0.38899500
H	-1.44974500	-2.10373500	2.54789300
H	-0.80525200	-3.65487200	1.98804800
H	-1.77408900	-3.27928300	-0.27003400
H	-3.07943100	-2.89442800	0.86126900
H	-0.89097000	1.76990900	2.70027800
H	-2.34446700	2.15916700	1.80604300

H	-1.75554000	4.07738200	3.23519100
H	-0.12577900	4.15793200	2.55933200
H	-1.52209000	4.56891100	1.55482800
H	-1.68133100	3.91011400	-0.44120900
H	-2.46489000	2.39489500	-0.89704000
H	-1.64118900	3.41608700	-2.97043100
H	-0.03511000	3.67028300	-2.28039700
H	-0.59489900	2.02318600	-2.61810300
H	3.91466800	0.78744100	-2.07738700
H	2.36636200	0.47581600	-2.86172100
H	3.86164800	-1.51024800	-3.13137900
H	4.03255900	-1.65191900	-1.37599800
H	2.45602000	-1.92815100	-2.13867500
H	3.42763300	-0.85647100	0.92286600
H	2.96371100	0.61121900	1.75753500
H	5.43073300	0.55621500	1.43814800
H	5.24663300	0.35565500	-0.30813100
H	4.77922200	1.87750300	0.46362400
H	1.70693500	-3.82900400	1.43316500
H	2.52517400	-2.72329800	0.32343300
H	1.71480200	-4.58989500	-1.04890300
H	0.10123700	-4.49367800	-0.33395100
H	0.66780000	-3.19663900	-1.39882900
H	2.34132800	-1.47092400	2.69460000
H	1.01180600	-2.37408500	3.40914300
H	1.24849800	-0.09537500	4.49772500
H	1.02297800	0.66212400	2.89892300
H	-0.30527300	-0.21624300	3.65033400
H	-3.82951500	-1.84430400	-1.54844200

H	-2.28343100	-1.81569300	-2.39618700
H	-3.90363200	-0.21957500	-3.45869000
H	-4.05720800	0.66550000	-1.93503700
H	-2.51035900	0.64833500	-2.80019100
H	-3.42268500	0.98083400	0.46113200
H	-2.96932600	-0.00343200	1.83819700
H	-5.43542400	-0.09926300	1.48018100
H	-5.21526300	-0.65920500	-0.18172200
H	-4.76509900	-1.70404900	1.17273500
N	0.01932300	-0.50872100	-2.05005000
N	0.02192900	-0.74646200	-3.16331800

Table S8. Optimized coordinates of $[FeN_2(depe)_2]^+$ for DFT calculations

1 2

Fe	-0.06418000	-0.06314900	-0.16045400
P	0.46432500	2.09722500	0.13062500
P	2.13243000	-0.39742300	0.06773500
P	-2.25876400	0.28364400	0.07239200
P	-0.60470900	-2.21030000	0.23292600
C	0.57732700	4.19815200	2.11098200
C	-0.13270700	2.90530800	1.69133000
C	0.72039200	3.25172000	-2.47777500
C	-0.00285500	3.37053600	-1.13207300
C	2.31474200	2.30832400	0.22736400
C	2.97547700	1.14360000	-0.51034700
C	4.26380600	-0.58334100	2.04196400
C	2.74910500	-0.57921400	1.80579900
C	4.37589500	-1.52691800	-1.38495900

C	2.93534100	-1.75366400	-0.90387600
C	-0.97130100	-3.51254000	-2.29653000
C	-0.19213900	-3.55368800	-0.97694200
C	-0.25769000	-2.12208100	3.03978700
C	-0.00212600	-2.98561100	1.80119100
C	-2.45213500	-2.40584600	0.39608900
C	-3.13247200	-1.28140900	-0.38419100
C	-4.29751000	0.27927400	2.12844700
C	-2.82503400	0.57487500	1.81962800
C	-3.03581000	1.51505300	-2.36663000
C	-3.21146400	1.57243800	-0.84538000
H	0.11036200	4.60290900	3.01432600
H	0.51697300	4.96669500	1.33540800
H	1.63352900	4.02442800	2.33396200
H	-0.06468400	2.15210000	2.48496200
H	-1.20116500	3.09731400	1.53698600
H	0.39388600	4.05479800	-3.14530500
H	0.51357800	2.30015500	-2.96981200
H	1.80401200	3.34716800	-2.35867200
H	0.19615600	4.35273100	-0.68701000
H	-1.08459500	3.29770900	-1.27460100
H	2.60233800	2.29287200	1.28435100
H	2.61500700	3.28076700	-0.17524400
H	2.80341000	1.21612700	-1.59008700
H	4.05653000	1.11191100	-0.34509300
H	4.47048700	-0.60166700	3.11676400
H	4.74539200	0.30698500	1.62745000
H	4.73483700	-1.46458900	1.59985000
H	2.30540500	-1.50134100	2.19231000

H	2.27439500	0.23526600	2.36681700
H	4.72597800	-2.41330400	-1.92318800
H	5.06662300	-1.34005600	-0.56015000
H	4.43108500	-0.67978500	-2.07392800
H	2.28677300	-1.91533200	-1.77154500
H	2.86896900	-2.65920600	-0.28772000
H	-0.67677500	-4.35862500	-2.92477700
H	-0.77882600	-2.59620800	-2.85634300
H	-2.04929400	-3.59293200	-2.12669000
H	-0.38102700	-4.50212800	-0.45755000
H	0.88324200	-3.50350800	-1.16663800
H	0.23416900	-2.54644300	3.92019700
H	-1.32739600	-2.05623300	3.26171300
H	0.11846900	-1.10417200	2.88954000
H	1.07044900	-3.17564700	1.67274400
H	-0.48292700	-3.96620700	1.90198500
H	-2.70134200	-2.33176700	1.46043900
H	-2.76062600	-3.39944400	0.05564100
H	-3.00312900	-1.42443000	-1.46174900
H	-4.20584100	-1.21890200	-0.17829100
H	-4.52926700	0.58253500	3.15425900
H	-4.52314300	-0.78770300	2.04293800
H	-4.97296700	0.82368600	1.46225100
H	-2.59975400	1.62520600	2.03202000
H	-2.17001100	-0.00960300	2.47325800
H	-3.62262800	2.30462500	-2.84526100
H	-3.37583600	0.55750300	-2.77185200
H	-1.99001600	1.64486700	-2.65347300
H	-2.89544000	2.54651500	-0.45282300

H	-4.26814000	1.45663900	-0.57690100
N	0.17051400	-0.25087600	-3.10543400
N	0.04080000	-0.16018000	-1.99058400

Table S9. Optimized coordinates of 5.

0 1

Fe 0.39770900 -0.09728200 -0.05281300

P 1.92063600 0.81258200 -1.31336000

P 1.41354100 -1.95804400 -0.47826400

N 0.81737800 1.12976600 2.60094900

N -0.08639600 -1.03692000 2.69241200

N 0.27681300 2.67432600 1.20727500

C -0.90730600 0.20332900 -1.16827500

N -1.65121100 -1.81725600 1.44401300

O -1.73921000 0.47706400 -1.97162600

C 0.33325000 3.26214600 2.46792500

C 0.66347100 2.28936200 3.35377900

C -0.50597600 -1.04791300 1.37283800

C 0.55536300 1.31649100 1.25161600

C 0.40851900 -3.42495000 -1.05689200

C -1.87150000 3.25434900 0.12507200

C -0.34431200 3.31523100 0.05038900

C -2.58037000 -2.00675800 0.33130000

C 1.05697200 -0.21949500 3.05221800

C 2.98587200 2.22667700 -0.73119400

C -0.94933300 -1.72167200 3.53972600

C 1.43993200 1.51023100 -2.97886200

C 3.74310400 1.97101300 0.57395700

C 2.65551700 -1.80966700 -1.86245800

C 3.24788900 -0.40119800 -1.83571300

C -2.53463000 3.79709200 -1.14288900

C -1.93021700 -2.21948100 2.74592100

C -4.64769500 -1.08285600 -0.84803500

C 2.40913300 -2.86462300 0.82664300

C -5.40121300 -2.41381400 -0.95784400

C -3.72394100 -0.98788900 0.37275800

C -0.36115700 -3.16858900 -2.35614400

C 0.97908800 0.43043400 -3.96353300

C -4.05846100 3.65074200 -1.10699700

C 3.70276900 -2.13130400 1.19438500

H 1.92594500 -0.60015300 2.50488600

H -2.26472400 4.85400600 -1.28016100

H 0.62256400 2.21947800 -2.80245500

H -6.09593200 -2.40121500 -1.80437500

H -5.37344800 -0.26167300 -0.79522100

H -2.79023700 -2.82511200 2.98556400

H -0.00538600 2.76181400 -0.82661000

H -4.05164200 -0.91104400 -1.75182400

H -4.71750400 -3.25658400 -1.10947600

H 3.42524700 -2.58832100 -1.79325400

H 1.75287300 -2.94706000 1.70233100

H -1.99808700 -1.87610500 -0.58098900

H 0.30916700 -3.17968700 -3.22175300

H 4.42870300 1.12213500 0.47902400

H -1.12590700 -3.93584800 -2.52221500

H 3.67945000 -0.10881600 -2.80136000

H 0.14345100 4.31340200 2.62012500

H 4.33817700 2.84858200 0.85277900

H -2.22216100 3.80785700 1.00704400

H 0.84217100 2.32744500 4.41709300

H -2.95094600 -3.03594200 0.37398500

H 0.52353800 0.88015800 -4.85242000

H -0.28625100 -3.64880800 -0.23773300

H -2.14029200 3.24887200 -2.00690300

H 1.82249900 -0.18417900 -4.29573900

H 0.01712000 4.34826800 -0.01542700

H -4.51898900 4.05095100 -2.01664400

H 1.06617300 -4.29799800 -1.16275500

H 2.33200700 3.09867300 -0.61824400

H 2.10554100 -1.96894100 -2.79543800

H -0.77504300 -1.81627400 4.60003800

H 1.20876100 -0.24333300 4.13225100

H 2.62984900 -3.88652200 0.49066600

H -4.33832500 2.59459700 -1.02489000

H 3.68862900 2.46070400 -1.54228500

H 3.04992800 1.75116400 1.38923900

H 4.13663800 -2.51351700 2.12529000

H 2.28485300 2.07662900 -3.39249600

H -4.30258700 -1.12417100 1.29719400

H 0.23758500 -0.22287700 -3.49625500

H -2.15018500 2.20332700 0.26369300

H -5.98370500 -2.61442700 -0.04982100

H -4.48778200 4.18276400 -0.24927700

H 4.45561800 -2.24291100 0.40677500

H -0.84989100 -2.18881500 -2.33260000

H 3.50836400 -1.05745700 1.31288200

H 4.04178000 -0.33785900 -1.08540900

H -3.27172500 0.00884900 0.41298400

Table S10. Optimized coordinates of $FeCp_2$ for DFT calculations

0 1

Fe	0.00000000	0.00000000	0.00000000
C	-1.63630700	0.10536100	-1.21321200
C	-1.63629300	1.18654900	-0.27489600
C	-1.63691800	-1.12118600	-0.47508000
H	-1.60703400	0.19891700	-2.29054100
C	-1.63672700	0.62806700	1.04314700
H	-1.60720900	2.24005000	-0.51891200
C	-1.63693700	-0.79812100	0.91938800
H	-1.60827100	-2.11695400	-0.89676200
H	-1.60816700	1.18575400	1.96961600
H	-1.60804200	-1.50684700	1.73613100
C	1.63630700	-0.10508100	1.21323700
C	1.63691800	1.12129600	0.47482300
C	1.63629200	-1.18648500	0.27516800
H	1.60703200	-0.19839000	2.29058700
C	1.63693700	0.79790900	-0.91957100
H	1.60827200	2.11716000	0.89627700
C	1.63672800	-0.62830700	-1.04300300
H	1.60720600	-2.23993000	0.51942500
H	1.60804200	1.50644800	-1.73647600
H	1.60816700	-1.18620600	-1.96934400

Table S11. Optimized coordinates of [FeCp2]+ for DFT calculations

1 2

Fe	0.00000000	0.00000500	0.00000000
C	1.69311900	1.19235800	0.26444600
C	1.76886900	0.58890300	-1.02505500
C	1.63778000	0.14457900	1.24004000
H	1.66325900	2.25474800	0.46633600
C	1.75669100	-0.82332500	-0.85705800
H	1.78021900	1.11369400	-1.97145800
C	1.67511000	-1.10565100	0.53955900
H	1.57878000	0.27416200	2.31220100
H	1.76155400	-1.55534700	-1.65399900
H	1.63640800	-2.08983200	0.98688500
C	-1.69315100	-1.19231000	-0.26469100
C	-1.63778300	-0.14433700	-1.24006900
C	-1.76888800	-0.58912600	1.02493000
H	-1.66329600	-2.25466000	-0.46679800
C	-1.67508000	1.10575400	-0.53933400
H	-1.57878200	-0.27370600	-2.31225600
C	-1.75666700	0.82313800	0.85723100
H	-1.78024300	-1.11411600	1.97122400
H	-1.63637400	2.09002600	-0.98646100
H	-1.76152400	1.55499300	1.65432500

Figure 57. Molecular structure of **2** with 50% probability ellipsoids. Solvent (CH_2Cl_2) molecules, a PF_6^- and a BPh_4^- counterion, and all hydrogen atoms not attached to iron are omitted for clarity.

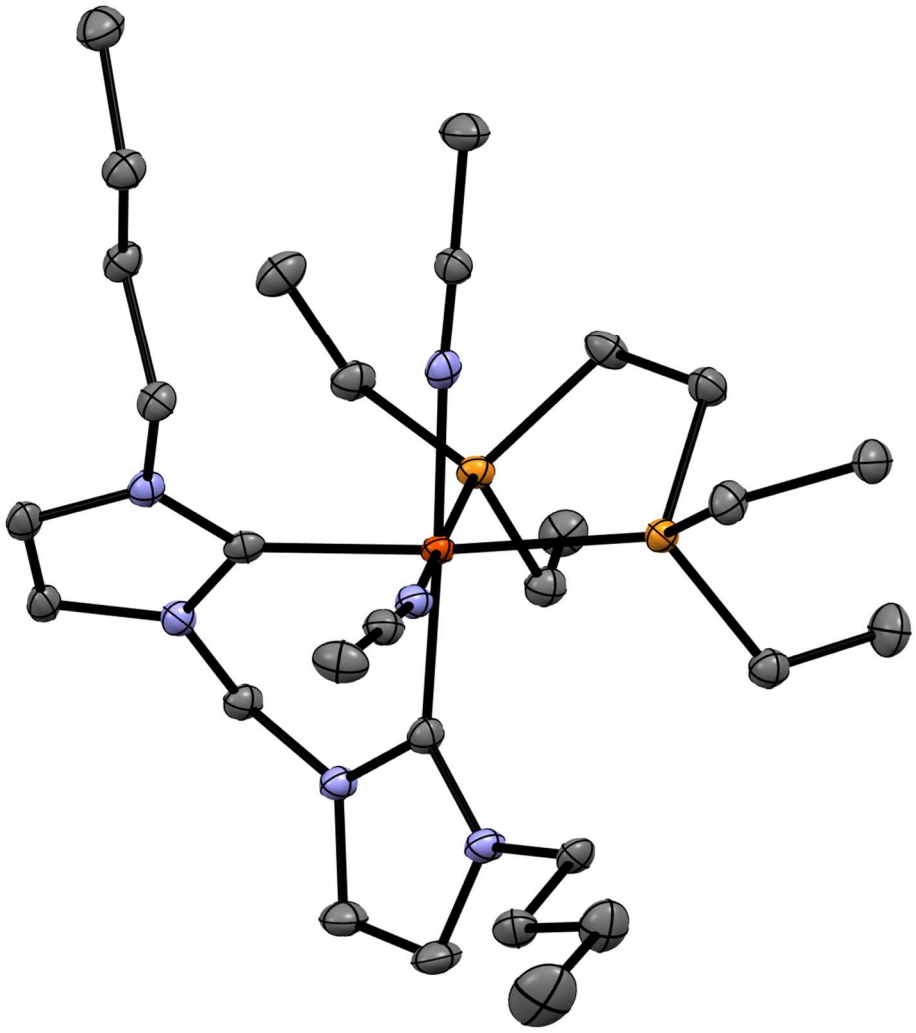

Complex: $[Fe(MeCN)_2(^{butyl}CC)(depe)][PF_6][BPh_4]$

Local Name: CA1321

CCDC: 2394085

Table S12. Crystallographic parameters for **2**.

CCDC number	2394085
Empirical formula	$C_{55}H_{78}BCl_4F_6FeN_6P_3$
Formula weight	1238.62
Temperature [K]	293
Crystal system	triclinic

Space group (number)	$P\bar{1}$ (2)
a [Å]	12.7534(4)
b [Å]	13.1143(5)
c [Å]	20.0807(6)
α [°]	76.017(3)
β [°]	74.960(3)
γ [°]	70.874(3)
Volume [Å^3]	3018.97(17)
Z	2
ρ_{calc} [gcm^{-3}]	1.363
μ [mm^{-1}]	4.877
F(000)	1146.455
Crystal size [mm^3]	0.222×0.139×0.135
Crystal colour	orange
Crystal shape	cube
Radiation	Cu K_α (λ=1.54184 Å)
2θ range [°]	4.63 to 138.83 (0.82 Å)
Index ranges	−15 ≤ h ≤ 15 −15 ≤ k ≤ 15 −23 ≤ l ≤ 24
Reflections collected	46024
Independent reflections	10857 R_{int} = 0.0428 R_{sigma} = 0.0285
Completeness to θ = 66.9682°	97.4 %
Data / Restraints / Parameters	10857/0/693
Absorption correction T_{min}/T_{max} (method)	0.67743/1.00000 (multi-scan)
Goodness-of-fit on F^2	1.0280

Final *R* indexes [*I*≥2σ(*I*)]	R_1 = 0.0411 wR_2 = 0.1145
Final *R* indexes [all data]	R_1 = 0.0422 wR_2 = 0.1172
Largest peak/hole [eÅ^{-3}]	1.29/−1.28

Figure 58. Molecular structure of **4** with 50% probability ellipsoids. Hydrogen atoms not attached to iron are omitted for clarity.

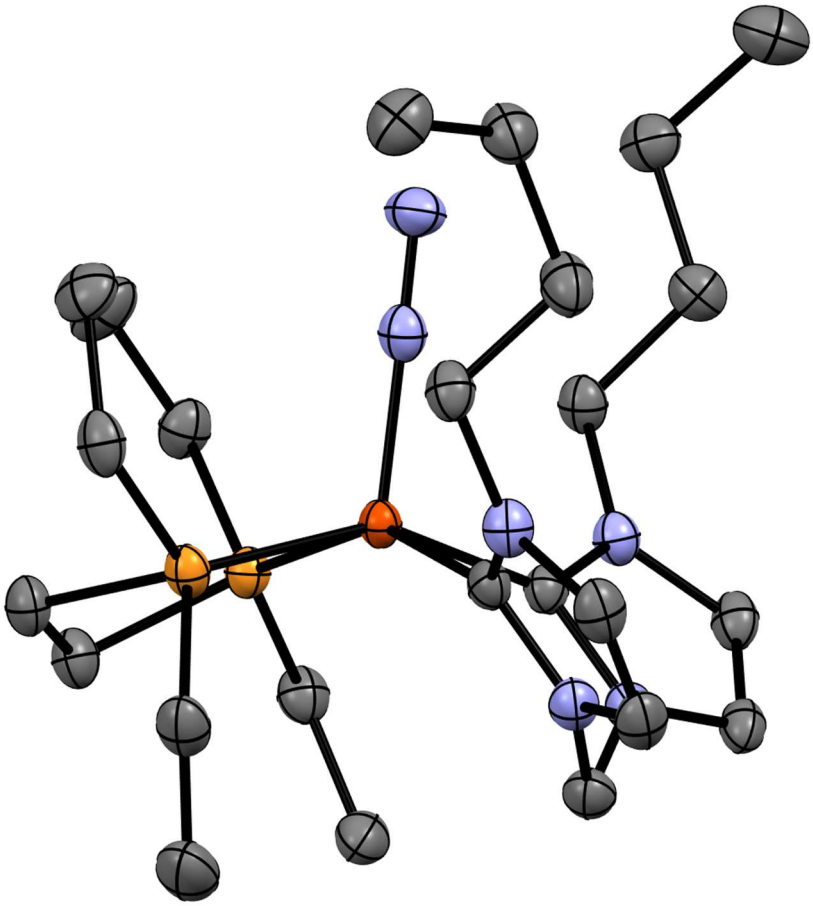

Complex: [Fe(N_2)(depe)(^{butyl}CC)]

Local name: CA56N2

CCDC: 2368195

Table S13. Crystallographic parameters for **4**.

	CA56N2
Crystal data	
Chemical formula	$C_{25}H_{48}FeN_6P_2$
M_r	550.49
Crystal system, space group	Monoclinic, $P2_1/c$

Temperature (K)	85K
a, *b*, *c* (Å)	9.0126 (1), 14.3811 (2), 22.2186 (2)
β (°)	98.161 (1)
V (Å^3)	2850.61 (6)
Z	4
Radiation type	Cu *K*α
μ (mm^{-1})	5.48
Crystal size (mm)	0.19 × 0.08 × 0.06 × 0.40 (radius)
Data collection	
Diffractometer	Dtrek-*CrysAlis PRO*-abstract goniometer imported rigaku-*D*TREK* images
Absorption correction	For a sphere *CrysAlis PRO* 1.171.43.95a (Rigaku Oxford Diffraction, 2023) Spherical absorption correction using equivalent radius and absorption coefficient. Empirical absorption correction using spherical harmonics, implemented in SCALE3 ABSPACK scaling algorithm.
T_{min}, T_{max}	0.307, 0.375
No. of measured, independent and observed [$I \geq 2u(I)$] reflections	41378, 5306, 5101
R_{int}	0.041
$(\sin \theta/\lambda)_{max}$ (Å^{-1})	0.607
Refinement	
$R[F^2 > 2\sigma(F^2)]$, $wR(F^2)$, S	0.030, 0.091, 1.04
No. of reflections	5306
No. of parameters	499
H-atom treatment	All H-atom parameters refined
$\Delta\rangle_{max}$, $\Delta\rangle_{min}$ (e Å^{-3})	0.32, -0.43

Figure S59. Molecular structure of **5** with 50% probability ellipsoids. Hydrogen atoms not attached to iron are omitted for clarity.

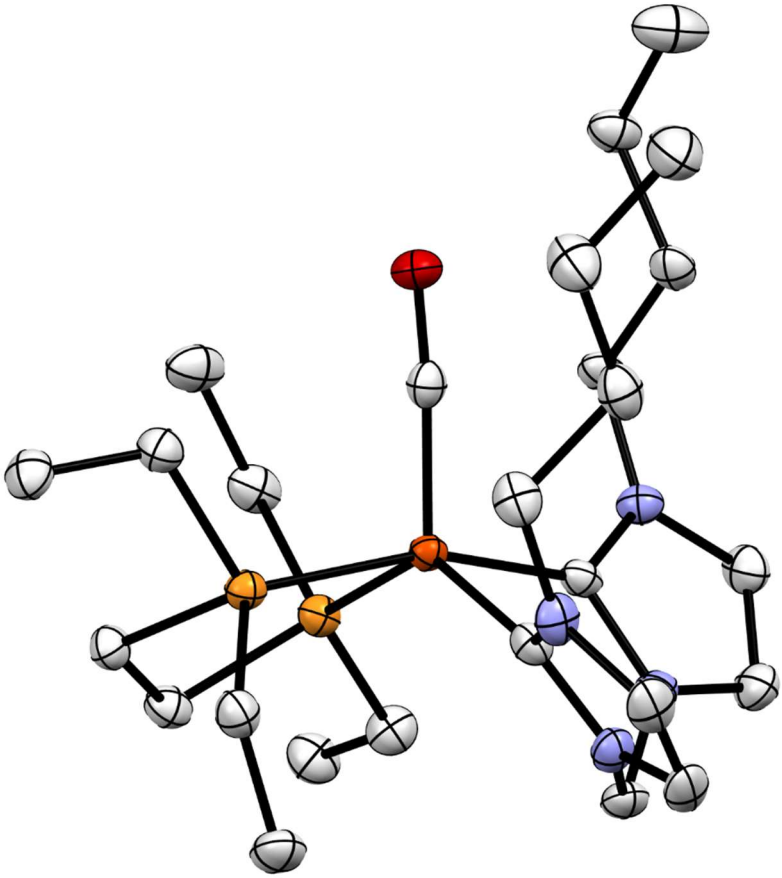

Complex: [Fe(CO)(depe)(^{butyl}CC)]

Local name: CA1368

CCDC: 2390974

Table S14. Crystallographic parameters for **5**.

CCDC number	
Empirical formula	$C_{26}H_{48}FeN_4OP_2$
Formula weight	550.47
Temperature [K]	293(2)
Crystal system	triclinic

Space group (number)	$P\overline{1}$ (2)
a [Å]	8.7819(3)
b [Å]	18.2197(4)
c [Å]	19.7713(4)
α [°]	67.588(2)
β [°]	86.730(2)
γ [°]	87.945(2)
Volume [Å^3]	2919.43(14)
Z	4
ρ_{calc} [gcm^{-3}]	1.252
μ [mm^{-1}]	5.361
F(000)	1184
Crystal size [mm^3]	0.192×0.115×0.068
Crystal colour	red
Crystal shape	plate
Radiation	Cu K_α (λ=1.54184 Å)
2θ range [°]	4.84 to 139.16 (0.82 Å)
Index ranges	−10 ≤ h ≤ 10 −21 ≤ k ≤ 21 −23 ≤ l ≤ 23
Reflections collected	19454
Independent reflections	19454 R_{int} = ? R_{sigma} = 0.0324
Completeness to θ = 67.684°	97.7 %
Data / Restraints / Parameters	19454/0/627
Absorption correction T_{min}/T_{max} (method)	0.70831/1.00000 (multi-scan)

Goodness-of-fit on F^2	1.002
Final R indexes [$I \geq 2\sigma(I)$]	R_1 = 0.0536 wR_2 = 0.1510
Final R indexes [all data]	R_1 = 0.0645 wR_2 = 0.1599
Largest peak/hole [eÅ^{-3}]	0.89/−0.56
Extinction coefficient	0.0020(2)

Computer programs: CrysAlis PRO 1.171.42.61a (Rigaku OD, 2022), CrysAlis PRO 1.171.42.61a (Rigaku OD, 2022), SHELXT 2018/2 (Sheldrick, 2018), olex2.refine 1.5 (Bourhis et al., 2015), Olex2 1.5 (Dolomanov et al., 2009).

References

(1) Broere, D. L. J.; Čorić, I.; Brosnahan, A.; Holland, P. L. *Inorg. Chem.* **2017**, *56* (6), 3140–3143.

(2) Doyle, L. R.; Heath, A.; Low, C. H.; Ashley, A. E. *Adv. Synth. Catal.* **2014**, *356* (2–3), 603–608.

(3) Alyea, E. C.; Malito, J. *Phosphorus Sulfur Silicon Relat. Elem.* **1989**, *46* (3–4), 175–181.

(4) Chakraborty, S.; Chattopadhyay, J.; Guo, W.; Billups, W. E. *Angew. Chem. Int. Ed.* **2007**, *46* (24), 4486–4488.

(5) Field, L. D.; Hazari, N.; Li, H. L. *Inorg. Chem.* **2015**, *54* (10), 4768–4776.

(6) Hirano, M.; Akita, M.; Morikita, T.; Kubo, H.; Fukuoka, A.; Komiya, S. *J. Chem. Soc. Dalton Trans.* **1997**, No. 19, 3453–3458.

(7) Gil-Rubio, J.; Cámara, V.; Bautista, D.; Vicente, J. *Organometallics* **2012**, *31* (15), 5414–5426.

(8) Komiya, S.; Akita, M.; Yoza, A.; Kasuga, N.; Fukuoka, A.; Kai, Y. *J. Chem. Soc. Chem. Commun.* **1993**, No. 9, 787.

(9) Gaussian 16, Revision C.01, Frisch, M. J.; Trucks, G. W.; Schlegel, H. B.; Scuseria, G. E.; Robb, M. A.; Cheeseman, J. R.; Scalmani, G.; Barone, V.; Petersson, G. A.; Nakatsuji, H.; Li, X.; Caricato, M.; Marenich, A. V.; Bloino, J.; Janesko, B. G.; Gomperts, R.; Mennucci, B.; Hratchian, H. P.; Ortiz, J. V.; Izmaylov, A. F.; Sonnenberg, J. L.; Williams-Young, D.; Ding, F.; Lipparini, F.; Egidi, F.; Goings, J.; Peng, B.; Petrone, A.; Henderson, T.; Ranasinghe, D.; Zakrzewski, V. G.; Gao, J.; Rega, N.; Zheng, G.; Liang, W.; Hada, M.; Ehara, M.; Toyota, K.; Fukuda, R.; Hasegawa, J.; Ishida, M.; Nakajima, T.; Honda, Y.; Kitao, O.; Nakai, H.; Vreven, T.; Throssell, K.; Montgomery, J. A., Jr.; Peralta, J. E.; Ogliaro, F.; Bearpark, M. J.; Heyd, J. J.; Brothers, E. N.; Kudin, K. N.; Staroverov, V. N.; Keith, T. A.; Kobayashi, R.; Normand, J.; Raghavachari, K.; Rendell, A. P.; Burant, J. C.; Iyengar, S. S.; Tomasi, J.; Cossi, M.; Millam, J. M.; Klene, M.; Adamo, C.; Cammi, R.; Ochterski, J. W.; Martin, R. L.; Morokuma, K.; Farkas, O.; Foresman, J. B.; Fox, D. J. Gaussian, Inc., Wallingford CT, 2016

(10) Tao, J. M.; Perdew, J. P.; Staroverov, V. N.; Scuseria, G. E. Phys. Rev. Lett. 2003, 91, 146401.

(11) Weigend, F.; Ahlrichs, R. Phys. Chem. Chem. Phys. 2005, 7, 3297–3305.

(12) Grimme, S.; Antony, J.; Ehrlich, S.; Krieg, H. J. Chem. Phys. 2010, 132

(13) (a) Klamt, A.; Schüürmann, G. J. Chem. Soc. Perkin Trans. 2. 1993, 2, 799–805. (b)Marten, B.; Kim, K.; Cortis, C.; Friesner, R. A.; Murphy, R. B.; Ringnalda, M. N.; Sitkoff, D.; Honig, B. J. Phys. Chem. 1996, 100, 11775–11788.